DEVELOPMENT OF A SYSTEM

TO MEASURE MARINE TURBULENCE.

Prepared by:

IAN CAMERON MAIN, B.Sc.(Elec.) Engineering, Cape Town.

Submitted to the University of Cape Town in partial fulfilment of the requirements for the degree of Master of Science in Engineering.

September, 1989

SYNOPSIS

Various transducers have been developed to measure turbulent shear in the ocean. The airfoil probe with it's piezoceramic beam encapsulated in a rubber airfoil has the simplest electronic processing system. However, the beam is very fragile and displays unpredictable thermal effects.

An airfoil probe with semiconductor strain gauges on an aluminium cantilever beam has been developed as an alternative to the piezoceramic beam. The probe was calibrated by exciting it with a known shear generated by the water flow from an oscillating nozzle. During the calibration the thermal sensitivity of the probe was established to be -1.7 % $^{o}C^{-1}$.

The probe, along with it's high gain, low noise processing system, is fitted to a tethered free-fall vehicle. A solid state data logger situated in the vehicle is used to record the data generated by the turbulence probe and a pressure transducer.

Field trials at St.Helena Bay and Hout Bay showed that the sensitivity of the system is 20 dB lower than that of similar systems using piezoceramic beams. The system is able to resolve turbulent dissipation levels above 10^{-8} W kg^{-1}, making it useful in regions characterised by a typical mixed layer (dissipation level of 10^{-6} W kg^{-1}); however, it's sensitivity is not adequate for deep sea measurements where dissipation levels may be as low as 10^{-10} W kg^{-1}.

/(ii)

ACKNOWLEDGEMENTS.

The financial contribution of the Institute of Maritime Technology, on which the project was dependant, is gratefully acknowledged.

Thanks are due to Mr A.W.D.Jongens of the Central Acoustics Laboratory, UCT Dept. of Electrical Engineering, the supervisor of this thesis. He motivated the writer throughout the project, provided technical input where required, was always available for advice and arranged the writer's participation in various conferences.

The advice and technical input of the undermentioned people, necessitated by the multi-disciplinary nature of this project, are gratefully acknowledged:

Mr H.Waldron, Senior Scientific Officer, UCT Dept. of Oceanography played a key role in defining the project goals, providing technical advice in the field of oceanography throughout the project. He was particularily helpful in calibrating the probe, and in organising and participating in the sea trials.

Dr H.Pierce of the UCT Dept. of Mechanical Engineering provided advice on the problems of resonating structures.

Dr C.Mercer of the UCT Dept. of Civil Engineering provided advice on Finite Element analysis.

Mr S.Schrire of the UCT Dept. of Electrical Engineering provided advice on the selection and procurement of electronic components.

Mr D.Kenyon of the UCT Electrical Engineering Workshop manufactured the casings of several probes and assisted

/(iii)

with some of the mechanical work in building the system.

Prof G.Brundrit, Head of the UCT Dept. of Oceanography provided advice on the theory of calibrating the probe.

Mr P.Hanekom of the UCT Diving Unit assisted in the pressure chamber tests, and skippered the ski-boat during sea trials.

CONTENTS

		PAGE
Synopsis.		(i)
Acknowledgements.		(ii)
Contents.		(iv)
List of Illustrations.		(ix)
Nomenclature.		(xi)
1.	INTRODUCTION.	1
2.	PHYSICAL PROPERTIES OF SUBMARINE TURBULENCE.	3
2.1	A DESCRIPTION OF THE VARIOUS SCALES OF OCEANIC MOVEMENT.	3
2.2	THE MAGNITUDE OF VELOCITY SHEARS WITHIN THE MICROSTRUCTURE.	4
3.	REVIEW OF THE VARIOUS MARINE TURBULENCE PROBES.	7
3.1	AIM OF THE REVIEW.	7
3.2	THE HOT FILM ANEMOMETER.	7
3.21	General Description.	7
3.22	Critical Review of the Hot-Film Anemometer.	8
3.3	ULTRASONIC SENSORS.	10
3.31	General Description.	10
3.32	Review of the Performance of the Ultrasonic Shear Profiler.	10
3.4	DOPPLER BACKSCATTER TECHNIQUES.	11
3.41	General Description of the Doppler-Backscatter Method.	11
3.42	A Review of the Performance of Acoustic Backscatter Techniques and Doppler Sonar.	12
3.43	The Laser Doppler Anemometer	13
3.5	AIRFOIL PROBES.	15
3.51	Historical Development of the Probe.	15
3.52	Review of the Performance of Airfoil Probes.	17
3.6	CONCLUSION.	20
4.	THE FEASIBILITY OF A STRAIN-GAUGED BEAM AS A TURBULENCE TRANSDUCER.	21
4.1	CHOICE OF BEAM CONFIGURATION.	21
4.2	CHOICE OF BEAM MATERIAL.	22

PAGE

4.3	CHOICE OF STRAIN GAUGE.	23
4.31	Physical Dimensions.	23
4.32	Sensitivity.	23
4.33	Compatibility with the Substrate.	24
4.4	REQUIREMENTS OF THE SIGNAL PROCESSOR.	25
4.5	CONCLUSION.	25
5.	DESIGN AND CONSTRUCTION OF AN AIRFOIL PROBE USING SEMICONDUCTOR STRAIN GAUGES.	26
5.1	DETERMINATION OF THE CANTILEVER BEAM DIMENSIONS.	26
5.11	Spatial Resolution.	26
5.12	Beam Senstitvity.	27
	5.121 The Relationship between Sensitivity and Natural Frequency.	27
	5.122 Determining the Relationship between Beam Thickness and Natural Frequency.	28
	5.123 Determination of the Desired Beam Thickness.	34
5.2	STRAIN GAUGE BRIDGE CRITERIA.	36
5.21	Configuration for Maximum Sensitivity.	36
5.22	Thermal Stability of the Bridge.	37
	5.221 The Active Arm.	37
	5.222 The Passive Arm.	38
	5.223 The Interconnecting Leads.	38
5.23	Balancing the Bridge.	39
5.3	DESCRIPTION OF AIRFOIL PROBE.	40
6.	DESIGN OF THE PROCESSING ELECTRONICS.	41
6.1.	GAIN REQUIREMENTS OF THE PROCESSOR.	41
6.2	BANDWIDTH REQUIREMENTS OF THE AMPLIFIER.	43
6.21	The High Frequency Band Limit.	43
6.22	Determination of the Low Frequency Cut-off Point.	43
6.3	DESIGN OF THE PRE-AMPLIFIER STAGE.	44
6.31	Determination of a Suitable Amplifier Configuration.	44
6.32	Theoretical Description of Pre-Amplifier Stage.	48
	6.321 Magnitude Response.	48
	6.322 Phase Response.	49

PAGE

6.4	SIGNAL CONDITIONING AND STORAGE.	49
6.41	Introduction.	49
6.42	The Differentiator Stage.	50
6.43	The Filter Stage.	51
6.44	The Calibration Stage.	52
6.45	The Sampling Procedure.	52
6.46	The Storage Module.	52
6.5	DESCRIPTION OF THE REQUIRED POWER SUPPLIES.	53
6.6	SHIELDING REQUIREMENTS.	53
7.	SIGNAL PROCESSING OF THE TURBULENCE DATA.	55
7.1.	OBJECTIVES OF SIGNAL PROCESSING.	55
7.2	POWER SPECTRAL ESTIMATION.	55
7.21	Classification of the Turbulence Signal.	56
7.22	Direct Spectral Estimation Using the Welch Method.	57
	7.221 Welch's Algorithm.	57
	7.222 Selection of a Suitable Data Window.	57
	7.223 The Use of a Spectral Window.	58
7.3.	PROCESSING THE TURBULENCE DATA IN THE TIME DOMAIN.	59
8.	CALIBRATION OF THE STRAIN GAUGE AIRFOIL PROBE.	60
8.1	OBJECTIVES OF THE CALIBRATION PROCEDURE.	60
8.2	THEORETICAL RESPONSE OF THE AIRFOIL PROBE TO TRANSVERSE VELOCITIES.	60
8.3	DEVELOPMENT OF A CALIBRATION PROCEDURE.	62
8.31	Simulating a Velocity Shear.	62
8.32	Review of Techniques Previously Used to Calibrate the Airfoil Probe.	62
	8.321 The Rotating Nozzle Technique.	62
	8.322 The Rotating Probe Technique.	64
	8.323 The Oscillating Probe Technique.	65
8.33	Feasibility of Previously Used Calibration Techniques.	65
	8.331 The Rotating Nozzle.	65
	8.332 The Rotating Probe.	66
	8.333 The Oscillating Probe.	66

PAGE

8.34	Construction of the Calibration Rig.	66
8.35	Minimisation of Background Noise in the Calibration Rig.	68
8.4	PROBE CALIBRATION.	70
8.41	Determination of the Calibration Coefficient.	70
	8.411 Derivation of the Calibration Coefficient.	70
	8.412 Band-limiting of Shear Simulation Data.	71
	8.413 Determining the Calibration Coefficient.	72
	8.414 Potential Errors and Uncertainty in the Calibration Procedure.	74
8.42	Determination of a Coefficient of Thermal Sensitivity.	75
	8.421 Static Response of the Probe.	75
	8.422 Dynamic Response of the Probe.	76
	8.423 Thermal Impulse Response of the Probe.	78
8.43	Effect of Probe Angle of Attack on Calibration Coefficient.	79
8.44	Effect of Hydrostatic Pressure on Probe Sensitivity.	79
8.45	Evaluation of Electronic Noise.	80
8.5	TRANSFORMATION OF CALIBRATION THEORY TO SPATIAL DOMAIN.	81
9.	DESCRIPTION OF TROUT SYSTEM.	83
9.1.	INTRODUCTION	83
9.2.	CONSTRUCTION OF THE MECHANICAL SYSTEM.	84
9.21	Description of the Vehicle.	84
9.22	The Probe/Vehicle Interface.	84
9.3.	SENSITIVITY SETTINGS OF TURBULENCE CHANNEL.	85
9.4	DESCRIPTION OF THE PRESSURE CHANNEL.	85
9.41	Description of the Pressure Sensor.	85
9.42	Description of the Amplifier.	86
9.43	Calibration of the Pressure Transducer.	86
9.5.	THE DATA LOGGING SYSTEM.	87
9.51	Power-Up of the Data Logger.	87
9.52	Triggering of the Turbulence Channel.	87

PAGE

9.53 Sampling Procedure. 87
9.54 PC/Data Logger Interface. 88
9.6 SOFTWARE PROCESSING. 88
9.61 MEMOD Downloading : Program READALL. 88
9.62 Data File Creation : Program DATASORT. 88
9.63 Data Processing : Program TROUT. 89
9.64 Shear Data Presentation (Time Domain) : Program TRACE. 89
9.65 Shear Data Presentation (Power Spectrum) : Program SPECTRUM. 90
9.7 SHEAR DATA INTERPRETATION. 91
10. PRESENTATION OF RESULTS OF FIELD TRIALS. 93
10.1 PRELIMINARY FIELD TRIALS : ST.HELENA BAY. 93
10.11 Introduction. 93
10.12 Deployment Results. 93
10.13 Discussion. 94
10.2 FIELD TRIALS : HOUT BAY. 96
10.21 Introduction. 96
10.22 Deployment Results. 96
10.23 Discussion. 97
11. EVALUATION OF SYSTEM PERFORMANCE. 99
11.1 SPATIAL RESOLUTION OF SYSTEM. 99
11.11 The High Frequency Cut-Off Scale. 99
11.12 The Low Frequency Cut-Off Scale. 99
11.2 THERMAL SENSITIVITY OF THE STRAIN GAUGE PROBE. 100
11.3 SENSITIVITY LIMITATIONS DUE TO ELECTRONIC NOISE LEVELS. 101
11.4 SENSITIVITY LIMITATIONS DUE TO MECHANICAL NOISE LEVELS. 101
11.5 PROBE RELIABILITY. 102
11.6 COST OF THE SYSTEM. 102
11.7 CONCLUSIONS. 103
12. RECOMMENDATIONS. 105
BIBLIOGRAPHY. 107
LIST OF REFERENCES. 109

LIST OF ILLUSTRATIONS

FIG.	TITLE	PAGE
2.1	Typical Shear Profile.	6
3.1	Schematic of Thin Film Probe Assembly.	8
3.2	Probe Arrangement for Ultrasonic Sensor.	10
3.3	Schematic of Original Airfoil Probe Transducer.	16
3.4	Schematic of Airfoil Sensor as used in the 1970's.	17
4.1	Cantilever Beam Airfoil Probe.	21
4.2	Young's Modulus for a Selection of Materials.	22
4.3	Bending Strain Gauges .	23
5.1	Comparison of Turbulence Spectra as Measured with Lift Sensing Probe and X-Wire Probe.	27
5.2	Typical Stress:Strain Curve for Rubber.	30
5.3	Physical Properties of Composite Beam.	30
5.4	Simple Line Element Model.	32
5.5	Variation of Natural Frequency with Beam Thickness - 1^{P} Model.	33
5.6.	Resonant Response of Prototype Airfoil Probe.	34
5.7	Spectrum of Shear Signal	35
5.8	Active Half-Bridge Configuration.	36
5.9	Bridge Circuit.	36
5.10	Traditional Bridge Balancing Technique.	39
6.1	Classical Instrumentation Amplifier.	45
6.2	Instrumentation Amplifier using Micropower Components.	45
6.3	LM607 Op-Amp Configured as a Differential Amplifier.	46
6.4	Comparison of LM163 Instrumentation and LM607 Operational Amplifiers.	47
6.5	Magnitude Plot of the Pre-Amplifier Response.	49
6.6	Magnitude Plot of Differentiator.	50
6.7	Magnitude Plot for 4^{th} Order Elliptic Filter.	51
6.8	Electronic System Shielding Schematic.	54

FIG.	TITLE	PAGE
8.1	Definition of Coordinate System Relative to the Probe Alignment.	60
8.2	Rotating Nozzle Calibrator.	63
8.3	Rotating Probe Calibrator.	64
8.4	Schematic of Calibration System.	67
8.5	Power Spectrum Showing Background Noise Caused by Turbulent Drainage.	68
8.6	Cross Section through Drainage System of Calibration Rig.	69
8.7	Power Spectrum Showing Background Noise due to Laminar Drainage.	70
8.8	Calibration Curve Showing Noise Level.	73
8.9	Calibration Curve Deduced by Linear Regression.	74
8.10	Determination of Thermal Sensitivity.	76
8.11	Dynamic Thermal Response.	77
8.12	Electronic Noise Levels at Different Sensitivity Settings.	80
8.13	Spectrum of Electronic Noise.	81
9.1	Block Diagram of TROUT System.	83
9.2	Table of Probe Sensitivity Settings.	85
9.3	Power Spectral Estimation Algorithm.	91
10.1	Turbulence Spectrum : St.Helena Bay.	94
10.2	Shear Trace in Presence of Strong Thermocline.	95

CHAPTER 1

INTRODUCTION

The physical properties of the ocean microstructure are not yet fully understood. An understanding of the physical characteristics of the microstructure velocity field is relevant to the fields of both oceanography and underwater acoustics.

Oceanographers are becoming aware of the fact that small-scale variations in temperature, salinity and velocity, and the associated small-scale vertical mixing play an important role in general circulation.

The Department of Oceanography at the University of Cape Town is involved in identifying turbulent layers in the water column. The aim is to correlate these layers with the vertical flux of phytoplankton nutrients, ie. nitrates, silicates and phosphates. To fulfil this objective, an instrument which is able to measure variations in the microstructure velocity field is required. The turbulence may then be analysed in the spectral domain, where the inertia and dissipation characteristics of the velocity field may be quantified.

In the field of underwater acoustics, a knowledge of the spectral and spatial magnitude of these turbulent fluctuations is important in understanding the effects of physical ocean processes on sound transmission. A study of the effects of microscale variations on acoustic signals is a major topic in current ocean acoustics research (R.C.Spindel, 1985).

The measurement of microscale velocity fluctuations in the ocean from a moving vehicle requires an instrument capable of high frequency response, fine spatial resolution and high sensitivity. Furthermore, the instrument must have a stable motion, falling freely through the water column rather than being cable-lowered from a ship.

This project is thus aimed at designing, constructing, calibrating and field testing an instrument having the properties mentioned.

This report first describes the expected physical properties of turbulent shear, and reviews the various instruments previously developed to measure this. The need for an alternative transducer is substantiated. The design of such a probe is then discussed, along with it's processing electronics and digital signal processing algorithms. The calibration of the probe is then considered and results are presented. The integration of the probe into a system capable of measuring turbulence in the field is then discussed. The results of field trials are presented. Finally, these results, together with those from the probe calibration are used to compare the characteristics of the system with those of other systems in use elsewhere.

CHAPTER 2

PHYSICAL PROPERTIES OF SUBMARINE TURBULENCE

2.1 A DESCRIPTION OF THE VARIOUS SCALES OF OCEANIC MOVEMENT

In order to understand the properties of the ocean microstructurre and turbulence on this scale, it is useful to have an understanding of the spatial characteristics of the various scales of marine flow fluctuation.

On the broadest level, background variations in temperature, pressure and salinity represent the "climatology" of the ocean. Vertical scales in this structure are consistent with mean ocean depths (order 5 km) and horizontal variations limited only by the size of the ocean basins. These background characteristics vary on a seasonal basis.

The next level is the mesoscale structure which is superimposed on the deterministic background structure. By definition, the mesoscale comprises spatial scales of tens to hundreds of kilometers, and time scales of days to several months. Complex rings, fronts, and eddy phenomena are characteristic of this class of ocean structure. It is estimated (R.C.Spindel, 1985) that 90% of the kinetic energy in the ocean is contained in mesoscale eddy fields. Variation in mesoscale characteristics can be analysed deterministically or as a stochastic perturbation of the background mean.

Finer scales of perturbation include internal waves, fine structure, microstructure and turbulence. These phenomena are generally treated as random processes. Internal waves exist in deep water, with wavelengths of the order of 150m,

and amplitudes of the order of several metres. They can also exist on shelves, where horizontal scales are reduced to between 100 m and 10 km, and vertical scales of 1-100 m. Time scales for internal waves vary from 10 mins to a few hours, and resultant horizontal currents from these disturbances are of the order of 0,05 ms^{-1}.

The ocean fine structure comprises areas of magnitude of 10-100 km on a horizontal scale, and 1-10 m on a vertical scale. It is characterised by a strata 25-40 m thick. The ocean fine structure spatially overlaps the internal waves described.

Finally, on the smallest scale, the ocean microstructure has a scale of the order of centimeters. Resultant turbulence and dissipation are caused by molecular processes. These processes are intermittent in time and space. Turbulence may be caused by mixing between pockets having uniform temperature and salinity, in statistically stable regions below the main thermocline.

These microstructure variations are the subject of current investigations; it is turbulence within the microstructure that is the topic of both acoustic and oceanographic study.

2.2 THE MAGNITUDE OF VELOCITY SHEARS WITHIN THE MICROSTRUCTURE

In order to design a sensor to detect turbulent velocity shears,it is necessary to know the approximate order of magnitude of the expected shears. The literature on the sensitivity of a variety of previously developed probes was reviewed to this end:

a) PROTAS, a shear probe using a neutrally bouyant

vane, described by J.H.Simpson (1971) is capable of resolving shears of 1 mm/sec over vertical separations of 30cm, ie: shears of $3.3 \times 10^{-3} s^{-1}$.

b) YVETTE, a free fall shear profiler described by D.L.Evans, M.Mork and T.Gytre (1979) can detect current variations of 0.05×10^{-3} cm s^{-1} over vertical separations of 10 cm, corresponding to shears of $5 \times 10^{-3} s^{-1}$. Evans et al claim that a shear of $5 \times 10^{-2} s^{-1}$ is very large in the ocean.

c) The hot-film anemometer described by R.E.Dingwell and F.B. Weiskopf (1981) meets the resolution requirements of 0,02 cm s-1 at 10 knots [0 dB Signal to Noise Ratio (SNR)] with an accuracy of velocity fluctuations of 0,1 cm s^{-1} at 10 knots. These values are not interpreted as velocity because the hot-film anemometer detects the axial, rather than the transverse component of the velocity field, which is required to measure shears.

d) A typical shear profile as recorded by R.G.Lueck and T.R.Osborn (1981) is shown in FIG. 2.1 It may be seen that the majority of shears are less than $1 s^{-1}$. The resolution of this instrument is of the order of $10^{-2} s^{-1}$.

It may be concluded that instrumentation currently used to detect turbulent velocity fluctuations has a resolution of between $10^{-3} s^{-1}$ and $10^{-2} s^{-1}$, depending on the type of instrument.

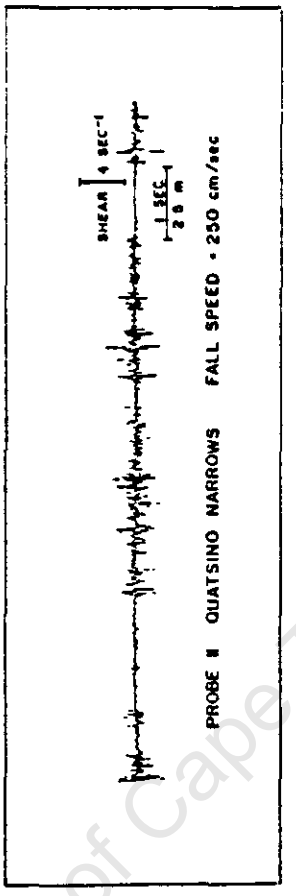

FIG.2.1 Typical Shear Profile
(R.G.Lueck and T.R.Osborn, 1981)

CHAPTER 3

REVIEW OF THE VARIOUS MARINE TURBULENCE PROBES

3.1 AIM OF THE REVIEW

The characteristics of transducers that have been developed to detect marine turbulence are described. These are compared in order to establish their relative merits (relevant to this project) and to justify the pursuit for an alternative sensor. The properties of the hot-film anemometer, ultrasonic sensors, airfoil probes, sonar and laser Doppler anemometers are reviewed and their suitability for this project is discussed in the conclusion.

3.2 THE HOT FILM ANEMOMETER

3.21 General Description

Hot-film probes consist of a thin metal sensing element having a resistance of 5 to 20 Ω , deposited on a substrate having high electrical and thermal insulating qualities, as shown in FIG.3.1. Films are used in preference to wires in liquid applications because they are better suited to withstand the associated hydrodynamic forces, and are less susceptible to contamination. The hot-film probe forms one arm of a bridge, with a feedback network that keeps the probe resistance constant. The flow of liquid past the probe is responsible for heat transfer, and an attending change in probe resistance. This change in resistance unbalances the bridge, and the feedback network readjusts the bridge voltage to achieve a new balance. Hence the voltage variations required to balance the bridge are proportional to the flow.

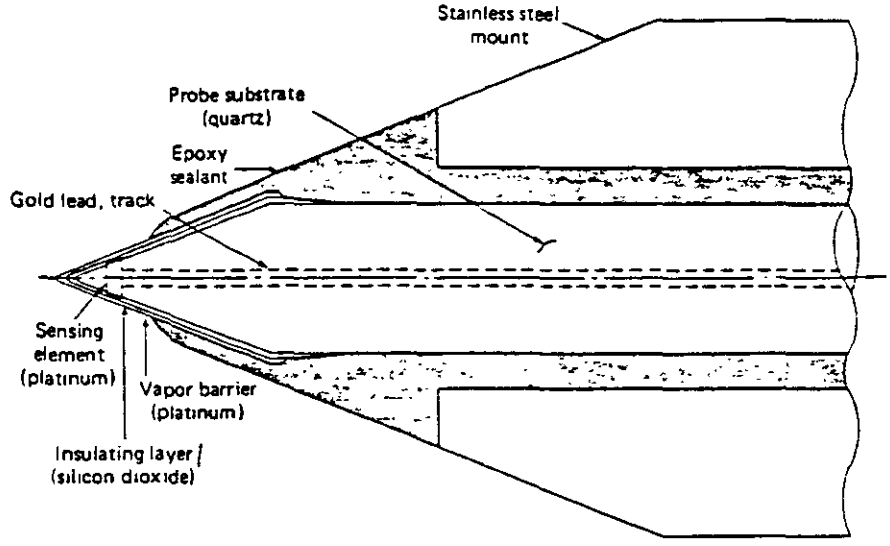

Schematic of thin film probe assembly, tip.

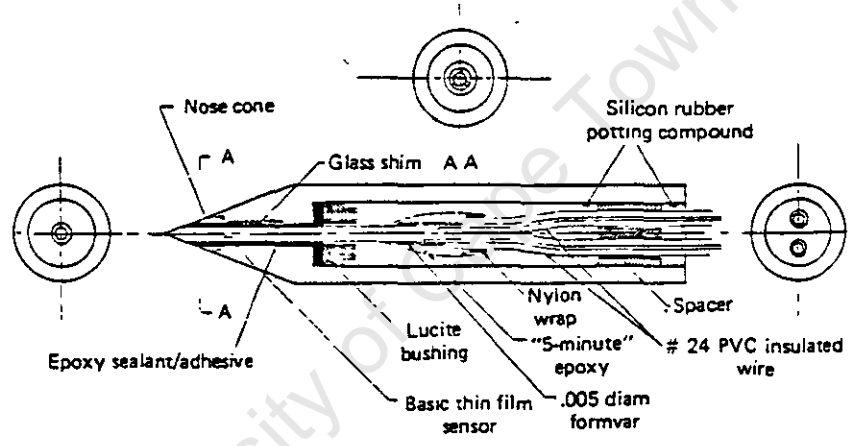

FIG.3.1 Schematic of Thin Film Probe Assembly.
(R.E.Dingwell and F.B.Weiskopf)

3.22 Critical Review of the Hot-Film Anemometer.

The hot-film anemometer has a high frequency response, varying from flat up to 500 Hz (as described in the review by H.R.Frey and G.J.McNally, 1973) to a typical decay of -6 dB @ 500 Hz, as is characteristic of the conical probe described by Dingwell et al (1981).

Hot-film anemometers have a high sensitivity.The instrument discussed by Dingwell et al has a resolution of

0,02 cm sec^{-1} @ 10 knots, with an accuracy of velocity fluctuations of 0,1 cm sec^{-1} @ 10 knots. However, the strongest asset of the hot-film (or hot-wire) anemometer is it's high spatial resolution. The relationship between bridge output voltage (V_{ac}) and particle displacement (ρ) is governed by the law:

$$V_{ac} = a_v(\frac{\rho}{d}) \qquad \ldots\ldots (1)$$

where a_v is a calibration coefficient dependant on frequency and d is the diameter of the hot-film sensor. A typical value is 300 μm, (P.S.Dubbleday, V.V.Apostalica and D.L.Diebel, 1988), making the instrument an attractive alternative for investigating inertial subrange and dissipation range of turbulence within the microstructure, where the spatial resolution of the probe is the determining factor.

The advantages of high sensitivity and spatial resolution of the hot-film anemometer are offset by it's unsuitability for field use. Shortcomings of this this type of probe are described in detail by Frey et al (1973) and Dingwell et al (1981).

These include the short lifetime of standard probes (10-100 hrs in laboratory conditions, and less than 21 hrs in field conditions), and the complexity of increasing this either by an inert platinum vapour barrier over the SiO_2 insulating layer (Dingwell et al), or by encapsulating the sensor in an elastomer boot filled with deionised water (Dubbleday et al). Other shortcomings include the downward drift in probe sensitivity due to deterioration of the film junction necessitating frequent calibration checks; also, the directional sensitivity of conical hot platinum film probes limits their use in determining the 3 spatial components of flow.

3.3 ULTRASONIC SENSORS

3.31 General Description

Shear profiles that utilise acoustic current meters are conceptually simple instruments comprising two ultrasonic pingers that transmit pulses in opposite directions along the same path. The difference in travel time is directly proportional to the average fluid motion along that path. The instrument described by Evans et al (1979) operates in this manner.

3.32 Review of the Performance of the Ultrasonic Shear Profiler

The transducer described by Evans et al is capable of measuring velocities of 1 mm sec^{-1}, a sensitivity of the same order of magnitude as the hot-film anemometer. However, the physical separation of the probes limits the spatial resolution of the instrument in two ways:

Firstly, the transit time of a pulse measured by the instrument electronics must be determined to a high degree of precision. Assume that two probes are spaced apart (distance d) in a mean flow V, as depicted in FIG.3.2:

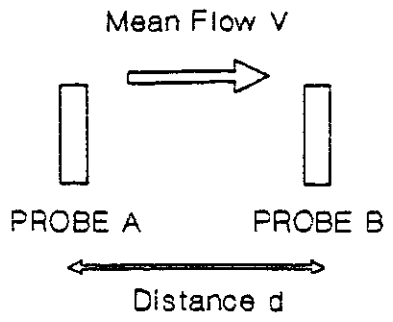

FIG.3.2 Probe Arrangement for Ultrasonic Sensor

The time it takes for a pulse travelling from A to B (t_{ab}) in water where the velocity of sound is c, is $t_{ab} = d/(c+V)$. The time for a pulse from B to A is $t_{ba} = d/(c-V)$. The instrument measures the difference in times, ie: $t_{ab}-t_{ba} = -2dV/c^2$.

If the probes are spaced 30 cm apart (as is the case with the probe used by Evans et al) and the mean flow velocity is 1 mms^{-1}, then for a velocity of sound of 1500 ms^{-1}, $t_{ab}-t_{ba} = -3x10^{-10}$ seconds. This value will fluctuate with physical changes of the water. Therefore, in addition to measuring transit times, the circuit must measure and compensate for electronic drift and changes in the speed of sound. The required precision increases as the probes are moved closer together.

Secondly, probes situated closer together than the 30 cm used by Evans et al will disturb the very structure that is being measured.

Thus, the effectiveness of ultrasonic instrumentation is limited to analysing vertical scales of 0.5 m and larger. These instruments are more suited to studying internal wave characteristics and fine structure, than the turbulent characteristsics of the inertial sub-range and dissipation region, where a spatial resolution of centimeter order of magnitude is required of the transducer.

3.4 DOPPLER BACKSCATTER TECHNIQUES

3.41 General Description of the Doppler-Backscatter Method

Doppler sensors can detect relative water motion by transmitting a high-frequency (sound or light) signal in a narrow beam, and measuring the frequency shift of the returned signal as it is scattered from particles in the

water. The attraction of this technique is it's remote measuring capability. In theory, velocity can be measured at a selected distance from the transducer without disturbing the velocity structure, as is the case with other techniques. The performance of Doppler Sonar and Acoustic Doppler instruments, as well as Laser Doppler Anemometers will be discussed.

3.42 A Review of the Performance of Acoustic Backscatter Techniques and Doppler Sonar

In their review of velocity measurements using Acoustic Doppler Backscatter, W.E.Woodward and G.F.Appell (1985) discuss the then state of the art in this technology. From the review, it is evident that the commercial devices available using acoustic backscatter techniques are primarily aimed at measuring mesoscale current variations. A typical specified precision is 3.7 cms^{-1} for a depth resolution of 2 m. The spatial resolution is inadequate for the measurement of microstructure disturbances. A system was developed for turbulence measurement in estuaries, but this never progressed beyond the research tool stage.

A high resolution Doppler Sonar system is described by R.Lhermitte (1983). This system has a velocity resolution of 0,2 cms^{-1} and a water depth resolution of 3,5 cm. The system has been used to measure water velocity and turbulence in a tidal channel. The technique requires the presence of a sufficient concentration of small targets acting as traces of water velocity from which the phase change between consecutive backscatter pulses is evaluated. The presence of air bubbles or organisms with propulsion capability tend to bias the velocity measurement.

The experimental layout comprised a fixed beam inverted Doppler Sonar which rested on the waterway floor, producing a sonar beam tilted at 45° from the horizontal.

The 200 kHz system had a range limited to 10-15 m which was adequate for use in the channel.

The system described has adequate spatial and velocity resolution to analyse dissipation due to microstructure turbulence. However, the range limitations and requirement of a fixed platform from which to monitor the turbulence, prevent the instrument from being used to map vertical shear profiles in a survey of the microstructure. Furthermore, to evaluate water velocity as a function of depth, a single Doppler Sonar would require either a scanning beam or several fixed beams pointed in different directions, because the Sonar only senses radial velocity , and evaluation of target motion as a vector would require radial velocities from different directions.

3.43 The Laser Doppler Anemometer

Using the same principle as the other Doppler-shift techniques described, the Laser-Doppler-Anemometer (LDA) measures the Doppler-shift of laser light scattered from small particles moving in the fluid. This method is well established in determining fluid velocity in pipes, where the fluid can be seeded with minute particles (micron order of magnitude) evenly distributed through the fluid.

Theoretical aspects of this approach are discussed by P.Buchhave, W.K.George and J.L.Lumley (1979) in their review of the measurement of turbulence with the LDA. The review also discusses the problems associated with this technology, which include the following factors:

Variations in the refractive index of the fluid have a detrimental effect on the signal to noise ratio of the output. In the case of seawater, the refractive index is primarily a function of salinity , which may vary

considerably through a typical vertical profile.

The measurement of low intensity turbulence requires the use of a burst-signal processor. Here, the movement of individual particles is monitored, as opposed to continuous processing where particle motion is averaged over the probe volume . This poses it's own problems, because the data rate is usually below that required to resolve small scale turbulence in a real-time mode (due to an inefficient concentration of seeding particles), thus complicating the extraction of statistical quantities from the randomly sampled data. The burst signal has to be analysed for the entire period that the particle is in the probe volume, for the samples to reproduce the desired Eulerian velocity field.

The only documented application of the LDA to the measurement of marine microstructure turbulence that has been discovered by the author in searching the literature in this field, is in the Annual Report of the Centre for Water Research at the University of Western Australia (1986). The Department of Environmental Fluid Dynamics is involved in the manufacture of a Microstructure Flux Profiler that incorporates an LDA to monitor the u and v components of velocity. It is difficult to evaluate the performance of this instrument from the very brief description which is given. The portable instrument does, however, require a National 32016 32-bit microcomputer system to handle data aquisition. The LDA signal processing involves Fourier Transforms of signals with bandwidths up to 100 kHz. The simplest Fourier Transforms algorithm requires a sustained computational throughput of 14 million floating point operations per second (Mflops), requiring 2 parallel processing systems having a combined throughput of 20-40 Mflops.

The source is a 5 milliwatt helium-neon laser. It is claimed that the instrument will be capable of resolving the three dimensional velocity field with cm order of magnitude resolution.

To date, there have been no publications on the performance of the instrument. It will be interesting to monitor publications from this University, in particular by J.Imbeger (the academic director of the project), to determine the success of this instrument.

Besides being technologically complex, the LDA is reliant on a pre-specified particle concentration in the deployment region. This may restrict it's deployment to regions where the salinity and nutrient concentration (seeds) are within specific operating limits.

3.5 AIRFOIL PROBES

3.51 Historical Development of the Probe

The first airfoil sensor was developed by T.E.Siddon and H.S.Ribner in 1965 to monitor turbulent velocity fluctuations in airflows. It consisted of a miniature aluminium aerofoil connected to a tapered cantilever beam embedded in a piezoceramic sensing element, as shown in FIG. 3.2.

For low values of turbulent intensity, the piezoelectric element produces an output voltage directly proportional to the transverse component of the turbulent velocity.

The most significant problem encountered with this design was obtaining an overall structural response free from resonant peaks over the frequency range of interest, with frequency components between 0 and 10 kHz contributing to

the frequency spectrum in a typical aerospace application. The resultant design had a fundamental natural frequency of 12.5 kHz.

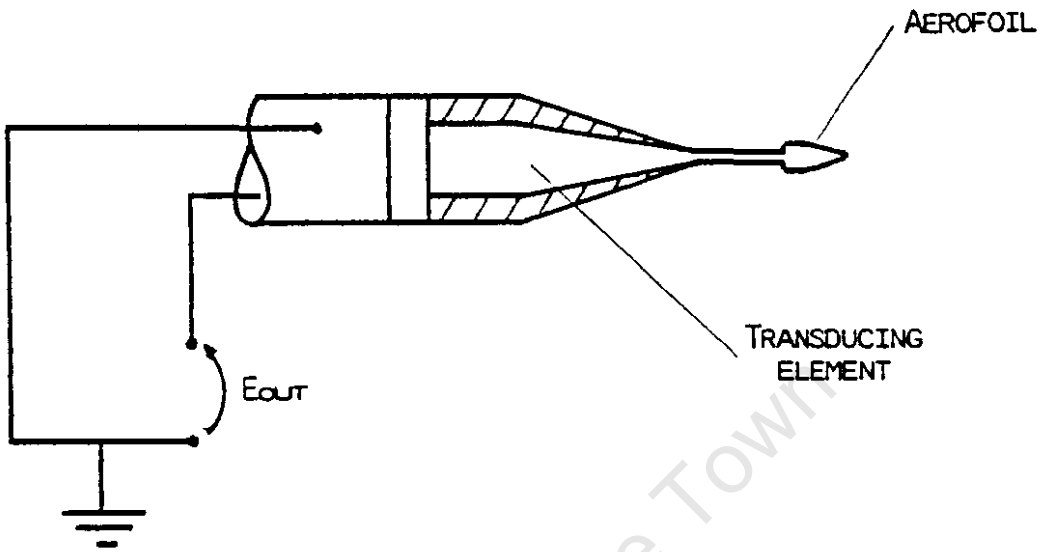

FIG.3.3 Schematic of Original Airfoil Probe Transducer.

The design was improved by T.E.Siddon (1971), when he replaced the aerofoil with an axisymmetric half-body of revolution at the nose of a cylindrical probe. The fundamental frequency of the beam-nosepiece was maximised by using an epoxy coated balsa nosepiece. This light configuration (FIG. 3.4) ensured a resonant frequency in excess of 15 kHz, and minimised inertial loading of the transducer arising from support vibration.

The application of this form of sensor was extended to oceanographic applications by T.R.Osborn (1974), the sensor construction being similar to that in Fig. 3.3., except for the balsa nosepiece being replaced by a moulded silicone rubber nose. A detailed description of the performance of the transducer is given by T.R.Osborn and W.R.Crawford (1980).

The probe has been deployed as a component of both retrievable instrumentation systems (N.S.Oakley, 1977), and expendable dissipation profiler (XDP) systems (R.G.Lueck and T.R.Osborn, 1981).

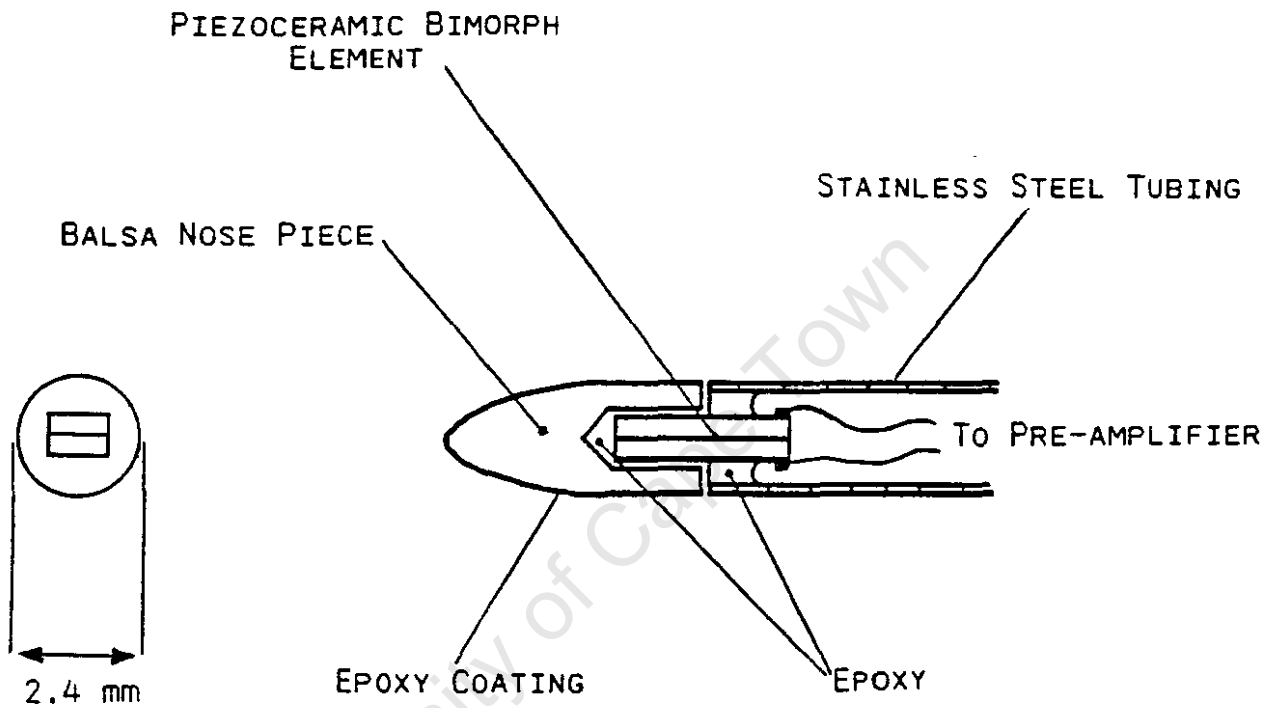

FIG. 3.4 Schematic of Airfoil Sensor as used in the 1970's.

More recently, the probe has been used to measure microstructure turbulence both in submarine canyons to a depth of 400 m (Lueck et al, 1984), and as part of a deep-sea instrumentation system where it has been deployed to depths in excess of 1 500 m (N.S.Oakley, 1988).

3.52 Review of the Performance of Airfoil Probes

The comprehensive documentation available on the results of field deployment of airfoil probes proves that their

performance compares favourably with the other turbulence measurement techniques discussed. The sensor is robust when compared with the hot-film anemometer. It's resolution of $10^{-2}s^{-1}$ is fine enough to analyse dissipation levels associated with microstructure shear.

The most attractive aspect of the airfoil probe is the simplicity of the processing system. The signal from the piezoelectric beam is amplified by a charge amplifier (the beam acts as a capacitively coupled voltage source), differentiated to present the data as a velocity shear, and finally stored or transmitted to the surface vessel. The result is a low maintenance processing system not requiring continuous specialist input.

It has been shown (T.E.Siddon, 1971) that the spatial resolution of the probe depends on the cross-section diameter of the airfoil, and that the probe resolves frequencies down to approximately 4 times the probe diameter. Typical diameters of probes are between 4.7 mm (T.R.Osborn and W.R.Crawford, 1980) and 6,0 mm (N.S.Oakley, 1977), resulting in a spatial resolution of between 19 and 24 mm.

The airfoil probe does have it's limitations, a number of which are commented on below:

Firstly, piezoelectric devices are sensitive to temperature variations. Experiments have shown (Osborn et al, 1981) that the sensitivity of the probe is dependant on the mean surrounding temperature, a factor of about +1% $^{\circ}C^{-1}$ (although this has been found to vary from probe to probe). Piezoelectric devices show pyroelectric effects, resulting in a low-frequency response to temperature changes. Osborn et al showed that a 1°C temperature change over 1 m resulted in a low frequency velocity shear of the order of

$2.5 \times 10^{-2}.s^{-1}$. Consequently, the low-frequency response of the probe is limited to between 1 and 0.1 Hz.

Secondly, piezoceramic bimorph beams are very brittle and have a limited life. Any form of mechanical shock is bound to break the sensing element. Lifetime is not a factor in expendable instruments, but in instances where a retrievable, reusable system has been desired, it has been necessary to build a few probes for each research mission. Each probe has to be calibrated individually because the axial alignment of the piezoceamic beam affects the sensitivity of the probe. Mechanical failure of the probe is characterised by the presence of large noise spikes associated with temperature changes. If the probe output is not monitored for each deployment, these noise spikes may contaminate the results of a significant portion of an oceanographic survey.

Thirdly, due to the high impedance output characteristics of the piezoceramic element, the probe is susceptible to noise between the sensor and the pre-amplifier. This does not seem to be a significant problem, as Lueck and Osborn (1980) describe the contamination in their system to be 100 V_{rms} in the 1-250 Hz band, corresponding to a root mean square (RMS) noise shear of $10^{-10}.W/m^3$.

Finally, the theory that predicts the output signal of the airfoil sensor is proportional to the transverse component of velocity, is only valid if the sensor has small angles of tilt and for an axial velocity much greater than the transverse velocity (justified in Chapters 8.31 and 8.411). Large angles of tilt of the probe ($>+15^{o}$) result in a non-linear output function due to viscosity effects on the probe (T.R.Osborn and W.R.Crawford, 1980). Thus, the hydrodynamic performance of the vehicle housing the probe is an important consideration when designing the system.

3.6 CONCLUSION

The suitability of the described sensors to the current project should be considered with reference to the desired spatial resolution of the probe , portability of the instrument, it's "user friendliness" (the users being Oceanographers and not Electronic Engineers), as well as the cost of design and manufacture (influenced by the state and availability of current technology).

Of the probes described, the hot-film anemometer and the airfoil probe are the only ones having the required spatial resolution and portability, along with relatively little technological complexity. Although the airfoil probe has a spatial resolution one order of magnitude lower than that of the hot-film anemometer, it proved to be adequate for the analysis of microstructure turbulence. The advantage of linearity and ease of calibration of the airfoil probe over the hot-film anemometer make it the more attractive alternative.

This project is therefore aimed at developing an airfoil probe which has a lower maintenance requirement than those used previously. This may be achieved by finding an alternative sensing element to the brittle piezoceramic beam currently used. Desirable characteristics of a new sensor include a longer lifespan, improved thermal characteristics and a higher signal to noise ratio than present probes.

CHAPTER 4

THE FEASIBILITY OF A STRAIN-GAUGED BEAM AS A TURBULENCE TRANSDUCER

A feasibility study of this nature was conducted by I.C.Main as part of an undergraduate thesis at the University of Cape Town in 1987. This section reviews some of the important factors to be considered.

4.1 CHOICE OF BEAM CONFIGURATION

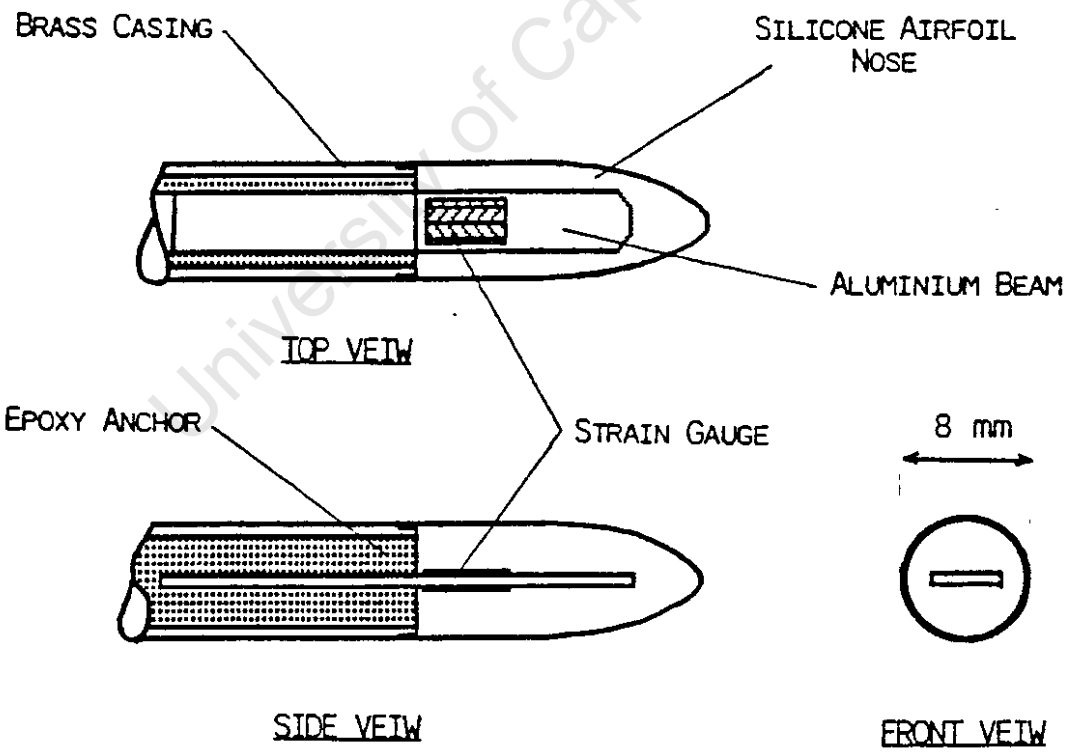

FIG. 4.1 Cantilever Beam Airfoil Probe

The most appropriate configuration is a cantilever beam anchored in an epoxy base, as shown in FIG. 4.1 For maximum sensitivity, the strain gauges must be mounted as close to the anchor as possible, in an active half-bridge configuration, where the bending moment is the greatest. The axis-symmetric silicone airfoil remains the same as that used for piezoceramic transducers.

4.2 CHOICE OF BEAM MATERIAL

In accordance with Euler-Bernoullian beam theory, the strain (ε) on a thin cantilever beam of length, width and thickness l, w and h, resectively, is given by the equation:

$$\varepsilon = \frac{6Fl}{wh^2E} \qquad \ldots\ldots (2)$$

where F is the applied force and E is the modulus of elasticity for the material. It is evident that the material that produces the largest strain for a given force is that with the lowest modulus. FIG. 4.2 lists the modulus of elasticity for a selection of materials.

Material	Elasticity [GPa]
Aluminium	69
Brass	90
Cast Iron	103-138
Copper Berrillium	131
Stainless Steel	179-193
Steel	200+

FIG. 4.2 Young's Modulus for a Selection of Materials

Substituting these values for E in equation (2) confirms that aluminium will produce the largest strain for a given applied force.

4.3 CHOICE OF STRAIN GAUGE

The suitability of the strain gauge for this application is determined by :

a) The physical dimensions of the strain gauge.
b) The achievable sensitivity of the gauge.
c) The compatibility of the gauge with the substrate.

4.31 Physical Dimensions

For maximum spatial resolution of the probe, the strain gauge must be as narrow as possible. This restricts the choice to the simple bending gauge, as shown in FIG. 4.3.

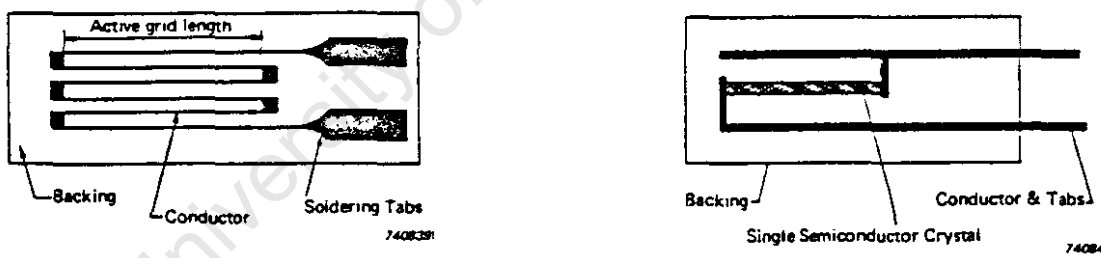

FIG.4.3 Bending Strain Gauges (Bruel and Kjaer).

4.32 Sensitivity

The sensitivity of a strain gauge is indicated by it's Gauge Factor (G)

$$G = \frac{\delta R}{\epsilon R} \qquad \ldots\ldots (3)$$

/24

where R is the static resistance of the strain gauge, and δR is the change in resistance for a given applied strain (ϵ). A Gauge Factor of 2.1 is typical for resistive bending strain gauges.

A probe utilising conventional resistive strain gauges has been designed and described by I.C.Main (1987). It was found that for the magnitude of strains expected, a Gauge Factor of 2.1 resulted in a SNR too low to retrieve the driving signal. It was proposed that a similar system be designed using semi-conductor strain gauges. These have a Gauge Factor of 120, providing a 35 dB sensitivity improvement. Some of this advantage may be lost due to the non-linear thermal behaviour and sensitivity associated with semiconductor strain gauges. The design of a system using semiconductor strain gauges is persued in Chapter 5.

4.33 Compatibility with the Substrate

The gauge backing material and the cement must be able to operate at the anticipated temperature and strain levels. Due to the moderate temperatures encountered in the ocean, and the low strains expected due to turbulence, the specifications of standard gauges are adequate.

The temperature expansion coefficient of the strain gauge should suit the aluminium to which it is to be attached. Semiconductor strain gauges specify a thermal coefficient as an apperant strain on steel (typically +11 $\mu\epsilon$ / $^{\circ}$C). However, if the gauges are used in a full bridge configuration, or if dummy gauges are used, the arrangement is thermally compensated.

4.4 REQUIREMENTS OF THE SIGNAL PROCESSOR

It will be shown in Chapter 6.1 that the output voltage from the strain gauged bridge has a microvolt order of magnitude, which may be compared with the millivolt order of magnitude signal resulting from an equivalent force on a PZT5B piezoceramic beam. This requires careful design of the amplifier stage if an adequate SNR of the output signal is to be achieved.

The overall gain of the system will be required to be in excess of 100 dB, in order to raise the output signal to levels compatible with a data-logging system. The bridge will require a high gain, low noise instrumentation pre-amplifier in the immediate vicinity of the strain gauges and the processing electronics. This instrumentation amplifier requires a high common mode rejection ratio of the order of 110 dB, and low thermal drift characteristics to minimise the errors in the output signal caused by the electronics.

4.5 CONCLUSION

It should be possible to replace the piezoceramic beam of the current airfoil probe with semiconductor strain gauges mounted on an aluminium cantilever beam, if a high gain , low noise amplifier is used.

CHAPTER 5

DESIGN AND CONSTRUCTION OF AN AIRFOIL PROBE USING SEMICONDUCTOR STRAIN GAUGES

5.1 DETERMINATION OF THE CANTILEVER BEAM DIMENSIONS

5.11 Spatial Resolution

It has been shown (Siddon, 1971) that the airfoil probe is able to resolve wavelengths down to about four times the probe diameter. FIG. 5.1. shows the probe response ($\phi_w(S)$) plotted against Strouhal frequency (S), where $S = fd/\bar{U}$, $\bar{U}$ being the mean flow of a round jet. This can be regarded as a measure of probe diameter: wavelength ratio, d/λ . The frequency response of the airfoil probe begins to fall when d exceeds $\lambda/4$.

Osborn and Crawford show that if the transfer function of a sinewave of wavelength λ is averaged over a length L, the result is the (Sin x)/x function, with $x = \pi L/\lambda$. This relation implies that the -3 dB point is at $\lambda = 2.25L$, and the point $\lambda = 4L$ corresponds to the -1 dB point. Thus, as the cross-sectional area of the airfoil decreases, so the spatial resolution increases.

The width of the cantilever beam is ultimately limited by the width of available strain gauges. The narrowest semiconductor bending gauges that Kyowa Electronics manufacture (Kyowa are the suppliers for this project) have a backing 5 mm wide. It should therefore be possible to manufacture an airfoil having a cross-sectional diameter of 7-8 mm. This is marginally larger than the 4.7-6 mm of previous airfoil designs, but the probe will still be capable of resolving wavelengths of 3.5 cm and longer.

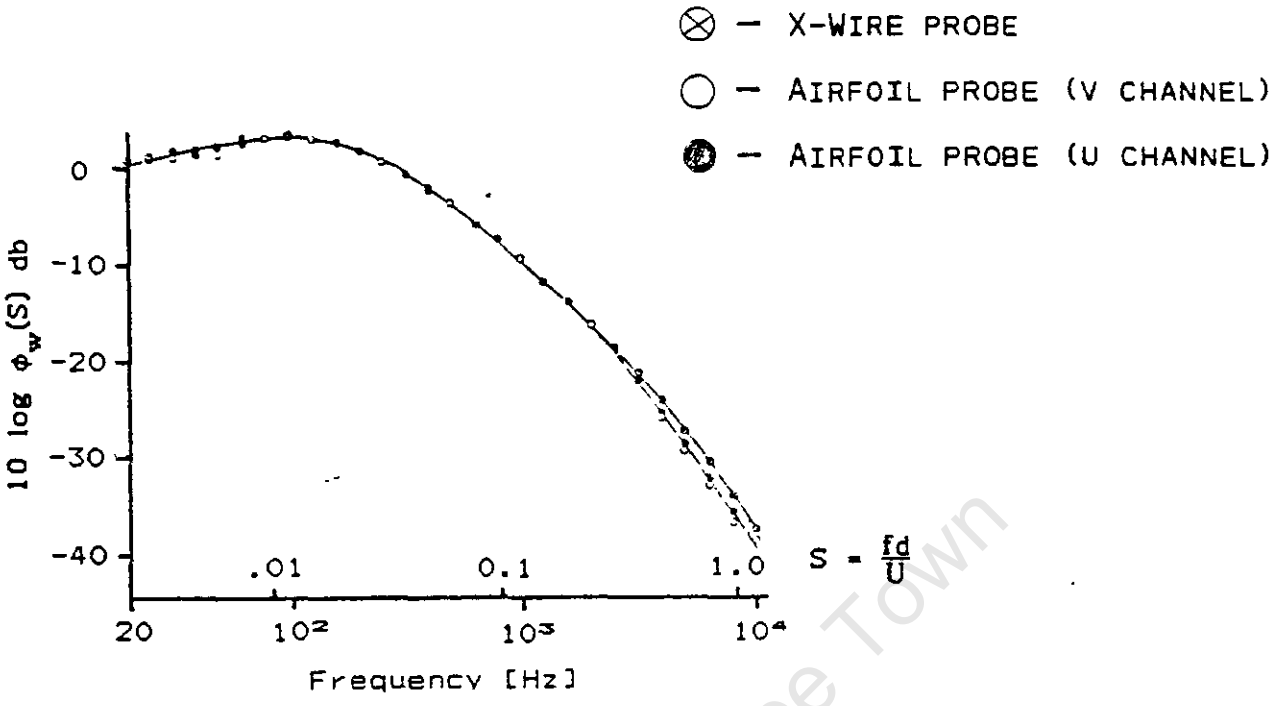

FIG. 5.1 Comparison of Turbulence Spectra as Measured with Lift Sensing Probe and X-Wire Probe (T.E.Siddon, et al, 1971).

5.12 Beam Sensitivity

5.121 The Relationship between Sensitivity and Natural Frequency

The relationship between the beam dimensions and probe sensitivity was described by Equation (2). It can be seen that the thickness of the beam is the single most significant dimension influencing beam sensitivity. If the width of the beam is set at 5 mm, as justified above, and the length is set at 20 mm (an aspect ratio comparable to other lift sensors), then the sensitivity of the probe is inversely proportional to the second power of beam thickness (h^2).

The sensitivity of the probe, however, is determined ultimately by the fundamental resonant response of the airfoil/cantilever beam combination. This can be attributed to the fact that the natural frequency of the beam becomes lower as the beam thickness is decreased. Eventually, for a thin beam, the resonant frequency encroaches into the frequency range of the expected turbulence driving signal, biasing the frequency response of the probe and contaminating the output signal.

5.122 Determining the Relationship between Beam Thickness and Natural Frequency

(i) Alternative Methods of Solution.

The problem arises in ascertaining the resonant response of the airfoil as a function of beam thickness in order to set the fundamental frequency at a predetermined value. In mechanical terms,the airfoil may be described as a complex thick beam with low aspect ratio. It does, therefore, not comply with Euler-Bernoullian beam theory, in which the shearing effects of the cantilever beam are neglected. Due to the complex nature of the beam structure (aluminium: silicone combination), the mathematical solution lies in solving the boundary conditions of a set of differential equations (Dr.H.Pierce, personal communication). This would require expert knowledge in the field of beam theory.

An alternative solution is to work on a trial and error basis, constructing probes of various thickness, and testing their response. This method is extremely costly in terms of the cost of the strain gauges and time in building probes which would later be discarded.

A feasible approach to solving the problem involves the creation of a finite element model and analysing the response using ABAQUS, a finite element analysis algorithm, in conjunction with the VAX/VMS computing system.

(ii) The Finite Element Model.

(a) General Approach to Finite Element Analysis.

A method of approaching the problem involves creating a one-dimensional beam model. The results of this analysis can be compared against the known resonant response of a prototype probe which has already been constructed. Parameters can be tuned until theory coincides with the known experimental values. The single dimensional model can be extended to a two-dimensional "beam in a plane model" which incorporates the effect of transverse shear deformation of the beam. This two-dimensional model would prove a more accurate representation of how the resonant frequency of the probe varies with the thickness of the aluminium cantilever beam.

The model is defined by representing the complex beam as a set of elements, each element approximating the physical displacement of the corresponding part of the real beam. The elements are then linked by a set of nodes which prevent the sides of neighbouring elements from separating or overlapping when the model deforms.

In the case of the cantilever beam, boundary conditions are set by fixing the appropriate nodes. The Finite Element Algorithm then requires the Elasticity, Poisson Ratio and Density (Mass) for both the aluminium and the rubber elements.

The Modulus of Elasticity of the Q3-3321 Silicone Moulding Rubber used, is 0.7 MPa at 100% elongation (Appendix 1), corresponding to Point A on FIG. 6.2 However, the Stress:Strain relationship for rubber is non-linear and has a pronounced hysterisis.

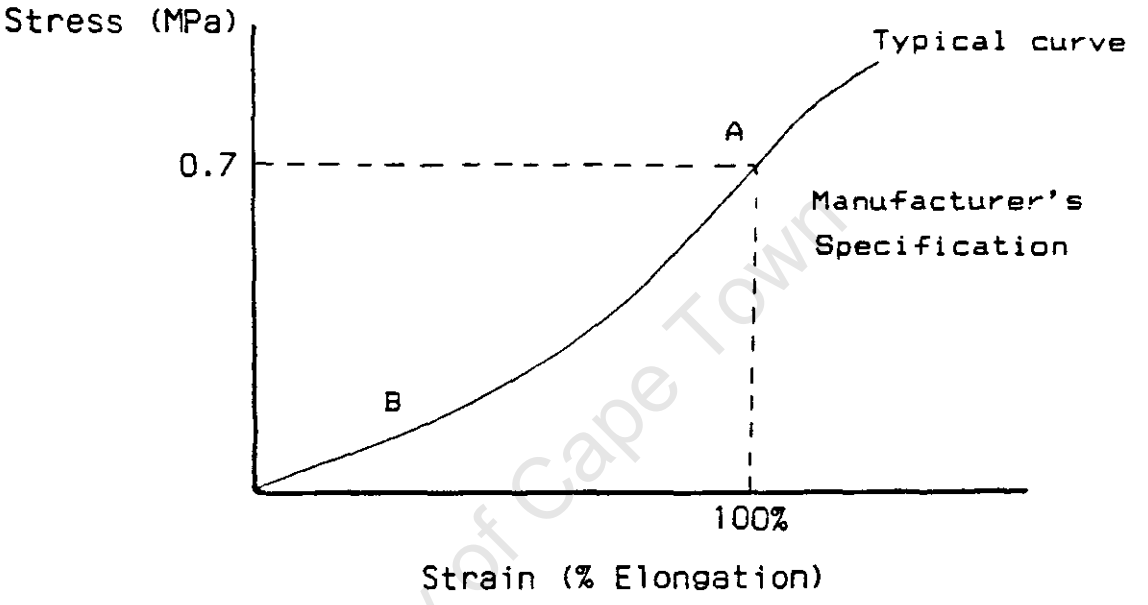

FIG. 5.2 Typical Stress:Strain Curve for Rubber.

PARAMETER	RUBBER	ALUMINIUM
Density (kg/m³)	900	2700
Poisson's Ratio	0.5	0
Young's modulus (MPa)	0.3-0.7	69 000

FIG. 5.3 Physical Properties of Composite Beam.

The Elasticity must therefore be modified to a value corresponding to a much lower strain. (In the natural frequency analysis, beam deflection is small and, therefore, very small strains are encountered). Region B on FIG. 6.2 would be more appropriate in order to estimate the Elasticity for the natural frequency calculation.

FIG. 5.3 gives the input parameters chosen for rubber and aluminium.

NOTES:

a) The Poisson's Ratio of aluminium is taken to be 0, and not it's actual value of 0.3, transverse shearing being neglected due to the high aspect ratio of the aluminium beam (less than 1 mm thickness x 20 mm length).

b) The rubber is assumed to be incompressible, with a Poisson's Ratio of 0.5. When the actual parameter is entered into the algorithm, a value of 0.499 is chosen to avoid theoretical singularities encountered in calculations involving incompressible materials.

(b) The One-Dimensional Finite Element Model.

A single line model is developed using linear Timoshenko beam elements, as shown in FIG.5.4. The aluminiumn beam is described by 4 line elements linked by 5 nodes. The elements are defined as having a rectangular cross-section. The silicone airfoil is approximated by a similar line element beam with a circular cross-section and nodes that coincide with those of the aluminium beam.

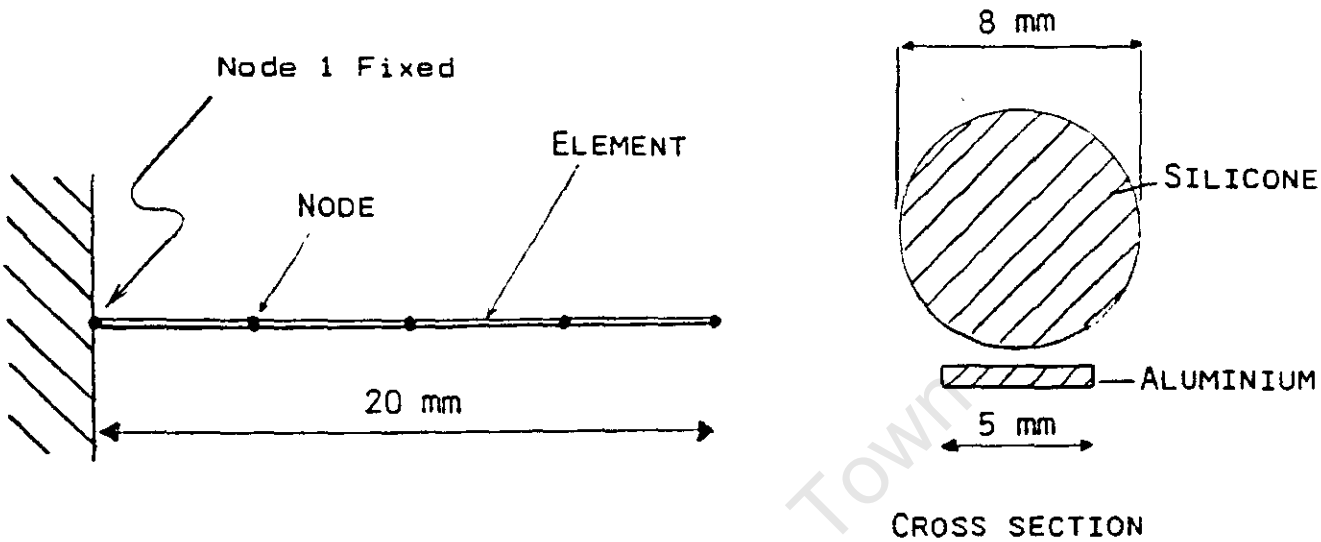

FIG. 5.4 Simple Line Element Model.

FIG. 5.5 shows the results of the analysis for the various thicknesses of aluminium. The elasticity of the silicone model was estimated at 0.5 MPa for this curve.

Point A corresponds to the calculated frequency for an input to the algorithm of 0.35 mm. A prototype probe of similar dimensions was constructed and the resonant response was found by blowing on the airfoil to obtain an approximate white noise forcing function. The output spectrum of the probe is shown in FIG. 5.6.

The resonant peak at 190 Hz is clearly visible in the plot. This should be compared with the theoretical value of 228 Hz (Point A on Fig. 5.5.) obtained using

Finite Element techniques. The discrepancy between the two values may be attributed to the Euler-Bernoullian assumptions used in the analysis of the line element model.

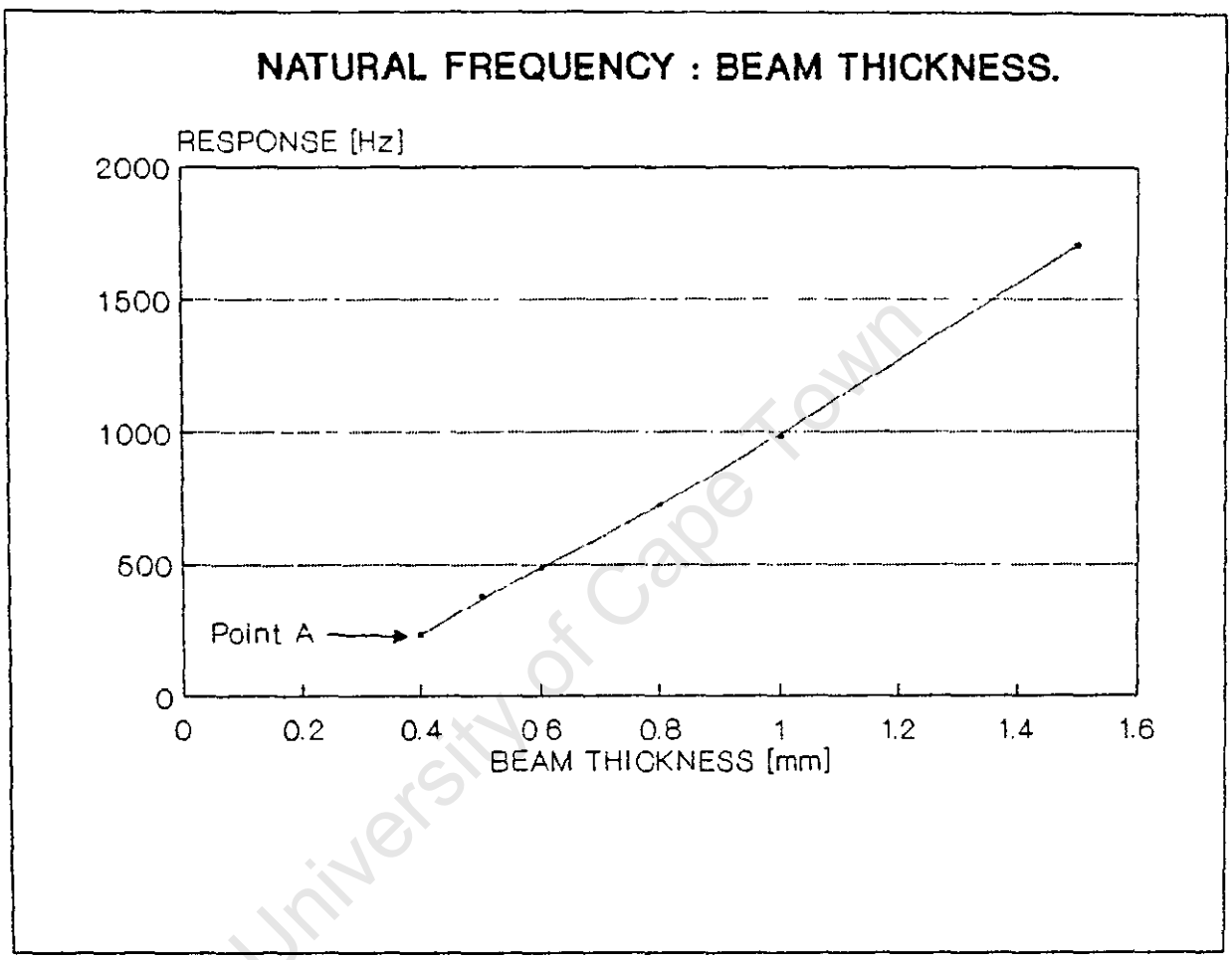

FIG. 5.5 Variation of Natural Frequency with Beam Thickness - 1ᴾ Model.

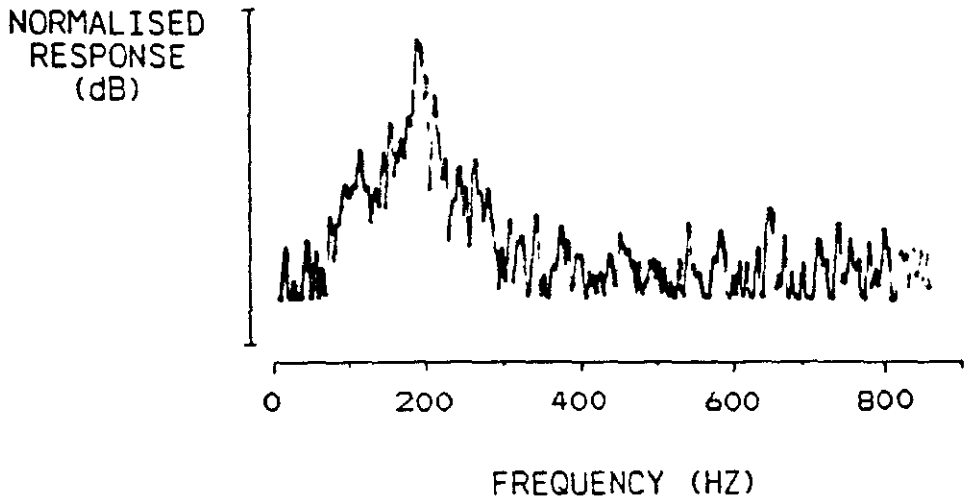

FIG. 5.6. Resonant Response of Prototype Airfoil Probe.

(c) Conclusion.

FIG. 5.5. allows a reasonable prediction of the resonant behaviour of the probe as the aluminium beam thickness increases. The resultant curve is adequate for the order of magnitude approximation required, and time did not permit a two-dimensional analysis.

5.123 Determination of the Desired Beam Thickness

Now that an estimate of the resonant behaviour is known, it is possible to set the natural frequency to a predetermined value. This value can be decided once the frequency range of the expected turbulence driving signal is known.

A typical airfoil probe (Lueck et al, 1981) is able to resolve spatial frequencies of the order of 100 Cycles per Meter (cpm), as shown in FIG. 5.7. The time-dependant frequency is obtained by multiplying this resolution by the expected fall speed of the probe.

Fall speeds of previously designed airfoil probes have varied between 0.5 ms^{-1} for retrievable instruments (N.S.Oakley, 1977) to as fast as 3 ms^{-1} for XDP instruments (Lueck et al, 1984).

Thus, if a fall speed of 1 ms^{-1} is selected, the frequency response of the probe should be flat up to 100 Hz.

Finally, evaluating this in terms of required beam thickness, FIG.5.5 shows that the beam will need to be at least 1 mm thick in order to keep it's natural frequency one order of magnitude higher than the expected 100 Hz driving signal.

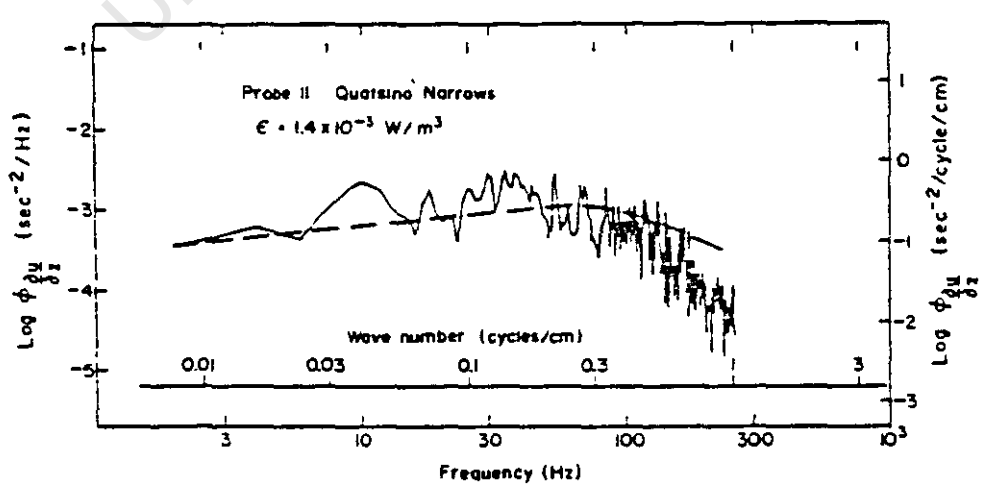

FIG. 5.7 Spectrum of Shear Signal
(R.G.Lueck and T.R.Osborn, 1981). /36

5.2 STRAIN GAUGE BRIDGE CRITERIA

5.21 Configuration for Maximum Sensitivity

The placement position of the strain gauges on the cantilever beam is shown in FIG. 4.1. In order to obtain maximum sensitivity from this arrangement, two strain gauges must form an active half-bridge, as shown in FIG. 5.8.

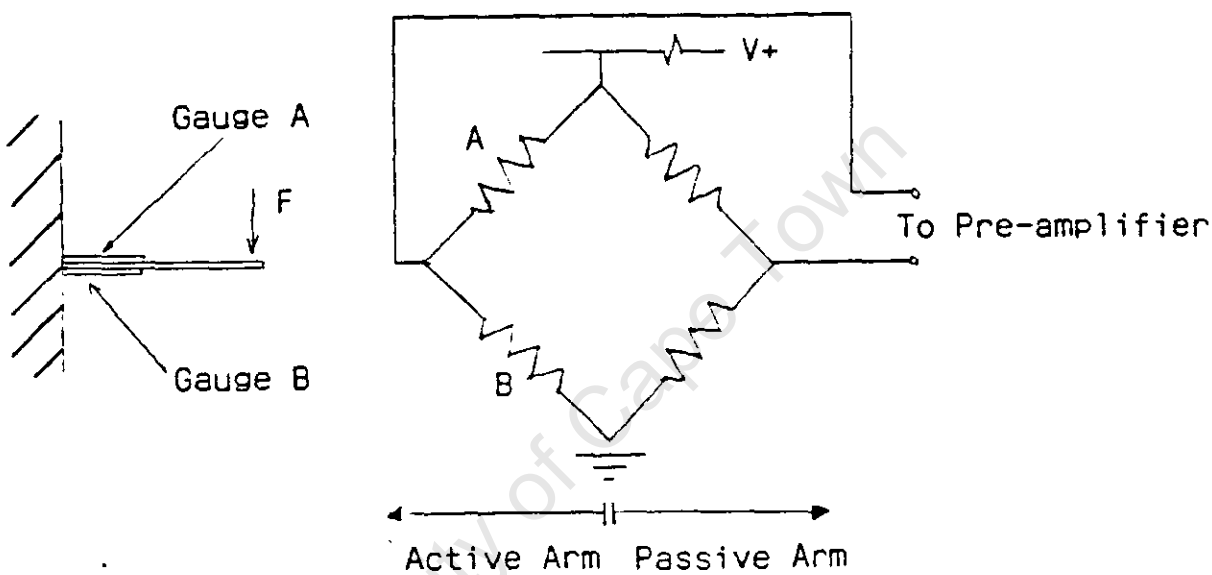

FIG. 5.8 Active Half-Bridge Configuration.

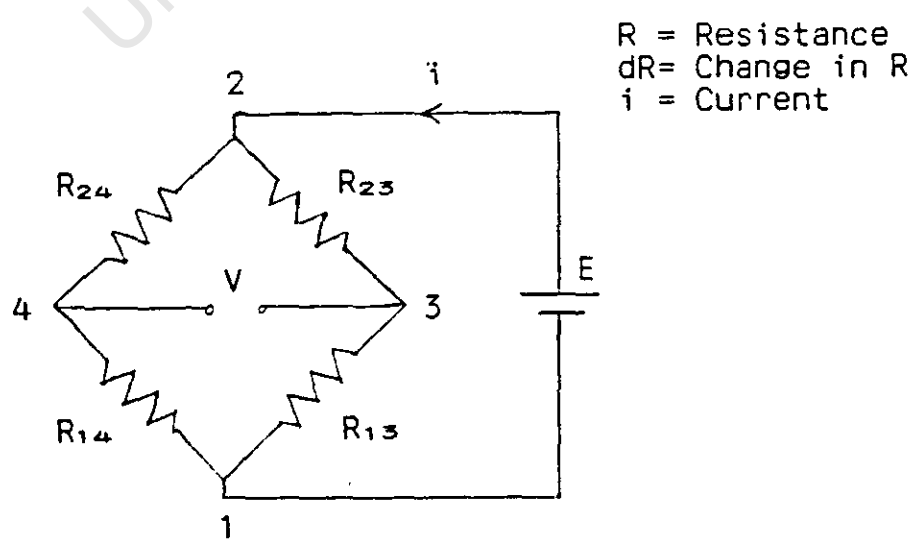

FIG. 5.9 Bridge Circuit.

The output voltage (V) from a bridge excited by a voltage (E) may be derived from the circuit in FIG. 5.9 as follows:

$$i_{241} = \frac{E}{R_{24} + R_{14}} \quad \ldots\ldots (4)$$

$$= \frac{E}{(R + dR) + (R - dR)} \quad \ldots\ldots (5)$$

$$= \frac{E}{2R} \quad \ldots\ldots (6)$$

$$V_{24} = i_{241} R_{24} = \frac{E}{2R} (R + dR) \quad \ldots\ldots (7)$$

$$V_{23} = \frac{E}{2} \quad \ldots\ldots (8)$$

$$\text{so } V_{43} = \frac{E}{2} - \frac{E}{2R} (R + dR) \quad \ldots\ldots (9)$$

$$= \frac{E\ dR}{2R} \quad \ldots\ldots (10)$$

5.22 Thermal Stability of the Bridge

5.221 The Active Arm

If the active strain gauges are well matched and experience an identical resistance change due to a given thermal gradient, there will be no apparent strain at the bridge output due to thermal drift. Furthermore, as long as the gauges are matched, expansion of the aluminium beam due to heating will cause the same apparent strain on both gauges, thus negating the resultant output drift.

5.222 The Passive Arm

Experience has shown (I.C.Main, 1987) that if the passive arm (FIG. 5.8) is made of carbon resistors, significant drifting occurs at the bridge output, as the bridge heats up. This can be attributed to uneven heating of the resistors due to mismatching and thermal variations within the physical layout of the bridge.

This effect can be minimised by replacing the resistors with compensation strain gauges mounted in close proximity, so that they experience the identical thermal variations.

5.223 Interconnecting Leads

It is important to ensure that the leads between the strain gauges and the bridge nodes are as short as possible to prevent spurious signals due to electronic noise and temperature-induced resistance changes.

The lead length can be minimised by mounting the passive compensation gauges on the aluminium beam immediately behind the active gauges (in the epoxy anchor). This has the added advantage of ensuring that all the gauges experience similar thermal conditions.

5.23 Balancing the Bridge

The traditional method of balancing a strain gauge bridge under no-load conditions, is shown in FIG. 5.10. A potentiometer is used to zero the effects of uneven potential divider ratios between the two arms.

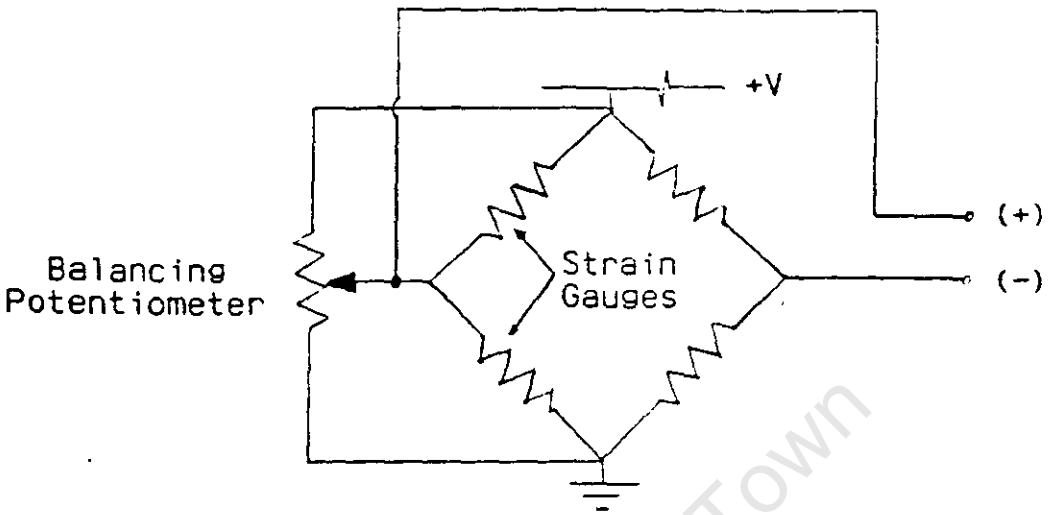

FIG 5.10 Traditional Bridge Balancing Technique.

This method was used by I.C.Main (1987) in a prototype design and was found to be most unsatisfactory. The bridge required continuous tuning due to thermal drift, as well as unbalancing caused by any permanent deformation of the cantilever beam.

This problem was solved by decoupling the bridge from the preamplifier of the transducer. This is justifiable for a few reasons:

a) The low frequency resolution of the probe is, in any event, restricted to a factor determined by the length of the vehicle housing the probe.

The airfoil will not be capable of resolving wavelengths longer than the length of the vehicle, because longer wavelengths advect the vehicle, changing it's angle of attack and making the sensitivity of the shear probe unpredictable. (Lueck et al, 1984).

b) The low frequency response of the instrument is likely to be affected by the thermal characteristics of the electronics and spurious signals due to any mismatch in the strain gauges.

c) Any D.C. signal output from the bridge would be the result of a constant transverse force on the beam caused by viscosity effects on an axially misaligned probe. This signal is not necessary in the evaluation of the velocity shear, which may be described as the derivative of the transverse force on the beam.

5.3 DESCRIPTION OF AIRFOIL PROBE

An airfoil probe was constructed using two KSP-2-E4 semiconductor strain gauges (Kyowa Electronics, Japan) mounted on an aluminium beam 1 mm thick (as justified in Chapter 5.123), 5 mm wide and 80 mm long. Two aluminium compensated conventional foil gauges (KFC-2-C1-23) were mounted on the beam, inside the probe as the compensating passive arm of the strain gauge bridge. A longitudinal view through the probe is given in Appendix 23. The silicone airfoil was moulded from Dow Corning Q3-3321 RTV High Strength Mouldmaking Rubber (Appindix 1). The active length of the cantilever beam is 20 mm and the cross-sectional diameter of the airfoil is 8 mm. The method used to construct the probe is described by I.C.Main (1987).

CHAPTER 6

DESIGN OF THE PROCESSING ELECTRONICS

6.1 GAIN REQUIREMENTS OF THE PROCESSOR

In order to establish the gain required to amplify the expected bridge output signal to levels compatible with the data-logging system, the magnitude of the transverse force on the beam needs to be determined. This requires an estimate of the order of magnitude of the transverse component of the turbulent velocity flow.

The instantaneous cross force (F_p) caused by potential flow on a slender body of revolution, has been described by Allen and Perkins (1952) as:

$$F_p = \rho A V u \qquad \ldots\ldots (11)$$

where ρ is the fluid density, A is the cross sectional area of the probe, V and u are the axial and transverse components of velocity, respectively.

The diameter of the airfoil probe has been set at 8 mm to allow for the 5 mm width of the aluminium beam and the surrounding brass casing. This corresponds to a cross sectional area of 5×10^{-5} m^2. It was established in 5.123 that the fall speed of the vehicle housing the probe will be 1 ms^{-1}. This corresponds to the (V) component of the velocity.

It is difficult to estimate the transverse component of velocity (u) by examining typical shear profiles, as in FIG.2.1. However, it is evident that the resolution of the various instruments described in Chapter 3 varies between 1 and 10 mm s^{-1}.

The resultant cross force (F_p) is calculated by substituting these estimates into Equation (11). It may be seen that the the above velocities correspond to cross forces of between 50 μN and 0.5 mN on the probe.

The resultant strain on the cantilever beam is calculated using Equation (2). The beam dimensions derived in Chapter5 (l = 20 mm, w = 5 mm and h = 1 mm) are used in (2) with the values of F (the cross force) calculated above. These forces result in strains of between 0,017 με and 0,17 με .

Using Equations (3) and (10), it is possible to predict the output signal (V_{out}) from the strain gauge bridge, knowing that strain magnitudes of between 0,01 με and 0,1 με can be expected.

Recalling Equation (3),

$$G = \frac{dR}{\epsilon R}$$

and from Equation (10),

$$V_{out} = \frac{E}{2} \times \frac{dR}{R}$$

Substituting, $$V_{out} = \frac{E}{2} \times G \times \epsilon \qquad \ldots\ldots (12)$$

Semiconductor strain gauges have a maximum current rating of 20 mA. Therefore, for a specified gauge resistance of 116 Ω and a bridge excitation voltage (E) of 3 volts, the resultant current through each strain gauge will be 13 mA, well within the rated value.

Thus, for an airfoil probe utilising conventional strain gauges with a gauge factor (G) of 2.1, results in a bridge output voltage of:

$$E \approx 0.05 \rightarrow 0.5\ \mu V$$

and, for a probe using semiconductor strain gauges, with a gauge factor of 120, the resultant output voltage is:

$$E \approx 1 \rightarrow 10\ \mu V$$

It may be concluded that in order to amplify the output signal to 1 Volt, a signal comparable to the full scale input voltage of the data logger, the processor requires an amplification of about 126 - 146 dB for the case of a probe using conventional strain gauges, and about 100 - 120 dB for the semiconductor probe.

6.2 BANDWIDTH REQUIREMENTS OF THE AMPLIFIER

6.21 The High Frequency Band Limit

It has been established in Chapter 5.11 that the spatial resolution of the airfoil probe is limited to 4 times the probe diameter, corresponding to a resolution of 32 mm for the strain gauge probe being developed. This requires an amplifier with a flat response to a frequency of 32 Hz, if the vehicle housing the probe is to be deployed at a fall speed of 1 ms^{-1}. However, to allow for variations in fall speed, and the possible construction of smaller probes with significantly higher spatial resolution, the processor will be designed with a frequency response flat to 100 Hz. A cut-off frequency higher than this would require a correspondingly higher sampling frequecy, resulting in inefficient use of the memory of the data logger.

6.22 Determination of the Low Frequency Cut-off Point

In Chapter 5.23 it was established that the easiest method of balancing the strain gauge bridge was to limit the low

frequency response of the probe, motivated by the fact that the low frequency behaviour of the probe deviates from the predictable airfoil theory.

A suitable cut-off frequency must be determined which will restrict electronic and thermal drift without damping the signal which contains low frequency information useful in the analysis of the turbulence spectrum. If, for example, the low frequency response of the probe is limited to 1 Hz, the corresponding low frequency resolution of the vehicle/airfoil probe combination is 1 cpm. Resolving longer wavelengths would require a vehicle longer than the 1 meter long vehicle available, due to the tilt effects mentioned in 5.23 (a). Also, variations on wavelength scales of larger than 1 meter may be classified within the ocean fine structure, as described in Chapter 2, and become less important when analysing the turbulent microstructure.

6.3 DESIGN OF THE PRE-AMPLIFIER STAGE

6.31 Determination of a Suitable Amplifier Configuration

It has been suggested (Horowitz and Hill) that the best method of achieving the high CMRR required in the case of a strain gauge bridge amplifier, is to use the classical instrumentation amplifier, as shown in FIG. 6.1.

The prototype probe constructed by I.C.Main (1987) utilized this configuration, but due to the high gain demand of the system, the amplifier was found to have a poor noise performance.

Subsequently, the performance of an instrumentation amplifier using micropower OP220 and OP20, shown in FIG. 6.2, has been compared with the performance of a relatively new (1987) precision operational amplifier, the LM607C

(Data Sheet - Appendix 2), configured as differential amplifier, as shown in FIG. 6.3.

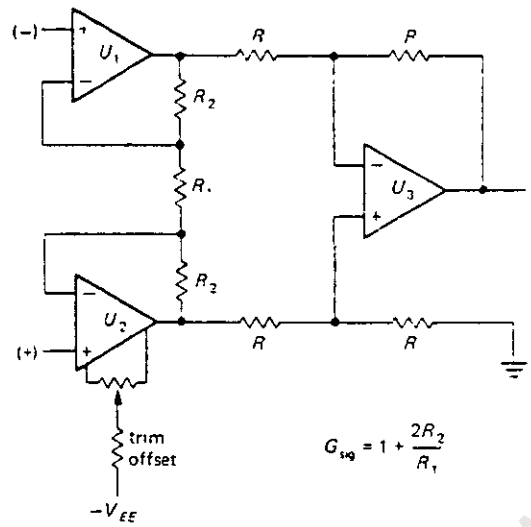

FIG. 6.1 Classical Instrumentation Amplifier.
(From Horowitz and Hill " The Art of Electronics ")

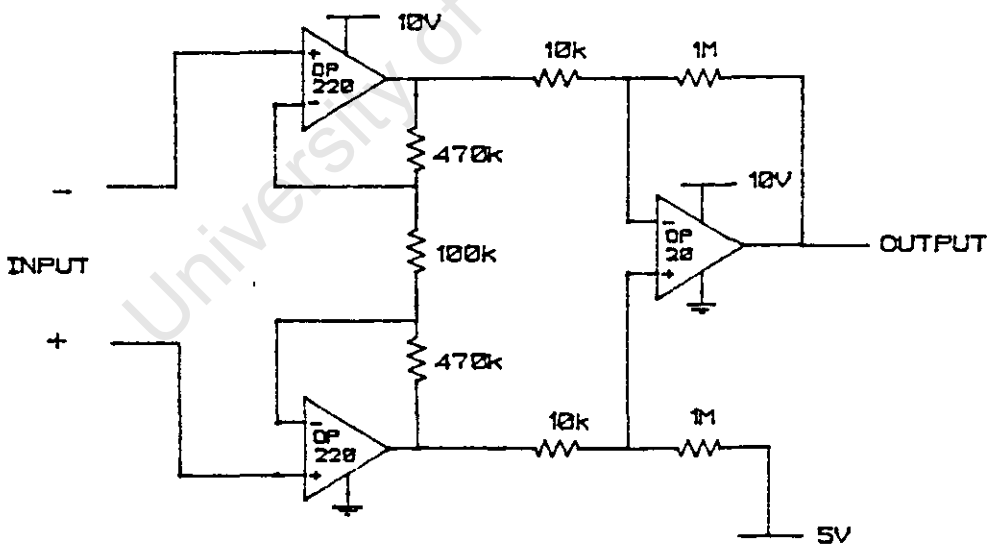

FIG. 6.2 Instrumentation Amplifier
using Micropower Components.

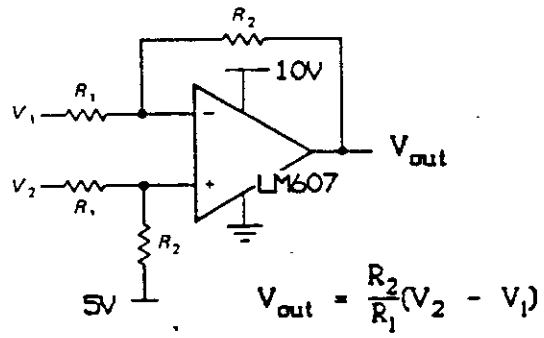

FIG. 6.3 LM607 Op-Amp Configured as a Differential Amp.

Both circuits were constructed using identical gain characteristics (60 dB), bandlimited by a first order low pass filter with f_{3dB} = 267 Hz. The differential inputs were tied together, and the outputs compared as follows:

	Output Noise (V_{rms})
Instrumentation Amp.	8.5 mV
Differential Amp.	3.6 mV

This demonstrates that the LM607 offers an advantage of more than 3 dB in Noise Power. The specified input offset voltage drift of both systems is of the same order of magnitude (1 $\mu V\ ^{o}C^{-1}$). Thus, the LM607 is the more attractive preamplifier alternative

An alternative device worth considering is the LM163 Precision Instrumentation amplifier which offers the classical instrumentation amplifier arrangement as a single integrated circuit. The specifications of the LM163 are compared with those of the LM607 in FIG. 6.4.

CHARACTERISTIC	UNITS	LM 607 Op-Amp	LM 163 Instr-Amp
Supply Range	V	3- 18	5- 18
Gain		variable	10,100,1000
CMRR-typical	dB	140	130*
CMRR-minimum	dB	110	120
Input Bias Current	nA	10	5
Input Offset Current	nA	0.5	1
Input Noise Voltage (0.1-10Hz)	μV_{p-p}	0.2	0.4*
Input Current Noise	pA_{p-p}	14	40
Slew Rate-typical	$V/\mu s$	0.7	1*
Input Offset Voltage Drift	$\mu V/^{o}C$	0.2	0.2** 10***

* For fixed gain: G=500,1000
** For fixed gain: G=500
*** For programmable gain: G=1000

FIG. 6.4 Comparison of LM163 Instrumentation and LM607 Operational Amplifiers.

It can be seen that the new generation of operational amplifier (LM607 - 1987) has characteristics comparable to those of the more dated (LM163-1983) instrumentation amplifier. The LM 607 has a typical CMRR 10 dB higher than that of the LM163, the advantage of continuously variable gain, lower input current noise and a wider supply range.

These factors, along with it's smaller size (easing the design for a preamplifier in the immediate vicinity of the strain gauge bridge) and lower price, all contribute to

the justification of the use of the LM607 as the preamplifier stage of the turbulence transducer.

6.32 Theoretical Description of Pre-Amplifier Stage

6.321 Magnitude Response

The LM607C Pre-amplifier circuit is shown in Appendix 3 The circuit may be analysed as follows:

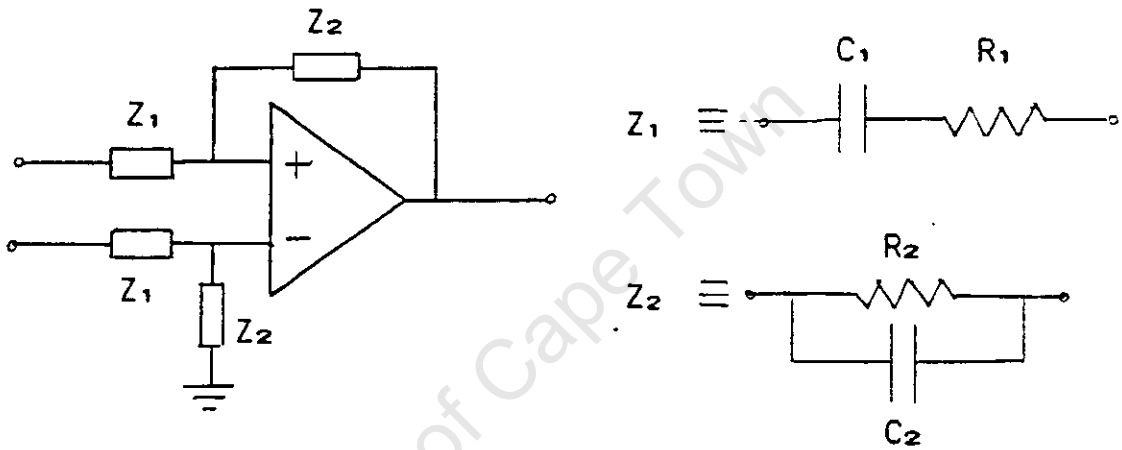

$$Z_1 = \frac{(\omega R_1 C_1)^2 + 1}{C_1} \qquad \ldots\ldots (13)$$

$$Z_2 = \frac{R_2}{\sqrt{(\omega R_2 C_2)^2 + 1}} \qquad \ldots\ldots (14)$$

For a differential amplifier,

the Magnitude Response $= \frac{Z_2}{Z_1}$ $\qquad \ldots\ldots (15)$

$$= \frac{\omega R_2 C_1}{\sqrt{[(\omega R_2 C_2)^2 + 1]\ [(\omega R_1 C_1)^2 + 1]}} \qquad \ldots\ldots (16)$$

The circuit, with component values as depicted in Appndx 3, is a band pass filter with a high frequency cut-off point f_{3dB} = 132 Hz.

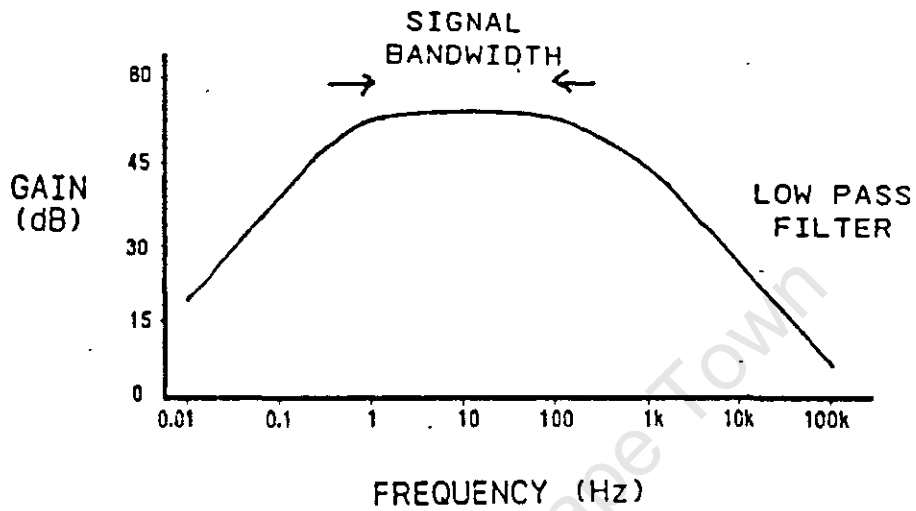

FIG. 6.5 Magnitude Plot of the Pre-Amplifier Response.

6.322 Phase Response

The phase response of the turbulence channel is immaterial. This is because there is no correlation between phases at different wavenumbers; therefore, meaningful statistical quantities are not affected by a variation of phase shift with frequency. (P.Bradshaw, 1971, p.145)

6.4 SIGNAL CONDITIONING AND STORAGE

6.41 Introduction

The low impedance signal from the pre-amplifier situated

immediately behind the airfoil probe in the nose of the vehicle is fed via a screened cable to the conditioning circuit board in the data logger.

The signal is differentiated, filtered, calibrated and sampled as an 8 bit data stream before being stored in a RAM memory module. This section discusses the characteristics of each of the stages mentioned.

6.42 The Differentiator Stage

The output signal from the strain gauge bridge, and hence the pre-amplifier, is a measure of the instantaneous cross-force on the aluminium cantilever beam corresponding to the instantaneous transverse component of velocity. In order to interpret the signal as a velocity shear (shear being the rate of change of instantaneous velocity), it must be differentiated over the bandwidth of interest. The circuit chosen (Appendix 4) has unity gain at 1 Hz, with a gain of 6 dB/octave from DC to 200 Hz. The 1 nF capacitor is included to roll off the gain above 1 kHz, reducing the high frequency noise associated with differentiators. The magnitude plot of the differentiator response is shown in FIG. 6.6.

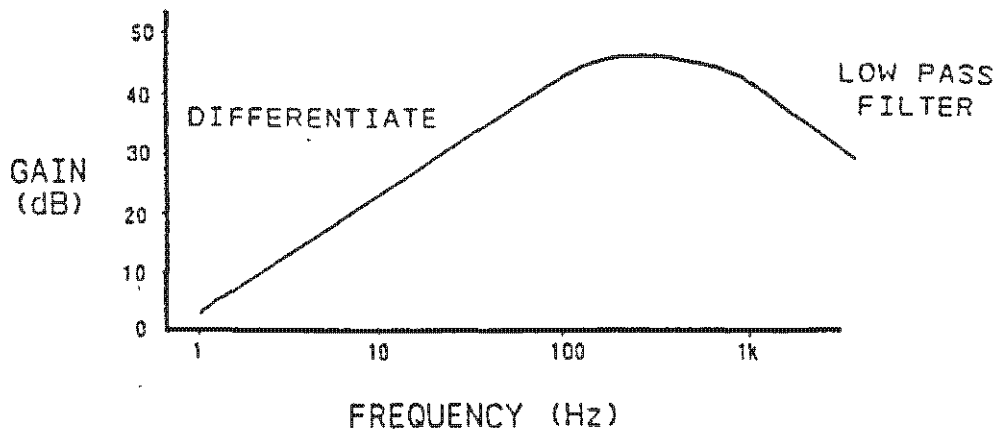

FIG. 6.6 Magnitude Plot of Differentiator.

6.43 The Filter Stage

The output of the differentiator is fed into a low pass anti-aliasing filter, which must be included before the signal can be sampled. To achieve maximum efficiency from the RAM module, the sampling frequency should be as low as possible. Using a fourth order elliptic filter with 0.5 dB ripple in the passband, the signal can be damped by 50 dB between the cut-off frequency (100 Hz) and a specified stop-band frequency of 250 Hz.
The procedure for designing the filter using an MF10 switched capacitor filter is given in Appendix 5, with the resulting circuit illustrated in Appendices 6a and 6b.

The steep roll-off of the filter is necessary to prevent aliasing caused by the sharp resonant peak expected near 1 kHz. The magnitude plot of the filter is shown in FIG. 6.7.

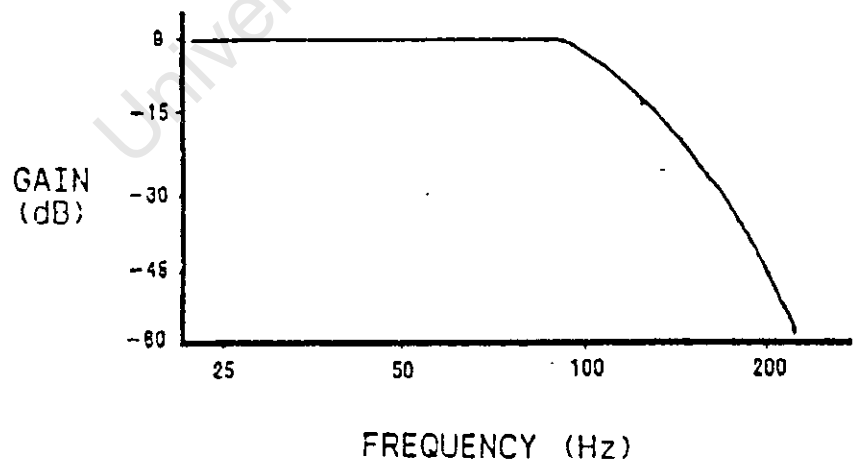

FIG. 6.7 Magnitude Plot for 4th Order Elliptic Filter.

6.44 The Calibration Stage

This final gain stage, shown in Appendix 7, is included to ensure that the full scale output from the turbulence channel is compatible with the full scale range of the A/D converter of the data logger. The various selectable gains are determined when the probe is calibrated (Chapter 8) and during field testing where the exact magnitude of the velocity fluctuations encountered by the probe become evident.

A DC shift potentiometer is included in the circuit to bias the input signal of the A/D to exactly the middle of the digital range.

6.45 The Sampling Procedure

It was established in 6.43 that the turbulence channel has a specified stop-band frequency of 250 Hz. The sampling theorem then dictates a sampling frequency of:

$$f_s = 2f_{stop\ band} \qquad \ldots\ldots (17)$$
$$= 500\ Hz$$

The data logger has been programmed to sample the turbulence channel at 500 Hz, multiplexing the signal with the two other channels, pressure and temperature, each sampled at 2 Hz to ensure adequate data to determine comprehensive profiles of the respective channels. (At this stage, a temperature transducer has not been included on board the vehicle - this profile can be constructed from a separate XDP trace).

6.46 The Storage Module

The three channels are multiplexed and stored as an 8 bit data stream in 512 kB of static RAM of a data logger

designed and programmed by the CSIR Division of Earth and Marine Sciences at Stellenbosch (Appendix 17). The sampling and storage is controlled by a Motorola MC146805 microprocessor, and two 2716 Eprom devices.

6.5 DESCRIPTION OF THE REQUIRED POWER SUPPLIES

The data logger is powered by a 6V lead-acid battery. The turbulence channel conditioning circuitry requires a stable 10V supply. This is achieved by using the Maxim 630 5-15V DC-DC convertor, as shown in Appendix 8. This voltage is then regulated at 10V, using a Ref 01 regulator with current boost, as shown in Appendix 9. A 5V rail is supplied, using the Ref 02 precision regulator, as shown in Appendix 10.

It was established in Chapter 6.1 that the strain gauge bridge requires a regulated 3V supply. This driver should be capable of supplying 26 mA and a stable voltage is essential to minimise spurious signals within the bridge. The precision 3V strain gauge bridge driver is shown in Appendix 11.

6.6 SHIELDING REQUIREMENTS

Due to the high gain requirements of the turbulence channel bridge amplifier, correct shielding of the system is critical. A schematic of the shielding arrangements is shown in FIG. 6.8.

Essential characteristics of this arrangement include:

a) Avoidance of possible paths for current loops within the shielding system, by ensuring that all ground planes are connected to earth at one point only.

b)Avoiding the use of the shield as the return path for any electrical signal.

c)The use of shielded cable between transducers and the processor.

d)Grounding the aluminium cantilever beam .

e)Using a double-sided printed circuit board having a ground plane on the component side.

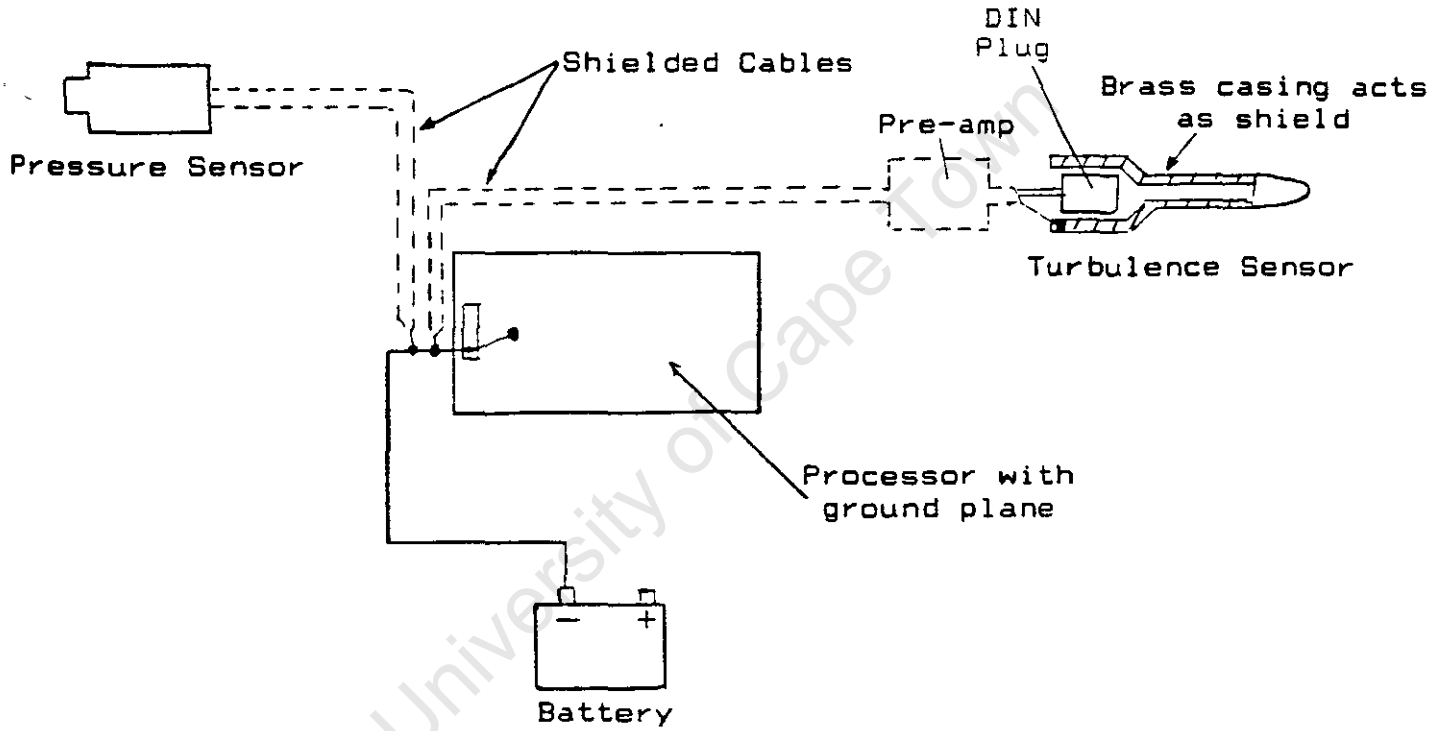

FIG. 6.8 Electronic System Shielding Schematic.

CHAPTER 7

SIGNAL PROCESSING OF THE TURBULENCE DATA

7.1 OBJECTIVES OF SIGNAL PROCESSING

Most of the theoretical work on turbulence (eg: P.Bradshaw, 1971) is concerned with the behaviour of wavenumber spectra and with the transfer of turbulent energy from low wavenumbers to high wavenumbers. Although the physics of turbulent dissipation is beyond the scope of this thesis, the wavenumber spectrum resulting from probe excitation is crutial in evaluating the probe performance. This spectrum gives an indication of the response of the system to excitation at various wavenumbers (laboratory turbulence simulation) and it is necessary in ascertaining whether results are contaminated through natural vibration of the probe and it's supporting vehicle, or aliasing of the sampled signal.

Therefore, the data generated by the turbulence probe should be transformed into a power spectrum displaying the spectral density, $\phi(\omega)$ as a function of radian frequency, ω .A second simple transformation, discussed in Chapter 8.5, may be used to transfer the frequency spectrum to a wavenumber spectrum with $\phi(k)$ as a function of the wavenumber, k. This power spectrum, in conjunction with a time dependant shear trace (FIG. 2.1), may be used by oceanographers to analyse energy dissipation as a result of microstructure turbulence.

7.2 POWER SPECTRAL ESTIMATION

7.21 Classification of the Turbulence Signal

In order to find the optimum spectral estimation algorithm, Geckinli and Yavus (1983) suggest that a physical signal may be classified as one of the following:

a) A Finite Energy Signal.
b) A Periodic or Periodic-like Signal.
c) A Stationary Random Process.
d) A Non-Stationary Random Process.

A full description of each category is given by Geckinli and Yavus in their book entitled "Discrete Fourier Transform and it's Application to Power Spectra Estimation". The shear trace defined by the airfoil probe is a long duration physical signal with time varying features. Analagous to a speech signal, the shear trace cannot be assumed to be Finite energy in nature, Periodic, or the outcome of a Stationary process; it therefore fits into the fourth category.

The signal, x(t) therefore has an average autocorrelation function:

$$R_{av}(\tau) = \lim_{B\to\infty} \frac{1}{2B}\int_{B}^{B} E\{x(t+\tau)x^*(t)\}\, dt \qquad \ldots\ldots (18)$$

where 2B is the record length, τ is the correlation lag and E{ } denotes the ensemble average. The average power spectrum $S_{av}(f)$ is then given as:

$$S_{av}(f) = \int_{-\infty}^{\infty} R_{av}(\tau)e^{-j2\pi f\tau}d\tau. \qquad \ldots\ldots (19)$$

ie: $S_{av}(f)$ is the Fourier transform of $R_{av}(\tau)$.

If it is assumed that the time-averaged autocorrelation of the process is equal to the time-averaged autocorrelation of any of it's outcomes, then Equation 18 becomes:

$$R_{av}(\tau) = \lim_{B\to\infty} \frac{1}{2B}\int_{B}^{B} x(t+\tau)x^*(t)\, dt \qquad \ldots\ldots (20)$$

In practice, 2B is finite, covering all time varying features, and $R_{xx}(\tau)$ may be calculated for finite lag values truncated to the interval $|\tau| \leq \tau_m$. For stability of the spectral estimate, $\tau_m \ll B$.

7.22 Direct Spectral Estimation Using the Welch Method

7.221 Welch's Algorithm

The Welch method of power spectral estimation is well described by C.H.Chen (1982). A brief summary of the algorithm follows:

The spectral components, $\hat{S}_i(\omega)$, of an N point data sequence, windowed by a windowing function W_n may be estimated using:

$$\hat{S}_i(\omega) = \frac{1}{N} \sum_{n=0}^{N-1} | x_{n+iN} W_n e^{-j\omega n} |^2. \qquad \ldots\ldots (21)$$

This algorithm gives spectral estimates at frequencies:

$$f = \frac{k}{N\Delta t} \qquad [k = 0, \pm 1, \pm 2, \pm 3, \ldots \pm\frac{N}{2}] \qquad \ldots\ldots (22)$$

If N is selected to be 2048 (suitable for a 1024 point Fast Fourier Transform) and a sampling frequency of 500 Hz is used (Equation 17), then the resultant spectral resolution is 0.244 Hz.

7.222 Selection of a Suitable Data Window

C.H.Chen (1982) demonstrates the smearing effect of a variety of simple data windows on an input signal comprised of 2 sinusoids and random noise. He then shows that for a poor SNR, the Hanning window is the most effective window for preserving the sinusoidal peaks.

During probe calibration, the probe is stimulated by a sinusoidal forcing function, and preservation of the resultant spectral peak is important. Thus, a Hanning window is well justified. Furthermore, the spectrum shown in FIG. 5.8 (R.G Lueck and T.R.Odborn, 1981) has been derived using a Hanning window. If that spectrum is to be used as a comparison with resultant spectra from the strain gauge probe, both estimates should be derived through the same procedure

For a record length NT, the Hanning window is defined as:

$$W(t) = \begin{cases} \frac{1}{2}(1 + \cos\frac{2\pi t}{NT}) & |t| < \frac{NT}{2} \\ 0 & |t| > \frac{NT}{2} \end{cases} \quad \ldots\ldots (23)$$

7.223 The Use of a Spectral Window

If the direct method of power spectral estimation is used, the autocorrelation is estimated over an interval $|\tau| \leq T$, where T is the length of the process. The resultant spectrum has a variance inversely proportional to T.

This variance could be reduced by circularily convoluting the spectral estimate (resulting from Equation 21) with a spectral window. However, if the average of many spectral estimates is to be taken, as is the case with a shear trace, there is no need for a spectral window (N.C.Geckinli and D.Yavus, 1983) as the process of averaging reduces the variance.

7.3 PROCESSING THE TURBULENCE DATA IN THE TIME DOMAIN

The output signal from the turbulence channel is directly proportional to the turbulent velocity shear. Therefore, this data may be presented directly, once the coefficient relating the system output voltage to the velocity shear is known.

CHAPTER 8

CALIBRATION OF THE STRAIN GAUGE AIRFOIL PROBE

8.1 OBJECTIVES OF THE CALIBRATION PROCEDURE

The calibration procedure is aimed at describing the system output (e_o), shown in FIG.8.1, in terms of a known, controllable, driving shear (du/dt).

The effects of temperature and pressure fluctuations on the probe sensitivity should be determined, along with an investigation into the effect of angle of attack on the calibration coefficient. The electronic noise generated by the system must be described in terms of RMS shear, if the system performance is to be compared effectively with the performance of other airfoil probes. Finally, the theory supporting the time dependant turbulence simulation in the calibration situation should be modified so that it may be applied to the spatial dependant shear (du/dz) encountered in the field.

8.2 THEORETICAL RESPONSE OF THE AIRFOIL PROBE TO TRANSVERSE VELOCITIES

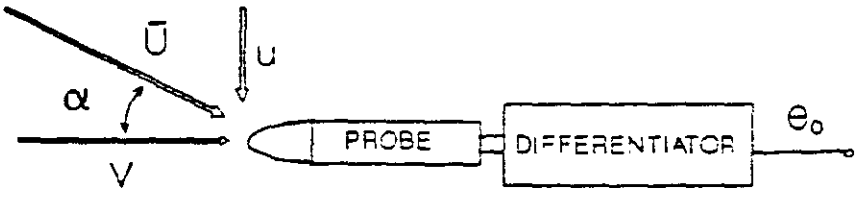

FIG. 8.1 Definition of Coordinate System Relative to the Probe Alignment.

The probe may be described as an axis-symmetric airfoil of revolution mounted so that the mean velocity ($\bar{V}$) is aligned with the axis of revolution (FIG. 8.1).

Allen and Perkins describe the cross force (f_p) for a slender, inlclined body of revolution in an inviscid flow of speed ($\bar{U}$) and angle of attack (α), which is assumed to be small, as:

$$f_p = \frac{1}{2} \rho \bar{U}^2 \frac{dA}{dx} \sin 2\alpha \qquad \ldots\ (24)$$

where ρ is the fluid density, and $\frac{dA}{dx}$ is the rate of change in body cross-sectional area longitudinally along the probe. (In this discussion, it is the cross force which is perpendicular to the airfoil, not the lift force which is perpendicular to the mean velocity vector, that is being analysed. Siddon et al (1965) give a derivation involving the lift force).

Equation (24) is correct to the second power in α in an inviscid flow. The total cross force exerted on the probe (F_p) is derived by Osborn et al (1980) by integrating (24) along the length of the probe from it's tip, where A=0, to it's base, where dA/dx=0:

$$F_p = \int f_p \, dx \qquad \ldots\ (25)$$

$$= \tfrac{1}{2}\bar{U}^2 \rho A \sin 2\alpha \qquad \ldots\ (26)$$

Using the double angle relation for sin 2α :

$$F_p = \rho A V u \qquad \ldots\ (27)$$

There is a second cross force, F_v, due to viscous effects, which is proportional to the square of the cross-stream velocity:

$$F_v = B \cdot \frac{1}{2}\rho U^2 \sin|\alpha| \sin \alpha \quad \ldots\ldots (28)$$

where B is a constant of proportionality.

Thus, the output is only linear in the cross-stream velocity for small angles of attack (ie: small α), where the cross force due to the pressure dominates, and F_v may be neglected.

The final step in the theoretical derivation of the transfer function of the airfoil probe is obtaining the relationship between the cross force (F_p) and the resultant output signal from the processor. This procedure was described in Chapter 6.1.

8.3 DEVELOPMENT OF A CALIBRATION PROCEDURE

8.31 Simulating a Velocity Shear

As described in Chapter 6.42, the airfoil probe measures the magnitude of velocity shear ie: the rate of change of cross force (F_p) on the beam. Therefore, it cannot be calibrated by being deployed in a constant flow (analagous to DC excitation). The flow needs to be modulated sinusoidally to generate a time-dependant cross force to stimulate the sensor. Three methods that have been used to do this are described below.

8.32 Review of Techniques Previously Used to Calibrate the Airfoil Probe.

8.321 The Rotating Nozzle Technique

T.E.Siddon (1971) used a rotating nozzle, as depicted in FIG. 8.2.

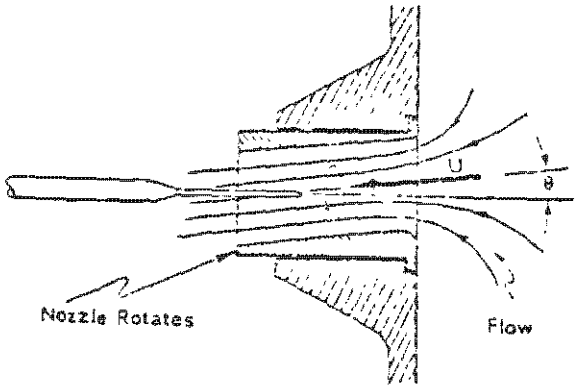

FIG. 8.2 Rotating Nozzle Calibrator.
(T.E.Siddon, 1971)

The probe is positioned in an airflow which is forced to swirl, due to the inclination of the nozzle passageway. Hence the probe experiences a sinusoidally fluctuating cross flow. The relationship between the cross component of flow [V(t)], the mean flow ($\bar{U}$), and the angle of inclination (θ), is given as:

$$\frac{v(t)}{\bar{U}} = \theta_0 \sin(2\pi ft) \qquad \ldots\ldots (29)$$

and the probe sensitivity (S_v) is determined from:

$$S_v = \frac{2e_{rms}}{q\theta} \quad \text{[mV per mm water]} \qquad \ldots\ldots (30)$$

where e_{rms} is the RMS output voltage, and q is a measure of the dynamic pressure of the jet:

$$q \approx \frac{1}{2} \rho \bar{U}^2 \qquad \ldots\ldots (31)$$

It should be noted, however, that Siddon's probe was used to measure airflow turbulence, allowing for a nozzle which could be rotated in an air lubricated bearing.

T.R.Osborn (1974) describes a similar apparatus used to modulate a water jet. However, a high mean flow of between 100 and 145 cm s^{-1} was required because the instrument did not operate at lower water velocities. This is probably due to the numerous problems associated with designing a rotating water nozzle which has a self-sealing mechanism.

8.322 The Rotating Probe Technique

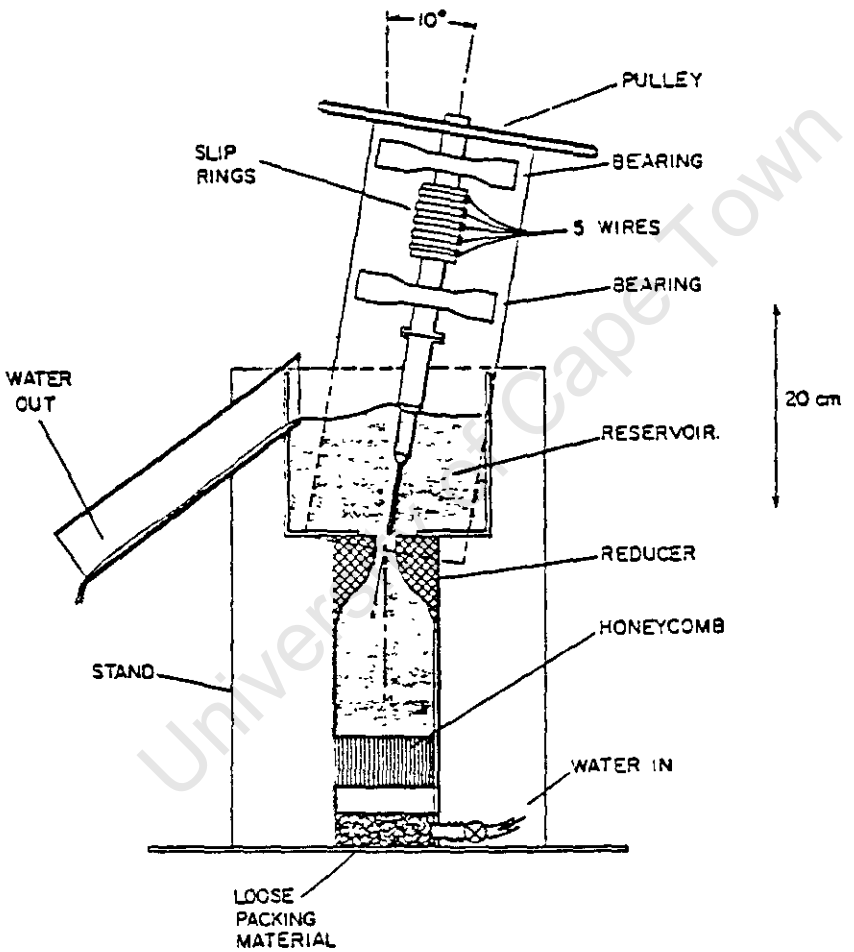

FIG. 8.3 Rotating Probe Calibrator.
(T.R.Osborn and W.R.Crawford, 1980)

The calibration apparatus used at the University of British Colombia (described by T.R.Osborn et al, 1980) comprises a jet which discharges vertically into a tank of water, with the tip of the probe mounted above the outlet at an angle, as shown in FIG. 8.3.

The probe is rotated about it's axis, generating a sinusoidal voltage. Slip rings are used to bring the supply voltage to the preamplifier, and to transmit the output signal to an RMS meter.

This method has been implemented successfully, and is described in detail by Osborn et al.

8.323 The Oscillating Probe Technique

N.S.Oakey (1977) describes a calibration procedure which avoids the use of rotating parts. The probe is oscillated through a small angle (1° - 5°) in the mean flow at various frequencies (0.1 - 10 Hz) by a mechanical driver. A theoretical description of the procedure is given by Oakey (1977).

8.33 Feasibility of Previously Used Calibration Techniques

8.331 The Rotating Nozzle

An investigation into the availability of a self-sealing nozzle led to the conclusion that most devices use the dynamic pressure to seal the bearing. This restricts the range of mean velocities through the nozzle, as described by Osborn (1974). It became evident that the nozzle and seals would need to be designed and machined, resulting in a costly and time consuming procedure.

8.332 The Rotating Probe

This technique was used by G.S.Anderson (1986) in an undergraduate project at the University of Cape Town. It was found that the noise generated by the slip-ring contacts and the driving motor seriously contaminated the output signal, introducing unacceptable uncertainty into the calibration coefficient.

It is expected that, due to the high gain requirement of the strain gauge preamplifier (relative to that of the piezoceramic probe), and the requirement of a stable, noise free supply for the strain gauge bridge, that the noise contamination of a system using slip rings will be at an unacceptable level.

8.333 The Oscillating Probe

This appears to be the simplest of the techniques that have been described. It is unrestricted in the usable range of water velocities and modulating frequencies. Although no details of the system are given by Oakey (1977), the concept of a mechanical driver appears to be simple.

8.34 Construction of the Calibration Rig

The feasibility study described in Chapter 8.33 above, motivated the design of an economical and effective oscillating calibration system, as opposed to the rotating systems mentioned. An investigation into alternative designs revealed that it would be easier to design a mechanical driver that oscillates the water flow over a stationary probe than the Oakey system of oscillating the probe in a laminar flow.

The system comprises a nozzle which oscillates about it's

outlet, the probe remaining fixed in the flow. The nozzle is fitted with a honeycomb insert to ensure laminar flow at it's outlet. Flow rate is controlled by a valve upstream of the nozzle, allowing control of the mean velocity over a range 0.4 - 2 ms^{-1}. The nozzle is driven, via a crank and levers , by a variable speed motor, continuously variable over a range 0 - 10 cycles/second. A schematic of the system is given in FIG. 8.4.

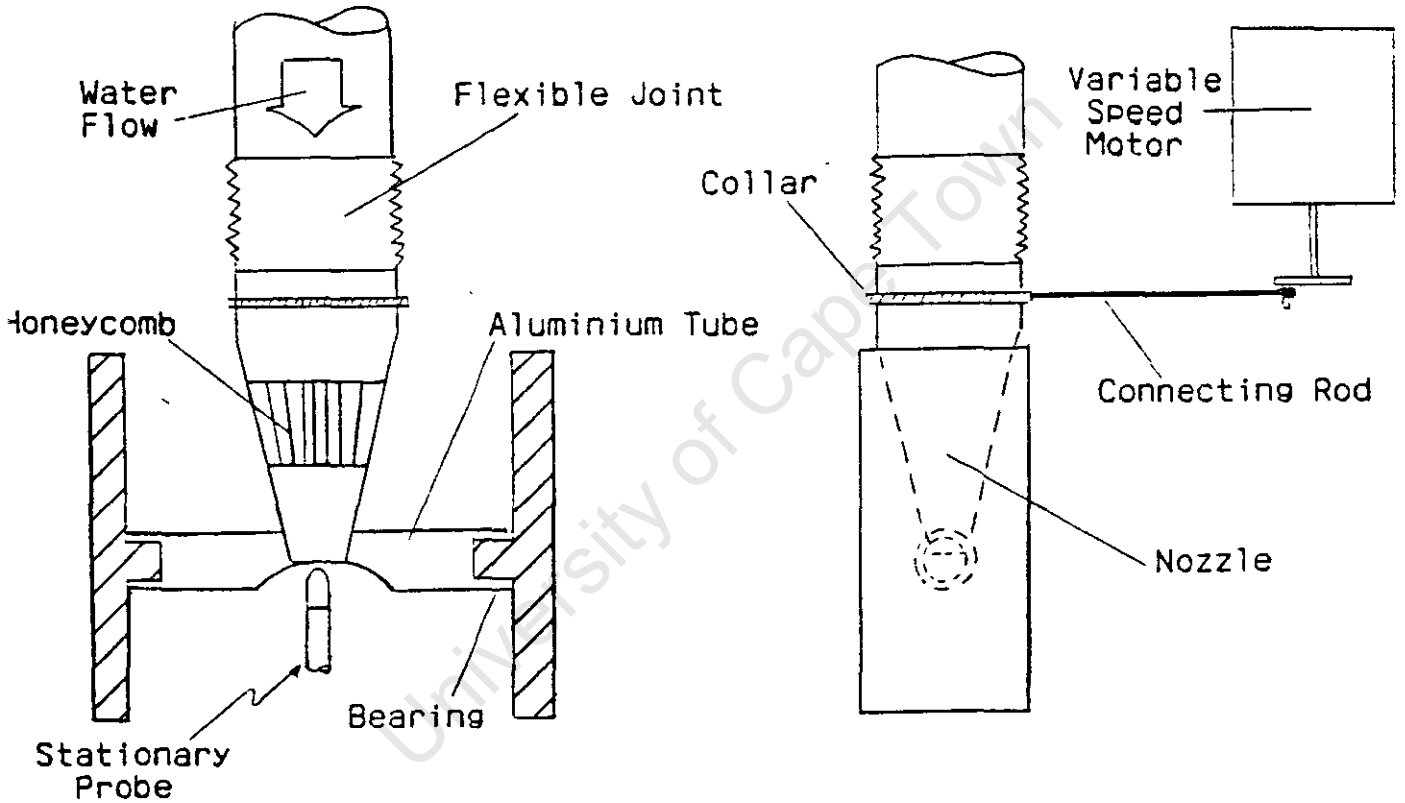

FIG. 8.4 Schematic of Calibration System.

8.35 Minimisation of Background Noise in the Calibration Rig

Early experimentation with flow over the probe revealed that turbulence in the drainage system and dripping onto the probe supports caused unacceptably high levels of backgroung noise, especially in the frequency region 20 - 200 Hz, as shown by the spectrum in FIG. 8.5.

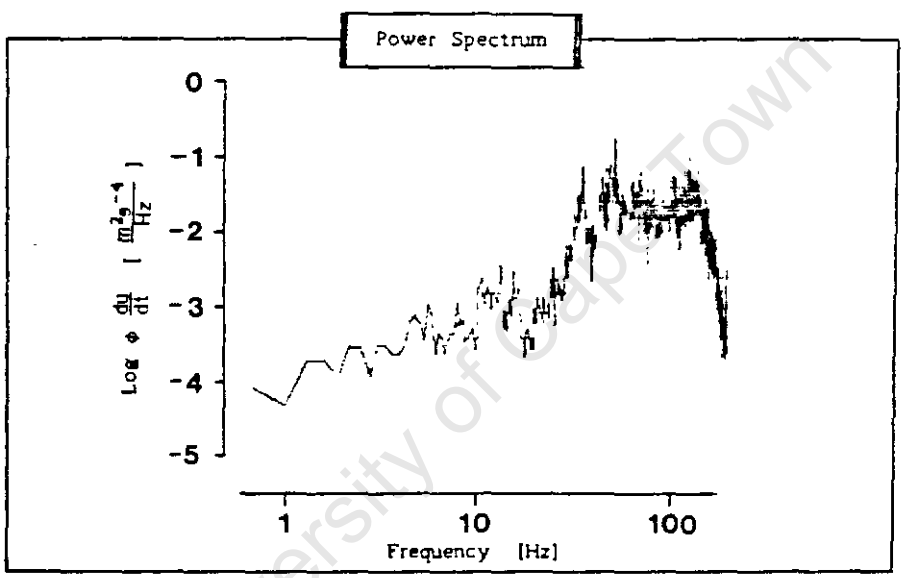

FIG. 8.5 Power Spectrum Showing Background Noise Caused by Turbulent Drainage.

The drainage system below the calibration rig was modified to ensure vibration-free flow. The final system, arrived at through a process of trial and error, is shown in FIG. 8.6. The Power Spectrum in FIG.8.7 shows the improved backgroung noise levels in comparison with FIG. 8.5.

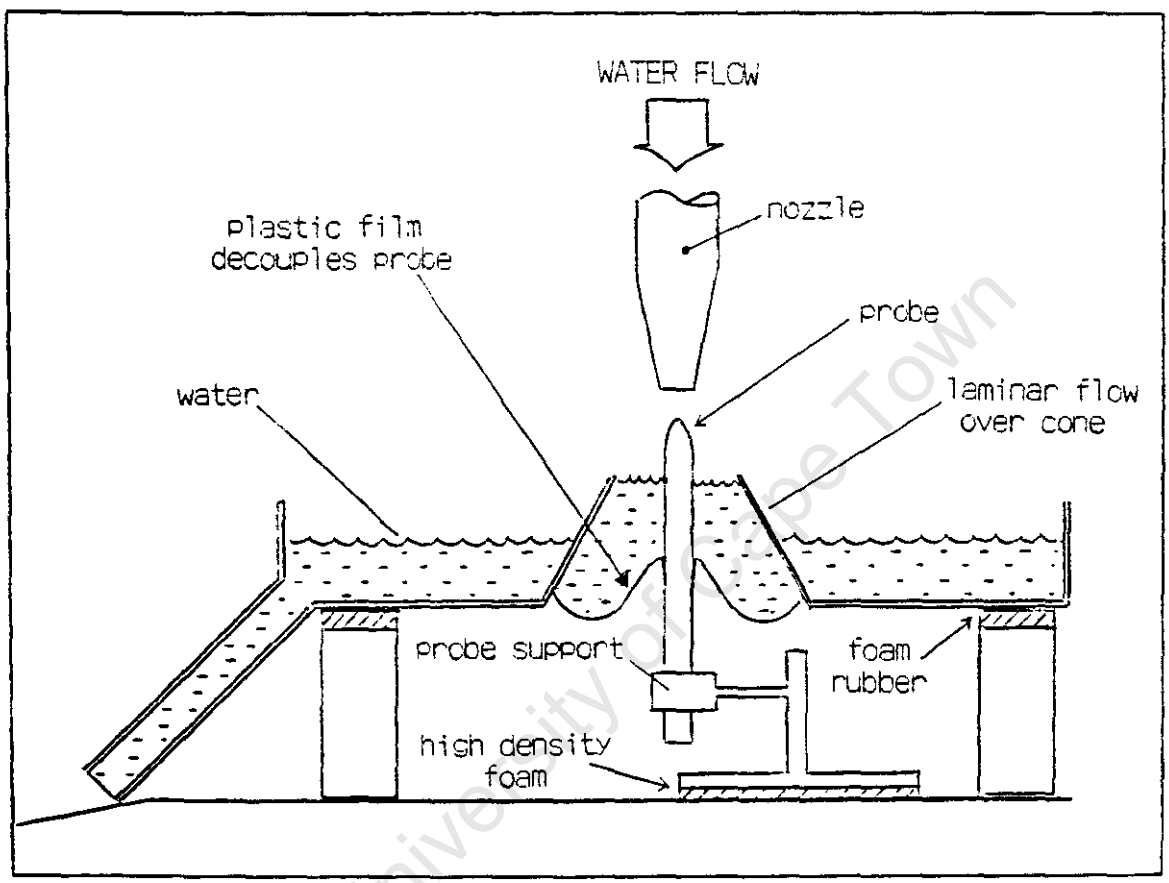

FIG. 8.6 Cross Section through Drainage System of Calibration Rig.

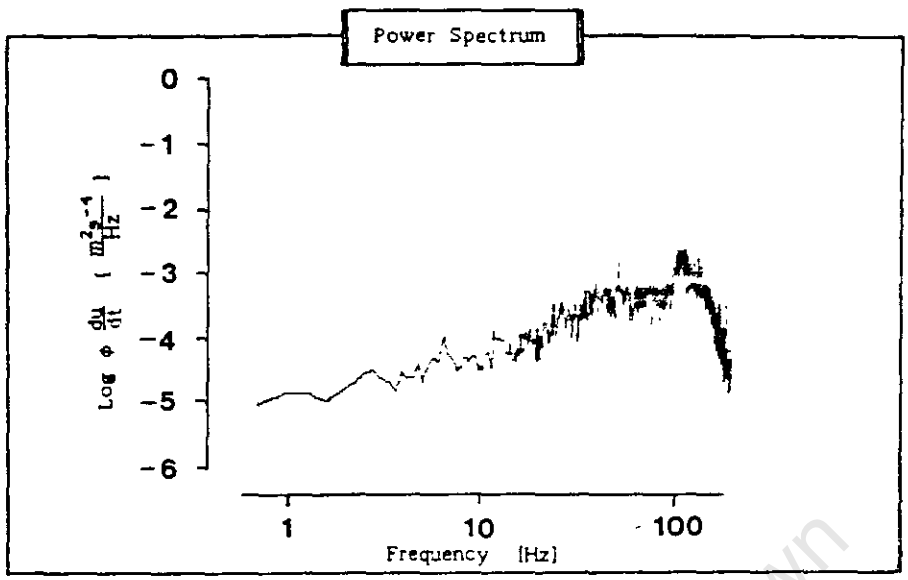

FIG. 8.7 Power Spectrum Showing Background Noise due to Laminar Drainage.

8.4 PROBE CALIBRATION

8.41 Determination of a Calibration Coefficient

8.411 Derivarion of the Calibration Coefficient

Using the coordinate system defined in FIG.8.1, the calibration coefficient, S, may be derived for the airfoil probe.

The transfer function of the airfoil probe has been described by Equation 27 in Chapter 8.2. The transverse force due to potential flow (F_p), is described in terms of the fluid density (ρ), the X-sectional area of the probe (A), and the axial and transverse components of velocity, V and u.

$$F_p = \rho AVu \qquad \ldots\ldots (32)$$

If α is small, then $u \approx \bar{U}\alpha$ and $V \approx \bar{U}$.

If α is now varied sinusoidally such that:

$$\alpha = \alpha_m \sin(\omega t). \qquad \ldots\ldots (33)$$

a time dependant shear, du/dt, is generated:

$$\frac{dF_p}{dt} = \rho AV\frac{du}{dt} \qquad \ldots\ldots (34)$$

Substituting Equation 33 into Equation 32:

$$F_p = \rho A\bar{U}^2\alpha_m \sin(\omega t) \qquad \ldots\ldots (35)$$

Due to the differential transfer function of the electronic system:

$$e_o \sim \frac{dF_p}{dt} \qquad \ldots\ldots (36)$$

$$e_o = S[\rho A\bar{U}^2\alpha_m]\ \omega \cos(\omega t) \qquad \ldots\ldots (37)$$

$$= S\rho AV\frac{du}{dt} \qquad \ldots\ldots (38)$$

Using Equation 37:

$$S = \frac{e_{opp}}{2\rho AV^2\alpha_m} \times \frac{1}{\omega} \qquad \ldots\ldots (39)$$

with e_{opp} denoting peak to peak output voltage.

8.412 Band-limiting of Shear Simulation Data

Preliminary trials using the calibration rig showed that the sinusoidal shear measured by the airfoil had a poor SNR , resulting from background noise. Because the maximum excitation frequency of the calibration rig is 10 cycles per second , it was decided to design a range of

Finite Impulse Response (FIR) low pass filters (software driven) with cut-off frequencies between 5 Hz and 50 Hz to reduce the variance of the calibration curve. The filters designed are 21 point FIR low pass filters, the design of which is discussed fully by N.B.Jones (1982). The input and output signals of 1 second of data into and out of a 10 Hz low pass filter are given for 2 probe excitation frequencies in Appendix 18. The data presented demonstrates the decrease in SNR as excitation frequency is decreased. (Note: the Y-axis scaling in these plots is arbitrary, as the calibration coefficient has not yet been determined).

8.413 Determining the Calibration Coefficient

Using Equation 39, the calibration coefficient (S) may be determined by plotting the system output (e_{opp}) at various excitation frequencies (ω), for constant values of α_m and V.

The probe was excited at 6 frequencies with water flowing at 0.72 ms^{-1} at the nozzle orifice. The angular excursion of the nozzle was limited to α_m = 3°. The resultant shear data was filtered by a low pass filter with f_{3dB} = 25 Hz. The system output was determined by calculating the RMS output over a 12 second period.

The results of the calibration process are shown in FIG. 8.8, from which it will be seen that for excitation frequencies below 3.4 Hz, the background noise level dominates.

The calibration coefficient has been calculated by discarding Point A (in FIG.8.8), the system output for excitation at 2.4 Hz, and calculating the slope of the curve passing through the 5 remaining points using a linear regression. The resultant best-fit line is shown in FIG. 8.9.

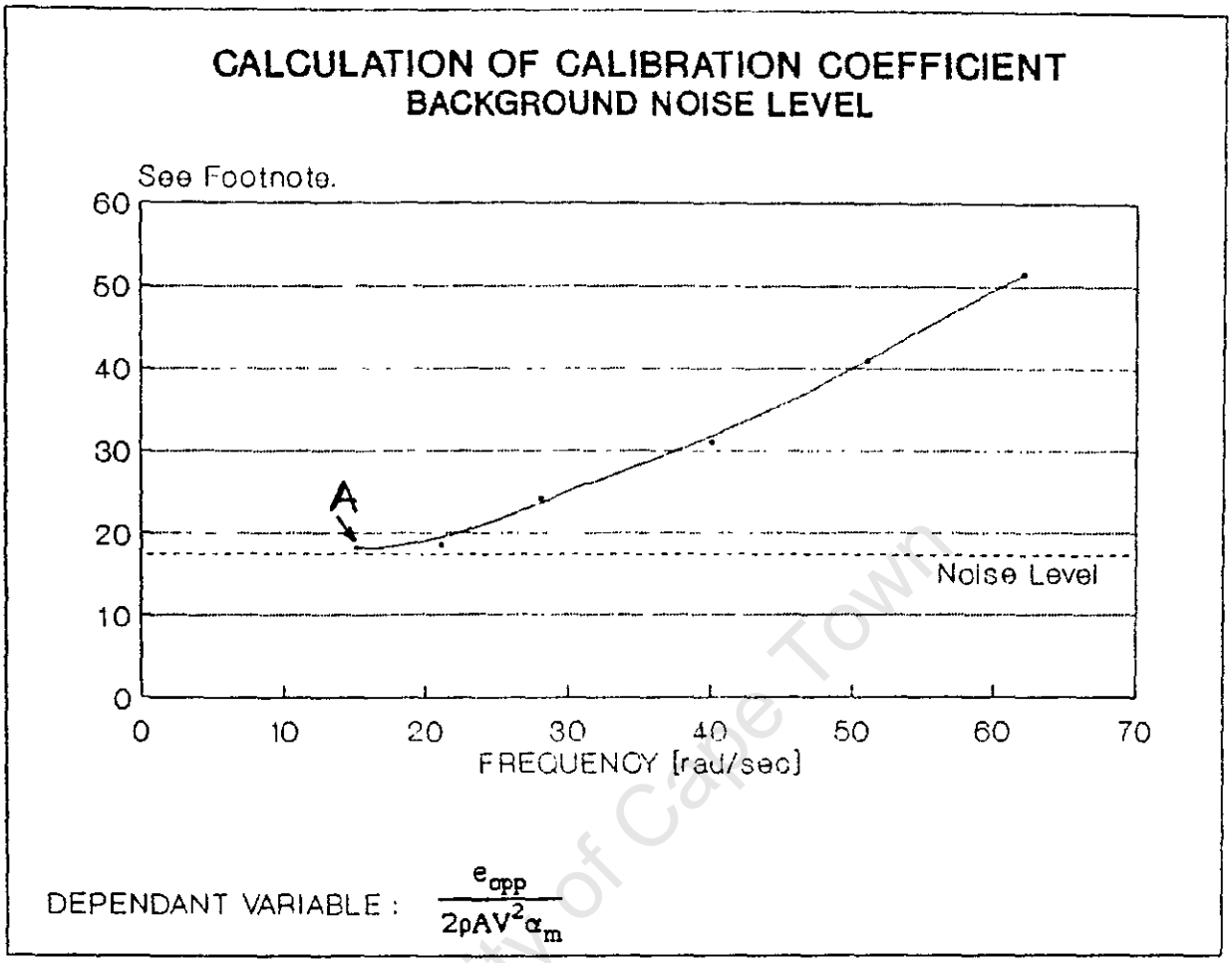

FIG. 8.8 Calibration Curve Showing Noise Level.

From FIG. 8.9, the calibration coefficient is determined by the slope of the curve. The constants ρ and A are 1000 kg m^{-3} and 5.03 x 10^{-5} m^2 respectively

The resultant slope, S = 0.80 $Vs^2kg^{-1}m^{-1}$, has a correlation coefficient of 0.996. The curve, with 4 degrees of freedom, has a confidence limit of over 99.9%

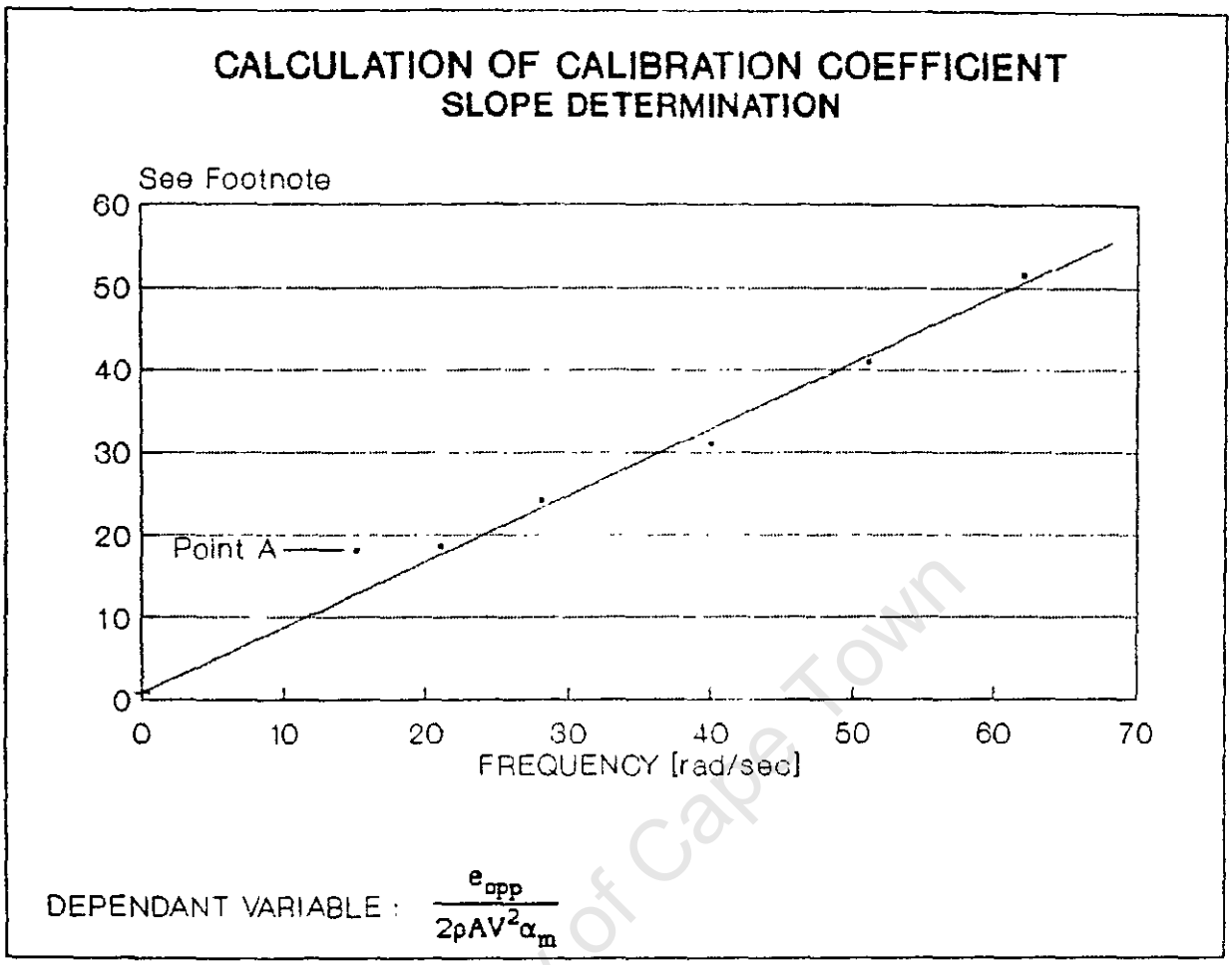

FIG. 8.9 Calibration Curve Deduced by Linear Regression.

8.414 Potential Errors and Uncertainty in the Calibration Procedure

Spectra resulting from the calibration process described in Chapter 8.413 displayed a pronounced sequence of odd harmonics. The spectra for calibration at 2.4 Hz and 9.8 Hz are shown in Appendix 19. These harmonics may be explained by the vibrational characteristics of the calibration rig. The transverse driving sinusoidal shear is biased by an additive

transverse vector caused by the vibration of the rig being transmitted through the water. However, [ref. Appendix 19, Spectrum B)] the power in the 3rd harmonic is 13.2 dB down on the fundamental, causing an error of less than 5%.

These harmonics may be reduced by increasing the angle, α_m , noting that α must remain small for the probe transfer function (Equation 27) and the theory supporting the calibration procedure (Chapter 8.411) to remain valid. By increasing α_m from 3° (as used during calibration) to 7°, the ratio of the fundamental to 3rd harmonic is increased to approximately 26.5 dB, an error of less than 0.3%, as shown in the relevant spectrum in Appendix 19 (Spectrum C).

8.42 Determination of a Coefficient of Thermal Sensitivity

8.421 Static Response of the Probe

The semiconductor strain gauges used have a specified coefficient of thermal sensitivity of - 0.17 % $°C^{-1}$. Due to changes in the density and elasticity properties of the beam/airfoil combination resulting from temperature changes, empirical verification of this coefficient was required.

The probe was calibrated at 3 temperatures within a range expected in the field. The other parameters of mean flow velocity and frequency were kept constant. The resultant RMS response at each temperature is presented as a velocity shear in FIG. 8.10 which depicts the best-fit straight line for the 3 points.

The slope of the curve is - 2.96 % $°C^{-1}$ (100% sensitivity is assumed at 14.0 °C, the temperature at which the probe was originally calibrated).

The correlation coefficient is - 0.99999 and, although there is only a single degree of freedom, the confidence limit is over 99.9 %.

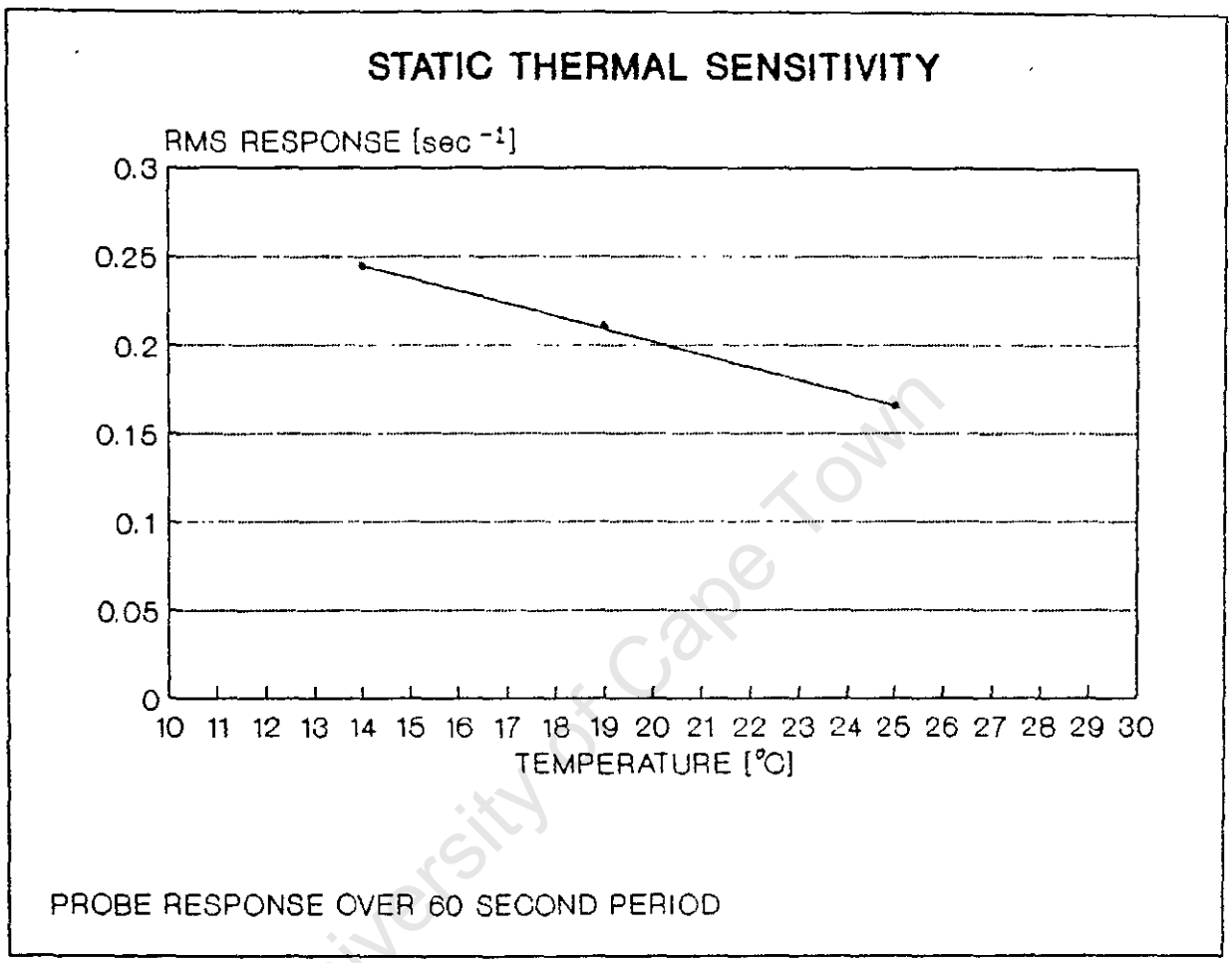

FIG. 8.10 Determination of Thermal Sensitivity.

8.422 Dynamic Response of the Probe

During the static tests described in Chapter 8.421, the probe was given time to reach thermal stability before the velocity shear at each temperature was measured. The resultant coefficient is inappropriate for field conditions where the probe is confronted with a continuous gradient, the steady state conditions in Chapter 8.421 never being achieved.

To simulate field conditions, the water temperature at the inlet of the calibration system was increased gradually from 14.0 °C to 23 °C over a period of 120 seconds. (Note: it was too difficult to replicate the negative temperature gradient which prevails in practice in the field). The curves of temperature vs time, and the resultant response vs time are given in Appendix 20. The probe response at various temperatures,neglecting thermal lag, has been plotted for various temperatures in FIG. 8.11.

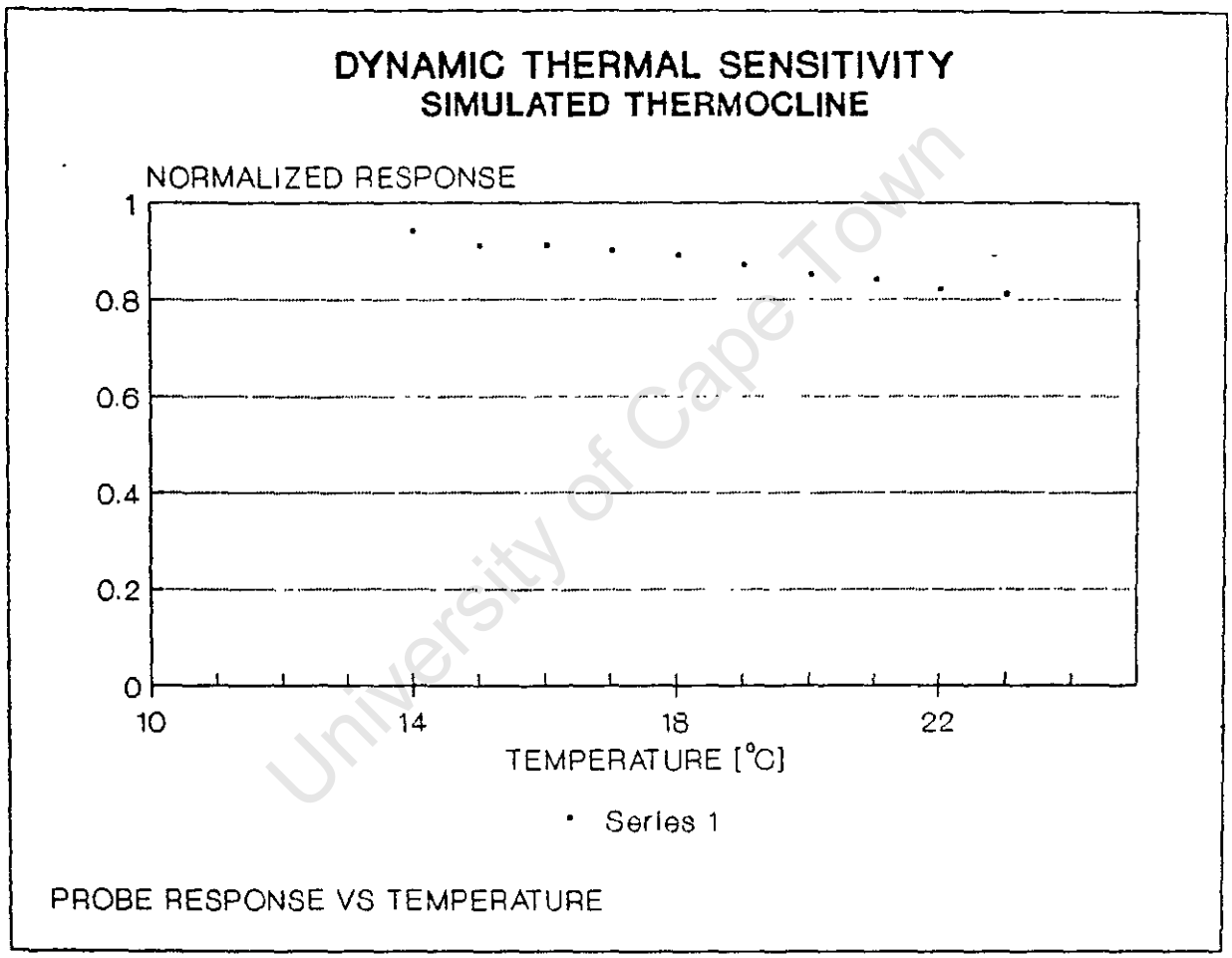

FIG. 8.11 Dynamic Thermal Response.

Using a linear regression, the probe response may be correlated against temperature. The correlation coefficient is - 0.96 and the confidence limit is 99.9 % for the 10 degrees of freedom used.

The resultant coefficient of dynamic thermal sensitivity given by the slope of FIG. 8.11 is - 1.36 % $^{\circ}C^{-1}$, compared to the static value of - 2.96 % $^{\circ}C^{-1}$ derived in Chapter 8.421. The dynamic coefficient is the more appropriate for evaluating field results, having been derived from simulated field conditions.

8.423 Thermal Impulse Response of the Probe

A step change in the temperature of the probe (eg: through deploying a warm instrument in cold water without allowing time for a steady state to be reached) may upset the thermal stability of the system if it is not well lagged. To evaluate the thermal stability of the system, an "impulse" of hot water (40 °C+) was introduced to the nozzle of the calibration rig without disturbing the flow velocity, after the probe had been given time to reach a steady state condition at 14 °C. The time response of the system was monitored. Graphs of both temperature and probe response as functions of time are given in Appendix 22.

The resultant response of the system depicts a low frequency oscillation in the probe sensitivity with a period of approximately 15 seconds. The temperature step of > 30 °C is far more severe than would be encountered in the field, but the curve shows that the thermal response is well damped. Any spurious shears arising from oscillations in the sensitivity have a frequency well below the 1 Hz cut-off frequency of the bridge/preamplifier decoupling filter discussed in Chapter 6.22.

8.43 Effect of Probe Angle of Attack on Calibration Coefficient

The derivation of the calibration coefficient (Chapter 8.411) required the assumption that the probe has a small angle of attack into the mean flow. The effect of the angle of attack on the probe's sensitivity was determined as per Chapter 8.413, except that the water velocity (V) and the excitation frequency (ω) were set at constant values, and the probe response (e_{opp}) was monitored for different angles of attack (α_m).

Due to the mechanical design of the calibration rig, the maximum angular excursion of the nozzle was limited from +7° to -7°. The uncertainty in the measurement of the nozzle angle was 1/2°, arising from mechanical slack in the system. Thus, the probe response was monitored for only three angular settings of the nozzle. The resultant calibration curve is shown in Appendix 21.

Due to the lack of data points, this procedure did not constitute a rigorous calibration, but the resultant slope of 0.76 $Vs^2kg^{-2}m^{-1}$ compares favourably with the value of of 0.8 calculated in Chapter 8.413. However, the curve, with it's correlation coefficient of r = 0.9997, is linear for angles of attack of up to 7°.

Thus, as long as the righting moment of the vehicle prevents angular excursions greater than about 7°, the viscosity effects discussed in Chapter 8.2 (Equation 28) may be neglected.

8.44 Effects of Hydrostatic Pressure on Probe Sensitivity

Kyowa have not published any data on the effect of pressure on the sensitivity of their semiconductor strain gauges, according to their local distributor, Peter Jones

Electronics. It is likely that any sensitivity changes will be as a result of temperature change due to pressure gradient. The probe is to be subjected to a gentle pressure gradient only (a 10 bar change over 100 seconds), and pressure induced temperature changes may thus be neglected.

8.45 Evaluation of Electronic Noise

The electronic noise generated by the processing electronics presents itself as an apparent shear at the output of the turbulence channel. This noise may be measured by monitoring the system response in a vibration-free laboratory environment, with no water flowing over the probe.

The noise was measured for three available sensitivity settings of the turbulence probe (x1, x4.7 and x10) and band limited to 100 Hz. The results are tabulated in FIG.8.12 in terms of both an RMS voltage and an apparent time-varying RMS shear (du/dt), using Equation 38 with a probe velocity V = 1 ms^{-1}.

Sensitivity	RMS Noise [mV]	du/dt [ms^{-2}]
x 1	9.0	0.2
x 4.7	18.6	0.096
x 10	25.7	0.062

FIG. 8.12 Electronic Noise Levels at Different Sensitivity Settings.

The noise is white, with a spectrum that is flat over the band 1 - 100 Hz. The power spectrum shown in FIG. 8.13 has been derived by monitoring 30 seconds of the system output, using the x10 sensitivity setting.

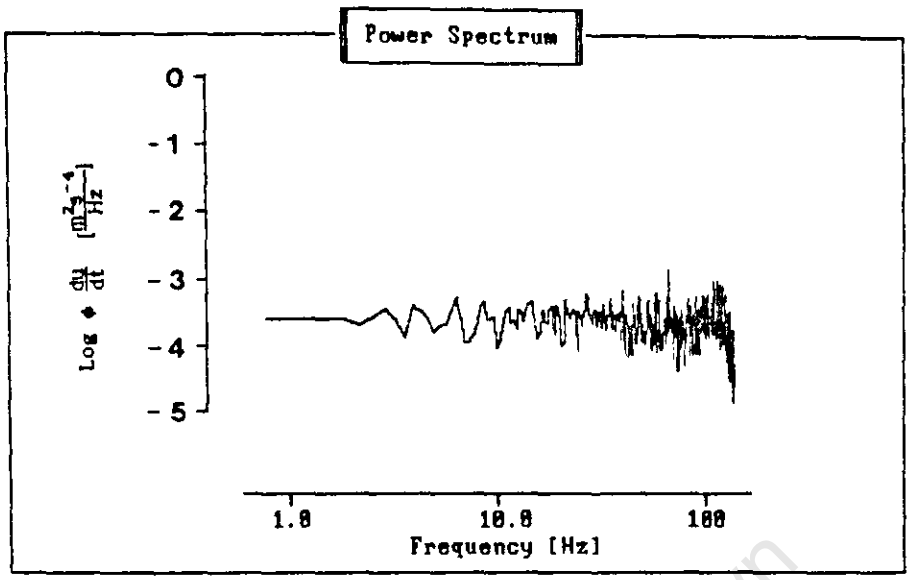

FIG. 8.13 Spectrum of Electronic Noise.

8.5 TRANSFORMATION OF CALIBRATION THEORY TO SPATIAL DOMAIN

Laboratory simulation of turbulence differs from turbulence encountered in the field , in that the time-varying component of velocity [u(t)] in the simulated case becomes a spatial variable [u(z/V)] in the field.

Consequently:

$$\frac{du}{dt} \Leftrightarrow V\frac{du}{dz} \qquad \ldots\ldots (40)$$

Furthermore, the time-dependant frequency (ω) may be related to the wavenumber (k), using the relationship:

$$\omega = kV \qquad \ldots\ldots (41)$$

as described by P.Bradwhaw (1971).

Equation 37 of Chapter 8.411 may be described in terms of spatial variables and becomes:

$$e_o(z) = S\rho AV^2\alpha_m k \cos(kz) \quad \ldots\ldots (42)$$

$$= S\rho AV^2\frac{du}{dz} \quad \ldots\ldots (43)$$

In practical terms, (V) is the terminal velocity of the probe/vehicle system as it penetrates the water column, denoted as (z) previously.

CHAPTER 9

DESCRIPTION OF TROUT SYSTEM

9.1 INTRODUCTION

This chapter is aimed at introducing the reader to the TROUT (Transducer for Research on Oceanographic Underwater Turbulence) system which was developed to measure turbulence and process data generated from deployments in the field. Each component and it's interface with the system is discussed briefly. An overview of the system is presented as a block diagram in FIG. 9.1.

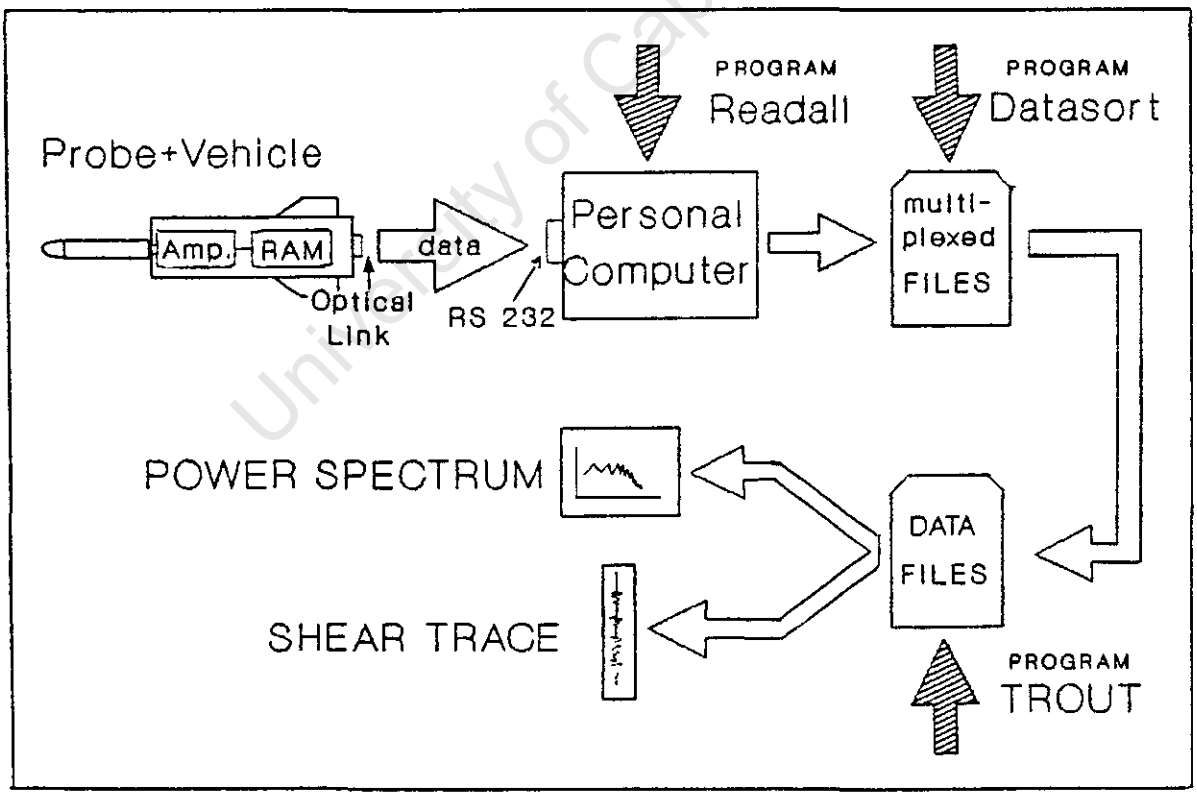

FIG. 9.1 Block Diagram of TROUT System.

9.2 CONSTRUCTION OF THE MECHANICAL SYSTEM

9.21 Description of the Vehicle

A longitudinal section through the vehicle is shown in Appendix 24. It is constructed from a tubular PVC casing having an inside diameter sufficient to accomodate the data logger which is shown in Appendix 17. The vehicle has a turned aluminium nosepiece at the front and a tightly fitted nylon collar at the rear. Four perspex fins are slotted into the nylon collar to improve the vehicle's stability. The vehicle's rear end is closed with a cover which is sealed with a single O-Ring, and secured with 8 screws fitting into the nylon collar.

The vehicle is suspended from the surface vessel by a slightly positively bouyant plastic cable having a safe operating load specification of over 80 kg. Success is critically dependant on the free-falling vehicle having a stable descent. Any vibration of the vehicle will be interpreted by the sensor a velocity shear, contaminating the results. This stability is achieved by designing the vehicle with a high aspect ratio and a strong righting moment (achievable by mounting ballasting weights as close to the vehicle's nose as possible. For the vehicle to fall at 1 ms^{-1}, the ballasting weight should be about 2-3 kg, as determined in the calculations in Appendix 25.

9.22 The Probe/Vehicle Interface

The system requires a probe that can be replaced in the field if it is damaged or if it fails. A screw-in probe is unacceptable due to the resultant twisting/breakage of the connecting leads to the preamplifier. The current design allows for a slide-in fitting, with a cap which screws over the probe, sealing onto O-Rings (shown in Appendix 26).

The probe is plugged into the preamplifier via a DIN plug fitted in the probe. The preamplifier is situated in the vehicle immediately behind the wiring channel to the probe.

9.3 SENSITIVITY SETTINGS OF TURBULENCE CHANNEL

Switch	Sensitivity	Calibration Coefficient	Full Scale Shear [s^{-1}] *
1	x 1	0.80	18
2	x 4.7	3.76	3.9
3	x 10	8.0	1.8
4	Unused	-	-

* A vehicle terminal velocity of 1 ms^{-1} is assumed.

FIG. 9.2 Table of Probe Sensitivity Settings.

The sensitivity of the turbulence channel may be changed by the DIP switch on the output stage of the turbulence channel (shown in Appendix 7). The full scale shear for each sensitivity setting is given in FIG. 9.2 which also shows the modified calibration coefficient.

9.4 DESCRIPTION OF THE PRESSURE CHANNEL

9.41 Description of the Pressure Sensor

The pressure sensor is a Sensotek Model MA miniature pressure transducer with temperature compensation (Appendix 12). The transducer is rated at 300 psi (200m of water), and produces a full scale output of 30.108 mV for a 10v supply.

The calibration record is listed in Appendix 13.

9.42 Description of the Amplifier

The bridge is driven by a similar power source to the strain gauge bridge of the turbulence channel. The circuit diagram is shown in Appendix 14. The pre-amplifier is an instrumentation amplifier utilizing an OP220 input stage (Input stages are matched, therefore thermal drift is low). The output stage is a micropower OP20 (Appendix 15).

The output voltage is matched to the A/D convertor of the data logger via a calibration stage which allows for calibration and DC shift (Appendix 15).

9.43 Calibration of the Pressure Transducer

As described in Chapter 9.41 the pressure transducer is rated for 300 psi (200 m of seawater) and 10 V excitation. To simplify the design of the voltage supply for the pressure transducer, it was decided to use the available 6 V battery supply, regulated at 5 V as opposed to using a DC-DC convertor to generate a 10 V power supply from the 6 V battery. This has the disadvantage of halving the full scale output voltage of the sensor. Furthermore, it was envisaged that the TROUT system would not be deployed to a depth greater than 50 m of water (75 psi), and the amplifier output was modified accordingly. Thus, the amplifier required a gain of 400 to match the resultant 3.76 mV full scale output of the transducer to the 1.5 V full scale input of the A/D convertor.

The pressure transducer was calibrated by simulating a system deployment to a depth of exactly 15 m of water in a decompression chamber. The resultant depth vs time trace is shown in Appendix 27, using a calibration coefficient of 48 dBar (equivalent to a full scale depth of 48 m of water).

9.5 THE DATA LOGGING SYSTEM

9.51 Power-Up of the Data Logger

The initialization procedure required to reset the data logger and prepare it for field use prior to sealing it in the vehicle is described in the data logger instruction manual included as Appendix 28.

As described in Chapter 6.5, the data logger is powered by a 6 volt lead-acid battery. To conserve power, the processor lies in a "wait-state" until pulsed by a signal via a magnetic reed switch fitted into the vehicle cover.

9.52 Triggering of the Turbulence Channel

Once the data logger is activated, it switches on the electronics of the turbulence channel, which are activated by a relay controlled by the processor. Thus, before deployment, the electronics are allowed to reach thermal stability. The data logger begins to monitor the pressure channel; once a pre-determined pressure is reached (5 m), the data logger begins recording data from the three channels.

9.53 Sampling Procedure

The three channels, temperature (inactive), pressure and turbulence are sampled, multiplexed and stored in RAM, as described in Chapter 5.45.

Sampling continues for 120 seconds, after which the data logger returns to it's wait-state until re-triggered by the reed. The RAM has the capacity to store results from eight successive deployments of the probe before it requires milking. Each file is headed by the date and time of deployment; the resultant file after each 120 seconds deployment is 60 480 bytes.

9.54 PC/Data Logger Interface

The data logger may be milked by interfacing it with a personal computer via an optical connection fitted into the cover of the vehicle. Thus, the data logger may be milked without opening the vehicle casing. The optical signal (1200 baud) is converted to a serial stream which is retrieved via the RS232 port of the PC. Milking is controlled by a program READALL developed by the CSIR at Stellenbosch; this stores the data as a hex file.

9.6 SOFTWARE PROCESSING

9.61 MEMOD Downloading : Program READALL

INPUT DATA: Data stored in RAM of data logger.
OUTPUT DATA: Multiplexed hexadecimal files.
DESCRIPTION:
The multiplexed files generated by READALL (one file for each probe deployment) have a format described in Appendix 29.

9.62 Data File Creation : Program DATASORT

INPUT DATA: - Multiplexed files generated by READALL.
OUTPUT DATA: - HEAD1 - HEADx
- TURB1 - TURBx
- PRES1 - PRESx
- TEMP1 - TEMPx
x Refers to the deployment number.
DESCRIPTION:
The files labelled HEAD contain the date and time of probe deployments. The files TURB, PRES and TEMP are the data files from the turbulence, pressure and temperature channels, respectively.
DATASORT was developed using Turbo Pascal V3.0 and is listed in Appendix 30.

9.63 Data Processing : Program TROUT

INPUT DATA: - All files generated by DATASORT.
- Full scale output of pressure transducer (calibrated at 48 dBar for this project).

OUTPUT DATA:- Display of date and time of all current deployments.
- Header file with date and time information.
- Pressure derived graph of depth vs time.
- Average fall speed of vehicle over any specified time interval.

DESCRIPTION:

This program (developed in Turbo Pascal) is menu-driven and requires minimal user input. Relevant data from the header file is listed on all graphic displays (depth characteristics, shear traces and power spectra) for identification purposes. The program is listed in Appendix 31. All the include files mentioned in the program listing are from the Graphic Toolbox and Numerical Methods Toolbox of Turbo Pascal.

9.64 Shear Data Presentation (Time Domain) : Program TRACE

INPUT DATA: - TURB1 - TURBx (Turbulence data files).
- Header file generated by Program TROUT.
- Calibration Coefficient of probe. (0.8 x Sensitivity Setting).
- Vehicle fall speed.

OUTPUT DATA: - Display shear trace in 1 second segments (for calibration purposes).
- Display shear trace in 10 second segments (for presentation of field results).

DESCRIPTION:

The program must be preceded by Program TROUT to generate the header file. A range of Finite Impulse Response low pass filters (5 Hz, 10 Hz, 25 Hz and 50 Hz) may be selected before displaying the data.

These are useful during probe calibration, as described in Chapter 8.412. These filters do not affect the original data files, but only the arrays that are plotted. A program listing is given in Appendix 32.

9.65 Shear Data Presentation (Power Spectrum) : Program SPECTRUM

INPUT DATA : - TURB1 - TURBx (Turbulence data files)
- Header file generated by Program TROUT
- Calibration Coefficient of probe.
- Vehicle fall speed.

OUTPUT DATA :- Power spectrum of shear trace over 0-200 Hz

DESCRIPTION:

This program (listed in Appendix 33) uses the Fourier Transform algorithms provided in Numerical Methods Toolbox, in conjunction with the Welch method of Power Spectral estimation (described in Chapter 7.22). A theoretical description of the process is given in Chapter 7. The process is summarised briefly in FIG. 9.3.

Each segment consists of 2048 data points (corresponding to about 4 seconds of data. Each segment may then be processed separately using the RADIX 4 FFT algorithm. The user selects the number of segments to be processed according to the active deployment time of the vehicle. A number of processing options are available, including Log/Linear selection for vertical scale, subtraction of interference, saving the processed spectrum as a file, replotting a previously processed spectrum and calculating the mean square shear over a specified band.

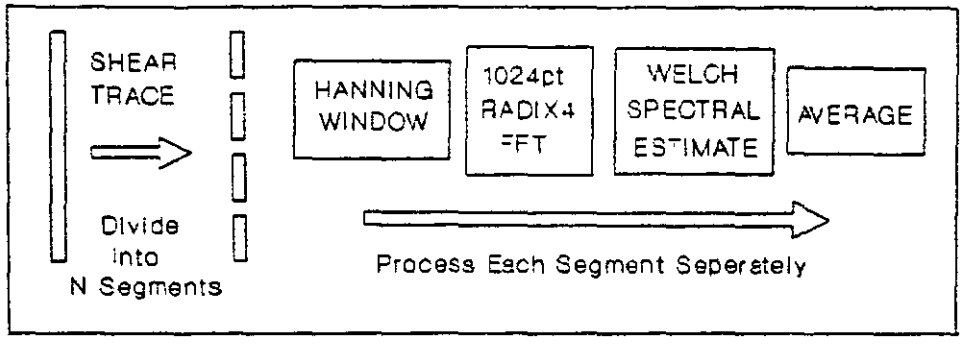

FIG. 9.3 Power Spectral Estimation Algorithm.

9.7 SHEAR DATA INTERPRETATION

Although the analysis of the turbulent shear data generated by the airfoil probe is beyond the scope of this project, it is important that the data can be interpreted in an oceanographic sense, in order to evaluate the system and effectively compare it's performance with previous systems.

The software algorithms discussed in Chapter 9.6 allow the user to present the data as either a time varying shear trace (with a choice of 1 second or 10 second time axis display), or as a power spectrum similar to that shown in Fig. 8.13. The user may use the program to calculate the RMS shear over a time interval (program TRACE), or to calculate the mean square shear $\overline{(du/dz)^2}$ over any specified frequency band (program SPECTRUM).

The mean square shear may be used to calculate the turbulent kinetic energy dissipation ϵ [Wkg^{-1}] of a turbulent field with a kinematic viscosity ν [m^2s^{-1}]. If the turbulent field is isotopic, then N.S.Oakey (1988) gives the dissipation as:

$$\epsilon = 7.5\ \nu\ \overline{\left(\frac{du}{dz}\right)^2} \qquad \ldots\ldots (44)$$

This value may be used to compare the effective noise levels of TROUT with that of other systems.

CHAPTER 10

PRESENTATION OF RESULTS OF FIELD TRIALS

10.1 PRELIMINARY FIELD TRIALS : ST. HELENA BAY

10.11 Introduction

Preliminary field tests were conducted at St.Helena Bay during July,1989. The tests were conducted from a ski-boat. The gradual slope of the sea bed permitted a depth of only 20 metes being attained after some 45 minutes travel from the harbour. A temperature profile revealed that typical winter conditions prevailed. A very weak thermocline existed (a change in temperature from 12.6 °C to 12.4 °C over a depth of 12 metres). This suggests that the water column was well mixed (due to the fresh winds which had prevailed over the previous few days). The system was deployed three times to depths of between 10 and 15 metres.

10.12 Deployment Results

The vehicle had a reasonably constant fall speed of 0.8 ms^{-1} over the depth range 0-8 m, before the drag of the retrieval rope disturbed the fall (the boat was not anchored and it's drift caused the the fall of the vehicle to be interupted about 5 m sooner than anticipated).

The sensitivity of the turbulence probe was set at x4.7 (corresponding to a full scale response to a shear of 3.9 s^{-1}). The resultant shear trace showed random noise spikes which were removed manually from the data sequence (these spikes could be a result of both the electronic noise of the system and collisions of the probe with small organisms in the water).

The spectrum resulting from the first 8 seconds of system deployment is shown in FIG. 10.1 below.

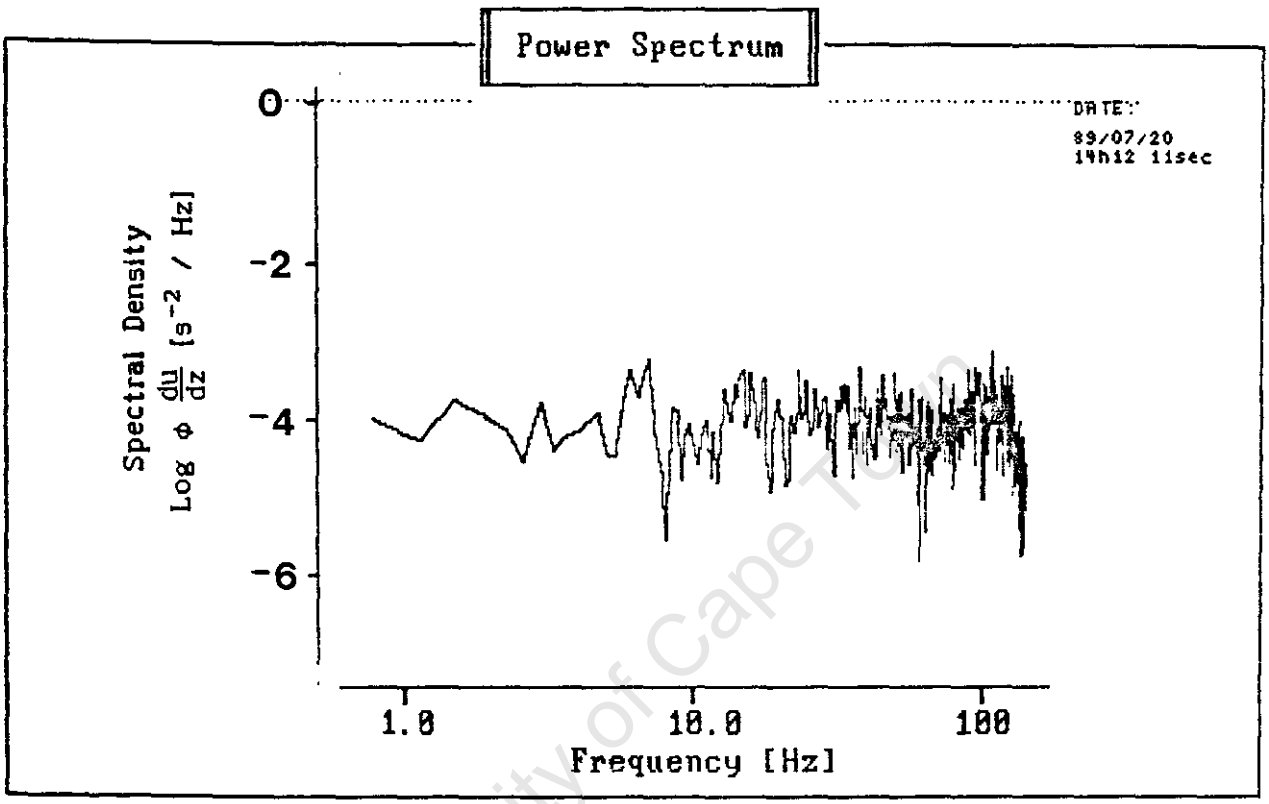

FIG. 10.1 Turbulence Spectrum: St.Helena Bay.

10.13 Discussion

Due to the short length of the data sequence, which is a consequence of the shallow water in which the system was deployed, the spectrum in FIG. 10.1 has a high variance (the spectrum is derived from only 2x2048 pt data segments, each windowed, transformed and averaged as described in Chapter 9.65). The absence of a pronounced boundary layer makes interpretation of the spectrum difficult.

It is not possible to separate the effective noise level of the system from possible turbulent excitation, as the shear trace (shown in Appendix 34) is not comprised of active and quiet regions, as is the case when a strong thermocline exists. A good example of such a trace is given by T.R.Osborn and W.R.Crawford (1979) and is shown in FIG. 10.2.

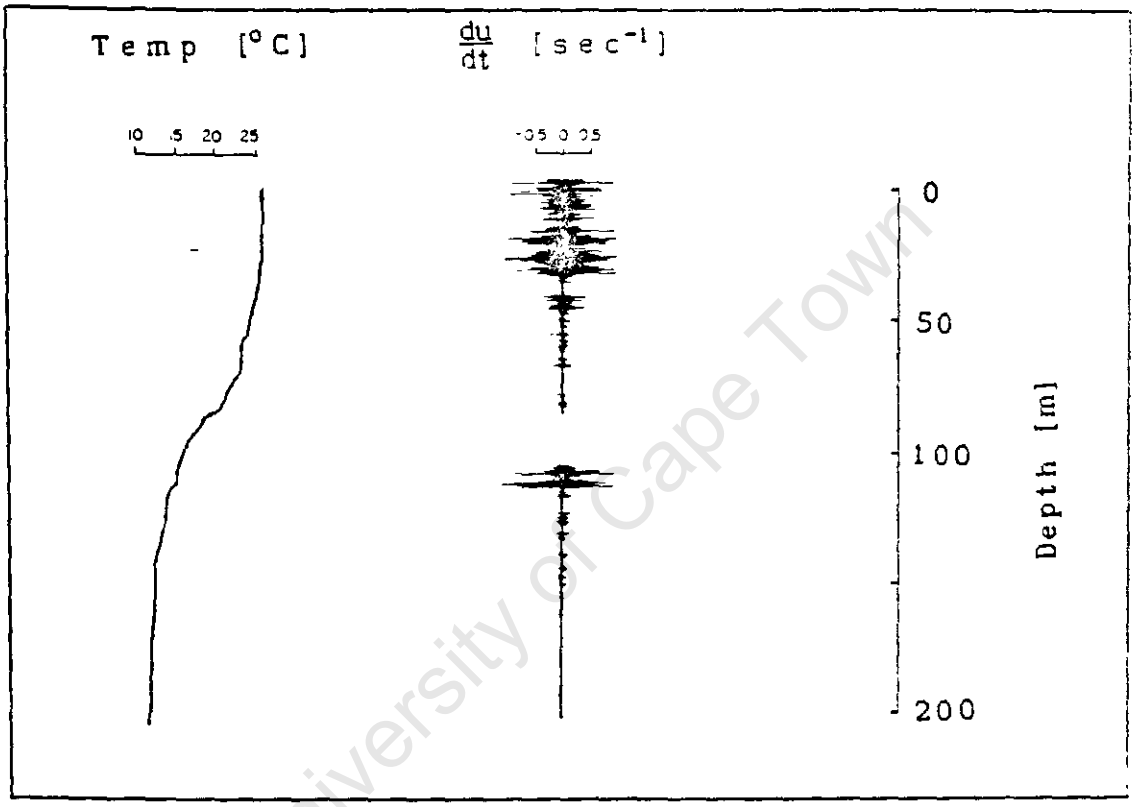

FIG. 10.2 Shear Trace in Presence of Strong Thermocline. (T.R.Osborn and W.R.Crawford, 1979.)

The above spectrum shows, however, that the system response is flat over the frequency range 1-100 Hz, and any vehicle vibration appears to be well damped (a spectrum with a lower variance resulting from a longer data sequence would give a better indication of the hydrodynamic stability of the vehicle).

The mean square shear for the spectrum shown in FIG. 10.1 is $2x10^{-3}$ s^{-2} over the frequency range 0-25 Hz. (Applying Equation 41 with a vehicle fall speed of 0.8 ms^{-1} and a band limit of 25 Hz, it can be seen that the energy of all wavelengths down to a scale of 32 mm is being considered, corresponding to the 3 dB cut-off in spatial resolution of the airfoil probe as discussed in Chapter 5.11)

The dissipation associated with a mean square shear of $2x10^{-3}s^{-2}$ may be calculated using Equation 44. If a kinematic viscosity of $1.3x10^{-6}m^2s^{-1}$ is assumed (N.S.Oakey, 1988), then the resultant dissipation is $2x10^{-8}Wkg^{-1}$.

It was intended that more field tests would be conducted in deeper water in the same area with the turbulence probe set at a higher sensitivity, but adverse weather conditions necessitated their cancellation.

10.2 FIELD TRIALS : HOUT BAY

10.21 Introduction

Following the inconclusive results obtained during the St. Helena Bay field trials (Chapter 10.12), it was decided to conduct further trials in an attempt to get a better evaluation of the system. Tests were conducted from a ski-boat in 40 m of water in Hout Bay during September, 1989. The temperature profile [shown in Appendix 35(a)] indicated a stratified sun-warmed surface layer with a reasonably constant thermal gradient varying from 17 °C at the surface, to 12 °C at 40 m.

10.22 Deployment Results

The system was deployed to a depth of between 25 and 30 m. The resultant pressure characteristic [Appendix 35(b)]

shows a constant vehicle fall speed of 0.9 ms^{-1} between 5 m (when the data logger was activated) and 26 m, where the fall was stopped by the retrieval rope.

The sensitivity of the turbulence probe was set at x10 (corresponding to a full scale response of 1.8 s^{-1}).

The spectrum resulting from the average of 5x4 second segments (5m - 25m) is shown in Appendix 35(c). A section of the accompanying shear trace is shown in Appendix 35(d). The spectrum is characterised by two distinct regions. The first is below 20 Hz (corresponding to a wavenumber k of 22 cycles/metre), where the gentle "hump" represents the turbulent energy region. The second region, above 20 Hz, is characterised by noise resulting from high frequency mechanical vibration generated as the water flows over the probe, and as the vehicle drags the retrieval rope behind it.

10.23 Discussion

As in the case of the St.Helena Bay tests, there was no strong thermocline (characterised by a constant thermal gradient in the surface layer, followed by a sharp temperature differential, as shown in FIG. 10.2). Therefore, turbulence dissipation levels were expected to be low.

The mean square shear for the spectrum shown in Appendix 35(c) is $7.5x10^{-4}s^{-2}$ over the frequency range 0 - 25 Hz. The associated turbulent dissipation, calculated in the same way as in Chapter 10.13, is $7x10^{-9}Wkg^{-1}$.

The noise shown in Apppendix 35(c) is at spatial frequencies higher than those resolvable by the probe and, therefore, does not significantly contaminate the turbulent energy region.

The dissipation levels calculated from the Hout Bay trials are 4.5 dB lower than those calculated for St.Helena Bay. This phenomenon may be explained by recalling that there was no thermal gradient in the water column in St.Helena Bay, suggesting that high levels of background turbulence (as opposed to turbulent strata - FIG. 10.2) were keeping the entire water column well mixed.

CHAPTER 11

EVALUATION OF SYSTEM PERFORMANCE

11.1 SPATIAL RESOLUTION OF SYSTEM

11.11 The High Frequency Cut-Off Scale

The ability of the system to resolve short wavelengths is limited by the diameter of the airfoil probe, as described in Chapter 5.11. The designed diameter of the probe for TROUT is 8 mm, limiting it's resolution to wavelengths above 32 mm (assuming a fall speed of 1 ms^{-1}). This was not verified during calibration because the generation of wavelengths of this scale would require a calibration rig capable of oscillating at frequencies of 1800-2400 rpm, a mechanically difficult task to construct.

The spectrum in FIG. 10.1 shows the system frequency response to be flat over the range 1-100 Hz; the spatial resolution of the system could be increased by constructing a probe of lesser diameter, and using it in conjunction with the TROUT system.

The 32 mm cut-off peak of the strain gauge probe may be compared with that of 18.8 mm for the piezoceramic airfoil probe (expendable) used by R.G.Lueck and T.R.Osborn (1985), and 24 mm for the piezoceramic airfoil probe (tethered vehicle) used by N.S.Oakey (1987).

11.12 The Low Frequency Cut-Off Scale

The ability of the system to measure long wavelengths is influenced by two factors.

Firstly, as described in Chapter 6.22, the system is unable to resolve wavelengths longer than the vehicle. In the case of TROUT, this corresponds to wavelengths > 1m. Secondly, the high pass filter separating the strain gauge bridge from the processor has a cut-off frequency of 1 Hz, also effectively limiting the low frequency resolution to wavelengths < 1m (assuming a vehicle fall speed of 1 ms^{-1}). Thus, if better low frequency resolution is desired, a longer vehicle will be required, with a bridge circuit having a different frequency characteristic. (It should be noted that for frequencies below 1 Hz, the thermal sensitivity of the electronics becomes critical, which should be considered).

The low frequency cut-off of 1m for the TROUT system is comparable to that of the piezoceramic probe used by N.S.Oakey (1977) and better than the 0.05m of the expendable piezoceramic probe used by Lueck et.al. (1985). The low frequency usefulness of piezoceramic transducers is inherently limited to about 1 Hz due to pyroelectric effects (T.R.Osborn and W.R.Crawford, 1980).

11.2 THERMAL SENSITIVITY OF THE STRAIN GAUGE PROBE

In Chapter 8.422, the thermal sensitivity of the semiconductor strain gauge probe was determined as -1.36% $^{o}C^{-1}$. This value should be compared to a typical thermal sensitivity of +1% $^{o}C^{-1}$ for a piezoceramic airfoil probe (T.R.Osborn and W.R.Crawford, 1980). The only significant difference between the two values is that there is an increase in sensitivity as the strain gauge probe penetrates a typical thermocline, whereas the piezoceramic probe has a comparative decrease in sensitivity under the same conditions.

11.3 SENSITIVITY LIMITATIONS DUE TO ELECTRONIC NOISE LEVELS

The power spectrum of the electronic noise level of TROUT is given in FIG. 8.13, from which the equivalent mean square shear and associated dissipation may be calculated. For an assumed vehicle fall speed of 0.8 ms^{-1} (the actual fall speed during the Hout Bay field trial), the noise has an equivalent RMS shear of 0.06 s^{-1} (bandlimited to 100 Hz) and 0.03 s^{-1} (bandlimited to 25 Hz). The associated dissipation levels of $3x10^{-8}$ Wkg^{-1} and $7x10^{-9}$ Wkg^{-1} respectively, are determined using Equation 44.

The electronic noise levels of the piezoceramic probe used by R.G.Lueck and T.R.Osborn (1981) corresponds to an RMS shear of $10^{-4}s^{-1}$ (bandlimited to 250 Hz), with an associated dissipation level of 10^{-13} Wkg^{-1} Unfortunately, from the selection of papers available on piezoceramic probes, this was the only value quoted.

11.4 SENSITIVITY LIMITATIONS DUE TO MECHANICAL NOISE LEVELS

The ultimate sensitivity of the system is determined by the background noise generated as water flows over the probe, the supporting vehicle and the supporting rope as it is dragged through the water column. An accurate estimate of the mechanical background noise level requires a water column having separate strata of turbulent activity and inactivity. These requirements were not met during the field tests of TROUT due to the winter weather conditions which prevailed. The effective noise level may, however, be estimated from the power spectrum of the Hout Bay trials [Appendix 35(c)].

The dissipation level over the frequency range 1-25 Hz is given in Chapter 10.23 as $7x10^{-9}$ Wkg^{-1}.

This value is significantly lower than the typical dissipation level for a mixed layer of 10^{-6} Wkg^{-1} (N.S.Oakey, 1988), and it may thus be assumed that the system was deployed in relatively quiet waters.

The effective noise level of approximately 10^{-8} Wkg^{-1} (Bandlimited to 100 Hz) should be compared with values of $4x10^{-10}$ Wkg^{-1} achieved by R.G.Lueck and T.R.Osborn (1981), and a value of 10^{-10} W/kg for EPSONDE, the instrument used by N.S.Oakey (1988).

The resolution of the probe may be evaluated by assuming a 0 dB SNR and substituting the estimated noise level of $10^{-8}s^{-1}$ into Equation 44. The resultant resolution is an RMS shear level of $3.2x10^{-2}s^{-1}$. This resolution is comparable to the values quoted for other systems in Chapter 2.2.

11.5 PROBE RELIABILITY

The semiconductor strain gauge probe manufactured for the TROUT system has proved to be extremely reliable. Only one probe has been constructed. It has survived a variety of calibration tests and field deployments. Previous research using piezoceramic probes, both at the University of Cape Town (G.S.Anderson, 1986) and elsewhere (T.R.Osborn and W.R.Crawford, 1980) has highlighted their fragility, many probes having been broken despite their having been handled with caution.

11.6 COST OF THE SYSTEM

The component costs incurred in the construction of the TROUT system have been approximately :

4 x Semiconductor Strain Gauges	R 450
10 x Conventional Strain Gauges	R 100
Electronic Components	R 250
Vehicle Construction	R 3 000
Data Logging System (including Software)	R 10 000
Pressure Transducer	R 2 000
Rope and Shackles	R 150
Total	R 15 950

Because the system is retrievable and the probe is rugged, maintenance costs are minimal compared with those of an expendable turbulence probe (R.G.Lueck and T.R.Osborn, 1985), the electronics of each expendable vehicle costing approximately $ 130.

11.7 CONCLUSIONS

Based on the above evaluation of the system, the following conclusions may be drawn:

a) The system has a spatial resolution comparable to that of other airfoil probes. Although the high frequency response is limited to wavelengths of 32 mm (versus about 20 mm), this may be improved if a probe having a smaller diameter is constructed.

b) The probe has a thermal sensitivity of similar magnitude but opposite sense to that of piezoceramic probes. No significant consequence of the latter aspect is apparant.

c) The electronic noise level of the strain gauge probe is higher than of the piezoceramic probe (about 50 dB). This is due to the comparitively higher amplification required for the strain gauge probe.

However, the electronic noise level does not determine the ultimate sensitivity of the system. The effective noise level (caused by background mechanical noise) is 20 dB poorer for the strain gauge probe but the noise level of the strain gauge probe is 20 dB lower than dissipation levels associated with a typical mixed layer.

However, in the deep ocean, dissipation levels may be 10^{-10} Wkg^{-1}, 20 dB lower than the present noise level of the system.

Under such conditions, the strain gauge probe will not have adequate SNR to detect the turbulence. (Under these conditions, the piezoceramic probe will have 0 dB SNR). Thus, the use of the TROUT system is limited to regions where there are moderate to high levels of marine turbulence (mixed layers with strong thermoclines, flooding tidal channels, etc.), having RMS shear levels of above $3.2 \times 10^{-2} s^{-1}$.

d) The semiconductor airfoil probe is more reliable than the piezoceramic airfoil probe.

CHAPTER 12

RECOMMENDATIONS

The following improvements are recommended in any further development of this system, based on the author's two years experience on this project, and on the conclusions in Chapter11.7 :

a) The probe should be redesigned with a reduced diameter to achieve an improved spatial resolution. The current spatial resolution of the probe is determined by the width of the Kyowa semiconductor strain gauges (5 mm) used for this project. Other manufacturers (eg: Entron, UK.) produce semiconductor strain gauges which will permit a probe diameter of about 4 mm (compared with the current probe diameter of 8 mm)

b) The vehicle should be redesigned to incorporate a stainless steel rather than a PVC casing, to increase the depth capability from 50 m currently to at least 200 m. Such redesign should also increase the length of the vehicle from it's current 1 m which is not consistent with that of other tethered free-fall vehicles (eg: the vehicle used by N.S.Oakey, 1988, is 4 m long); the resultant stronger righting moment will improve vehicle stability and reduce the effective noise level.

c) A temperature sensor should be incorporated into the system to facilitate deployment procedures and improve the accuracy of correlation between the measured variables. The data logger has a channel available for such a sensor.

This would obviate the current need for a separate temperature probe, which complicates procedures and does not ensure measurement of the temperature in the immediate vicinity of the probe.

d) The program SPECTRUM should be modified to permit comparison of the spectra for turbulent regions within a water column with those of quiet regions. This would require the facility to select separate spectra representing short intervals of the trace, instead of a single resultant time averaged power spectrum representing a complete deployment.

BIBLIOGRAPHY.

AGRAWAL, Y.C., W.E.TERRY and A.J.WILLIAMS 3rd, 1982
Backscatter laser velocimeter for energetic bottom boundary layers.
IEEE Journal of Oceanic Engineering,
Vol OE-7, No 4.

CARTER, G.D. and J.IMBERGER, 1986
Vertical rising microstructure flux profiler.
Journal of Atmospheric and Oceanic Technology,
Vol 3, pp 462-471.

MAIN, I.C. and A.W.D.JONGENS, 1988,
Development of a system to measure marine turbulence.
Seminar on Electroacoustics, SAAI.

MAIN, I.C., A.W.D.JONGENS, and H.WALDRON, 1989.
Development of a system to measure marine turbulence.
Seninar on Electroacoustics, SAAI.

MORRISON, R.
Grounding and Shielding Techniques in Instrumentation.
John Wiley and Sons, USA.

MOTT, R.L, 1978
Applied Strength of Materials.
Prentice Hall, New Jersey

ROBERTS, R.A. and MULLIS, C.T., 1987.
Digital Signal Processing,
Addison-Wesley Publishing Co., USA.

STREMLER, F.G., 1982.
Introduction to Communication Systems,
(Second Edition), Addison-Wesley Publishing Co.

THOMSON, 1971
Theory of Vibration with Applications.
Prentice Hall, New Jersey.

LIST OF REFERENCES.

ALLEN, H.J. and E.W.PERKINS, 1952
A study of effects of flow over slender, inclined bodies of revolution.
U.S..National Advisory Committee for Aeronautics, Report No. 1048.

ANDERSON, G.S., 1986
A probe to measure underwater turbulent velocity fluctuations.
Undergraduate Thesis, University of Cape Town.

BRADSHAW, P., 1971
An Introduction to Turbulence and it's Measurement.
Pergamon Press, Oxford.

BUCHHAVE, P., W.K.GEORGE Jr. and J.L.LUMLEY, 1979
The measurement of turbulence with the laser-Doppler anemometer.
Annual Review of Fluid Mechanics,
Vol 11, pp 443-503.

CHEN, C.H., 1982.
Digital waveform processing and recognition.
CRC Press, USA.

CRAWFORD, W.R. and T.R.OSBORN, 1979.
Microstructure movements in the Atlantic equatorial undercurrent during GATE.
Deep-Sea Research,
GATE Supplement, edited by W.Duing.

DINGWELL, R.E. and F.B.WEISKOPF, 1981
A hot-film anemometer for ocean turbulence measurements.
Oceans '81 IEEE 81CH1685-7, pp 468-472.

DUBBELDAY, P.S., V.V.APOSTOLICA AND D.L.DIEBEL, 1988
Developments in hot-film anemometry measurements of hydroacoustic particle motion.
Naval Research Laboratory,
NRL Memorandum Report 6188.

EVANS, D.L., T.S.ROSSBY, M.MORK AND T.GYTRE 1979
YVETTE-a free fall shear probe.
Deep Sea Research,
Vol 26/6A, pp 703-718.

FREY, H.R. and G.J.McNALLY, 1973
Limitations of conical hot platinum film probes as oceanographic flow sensors.
Journal of Geographical Research,
Vol 78, No 9, pp 1449-1461.

GARRETT, C. and W.MUNK, 1979
Internal waves in the ocean.
Annual Review of Fluid Mechanics,
Vol 11, pp 339-369.

GECKINLI, N.C. and D.YAVUS, 1983
Discrete Fourier Transform and it's Application to Power Spectra Estimation ,
ELSEVIER, New York.

HOROWITZ, P. and W.HILL, 1980
The Art of Electronics.
Cambridge University Press, Cambridge

IMBERGER, J. and A.J.McCOMB, 1986
Water Research 1986
Centre for Water Research, University of Western Australia

JONES, N.B., 1982
Digital Signal Processing.
Peter Peregrinus Ltd., UK.

LHERMITTE, R., 1983
Doppler sonar observations of tidal flow.
Journal of Geophysical Research,
Vol 88, No C1, pp725-742.

LUECK, R.G. and T.R.OSBORN, 1981
Expendable dissipation profiler
Oceans '81 IEEE 81CH1685-7, pp 377-381.

LUECK, R.G. and T.R.OSBORN, 1985
Turbulence measurement in a submarine canyon.
Continental Shelf Research,
Vol.4,No 6, pp 681-698.

MAIN, I.C., 1987
Development of a probe to measure marine turbulent velocity fluctuations.
Undergraduate Thesis, University of Cape Town.

NATIONAL SEMICONDUCTOR CORPERATION, 1985
Switched Capacitor Filter Handbook.

OAKEY, N.S., 1977
Octoprobe III:an instrument to measure oceanic turbulence and microstructure.
Bedford Institute of Oceanography, Canada,
Report No B1-R-77-3.

OAKEY, N.S., 1988
EPSONDE:an instrument to measure turbulence in the deep sea.
IEEE Journal of Oceanic Engineering,
Vol 13 ,No 3, pp 124-128.

OSBORN, T.R., 1974
Vertical profiling of velocity microstructure.
Jounal of Physical Oceanography,
Vol 4, pp 109-115.

OSBORN, T.R. and W.R.CRAWFORD, 1980
An airfoil probe for measuring turbulent velocity fluctuations in water.
Air-sea Interaction, Instrumentation and Methods.
Plenum Press, New York, pp 369-386.

ROBERTS, R.A. and C.T.MULLIS, 1987
Digital Signal Processing,
Addison-Wesley Publishing Co., USA.

SIDDON, T.E. and H.S.RIBNER, 1965
An aerofoil probe for measuring the transverse component of velocity.
AIAA Journal,
Vol 3 No 4, pp 747-749.

SIDDON, T.E., 1971
A miniature turbulence gauge utilizing aerodynamic lift.
Review of Scientific Instruments,
Vol 42, No 5, pp 653-656.

SIMPSON, J.H. 1972
A free fall probe for the measurement of velocity microstructure.
Deep Sea Research,
Vol 19, pp 331-336.

SPINDEL, R.C., 1985
Sound transmission in the ocean.
Annual Review of Fluid Mechanics,
Vol 17, pp 217-237.

VAUGHN, 1975
Application of Bruel & Kjaer Equipment to Strain Measurement.
Bruel & Kjaer, Denmark.

WOODS, J.D. 1969
On Designing a probe to measure ocean microstructure.
Underwater Science and Technology Journal.
J1 (1) pp 6-12.

WOODWARD, W.E. and G.F.APPELL 1986
Current velocity measurements using acoustic Doppler backscatter:A Review.
IEEE Journal of Oceanic Engineering, Vol OE-11, No 1, pp 3-6.

LIST OF APPENDICES.

APPENDIX.	TITLE.	PAGE.
1	Q3-3321 Silicone Moulding Rubber Specification Sheet.	A3
2	LM 607 Precision Operational Amplifier Data Sheet.	A4
3	Circuit Diagram for Turbulence Channel Pre-amplifier.	A5
4	Circuit Diagram of Differentiator.	A6
5	Design of MF 10 4th Order Elliptic Filter.	A7
6(a)	Circuit Diagram of MF 10 Switched Capacitor Filter.	A8
6(b)	Circuit Diagram of Filter Clock.	A9
7	Circuit Diagram of the Calibration Stage.	A10
8	Circuit Diagram of Maxim 630 5-15V Convertor.	A11
9	Circuit Diagram of +10V Regulator.	A12
10	Circuit Diagram of +5V Regulator.	A13
11	Circuit Diagram of +3V Strain Gauge Bridge Driver.	A14
12	Specification Sheet of Model MA Pressure Sensor.	A15
13	Calibration Record for Pressure Sensor.	A16
14	Circuit Diagram of the Bridge Driver for Pressure Sensor.	A17
15	Circuit Diagram of Pressure Channel Pre-amplifier.	A18
16	Circuit Diagram of Pressure Channel Calibration Stage.	A19
17	Details of Solid State Data Logger.	A20
18	Effect of 10 Hz Low Pass FIR Filter.	A22
19	Spectra Generated by Calibration Procedure.	A24
20	Dynamic Response of Probe: Thermocline Simulation.	A26

21	Calibration Curve Generated by Various Angles of Attack.	A27
22	Thermal Impulse Response of Probe.	A28
23	Detailed View of Strain Gauge Probe.	A29
24	Longitudinal View through Vehicle.	A30
25	Calculation of Ballast Weight required to Control Fall Speed.	A31
26	Exploded View of String Assembly.	A32
27	Deployment Simulation used to Calibrate Pressure Transducer.	A33
28	Data Logger Operating Instructions.	A34
29	Format of Multiple Data Records.	A37
30	Software Reference: Program DATASORT.	A38
31	Software Reference: Program TROUT.	A42
32	Software Reference: Program TRACE.	A50
33	Software Reference: Program SPECTRUM.	A60
34	Shear Trace Generated During Field Trials : St.Helena Bay.	A69
35(a)	Temperature Profile : Hout Bay.	A70
(b)	Deployment Pressure Characteristic : Hout Bay.	A71
(c)	Power Spectrum : Hout Bay.	A72
(d)	Shear Trace : Hout Bay.	A73

APPENDIX 1

Dow Corning® Q3-3321 RTV High Strength Silicone Elastomer. Mouldmaking Rubber.

From:
SILICONES & TECHNICA PRODUCTS
29 AUCKLAND STREET
PAARDENEILAND
PHONE: 51-2151/2

Dow Corning Silicones

Physical form	Medium viscosity two part silicone elastomer
Special properties	Very high tear strength, low modulus, high elongation
Applications	High strength flexible moulds also, potting and encapsulation of components, fabrication of silicone rubber parts

Description

Dow Corning® Q3-3321 RTV is a two part, medium viscosity silicone rubber. The base is white with a typical viscosity of 45,000 mPa.s and the clear catalyst has a viscosity of 100 mPa.s.
The base to catalyst mixing ratio is 20 : 1 by weight and the catalysed mixture cures at room temperature, within 24 hours to a flexible silicone elastomer.

General Properties

- High tensile strength (6MPa)
- Very high tear strength (24kN/m)
- High Elongation (400 %)
- Working time of 1 hour with catalysed mixture
- Material cures at room temperature within 24 hours even in thick section
  No exotherm during cure
- Cure not sensitive to inhibition
- Low shrinkage on cure (0.5 %)
- Excellent reproduction of fine detail
- Exceptional release characteristics
- Good heat stability
- Remains flexible down to - 65 °C
- Excellent dielectric properties over wide temperature range.

Applications

Dow Corning® Q3-3321 RTV is primarily designed for mouldmaking applications, where its viscosity and flow characteristics allow an excellent reproduction of fine detail. The low modulus, high tear strength, high elongation and excellent release characteristics permit easy demoulding and give a long mould life, even when deep undercuts are present.

Because of these features it is often possible to make a one part mould where previously a two part mould had to be used. Moulds made from Q3-3321 RTV can be used to cast a wide variety of materials, including : polyesters, polyurethanes, epoxies, plaster, wax and low melting point metal alloys.

Applications for these moulds include :
- Decorative furniture panels, grills and carvings
- Jewellery, buttons and decorative parts
- Works of art, statues, candles
- Prototype engineering parts and models.

Although primarily designed for mouldmaking, Dow Corning® Q3-3321 RTV can also be used to encapsulate electrical or electronic devices, where it provides excellent environmental protection from moisture, dirt, corona, weathering and corrosive atmospheres. Other applications include gasketing, sealing and the fabrication of silicone rubber parts.

Typical Properties

a) Materials as supplied	Q3-3321 Base	Q3-3321 Catalyst
Colour	white	clear
Viscosity mPas	45,000	100
Mixing Ratio by weight	20	1

b) Catalysed Mixture	
S.G.	1.21
Pot Life*	40 minutes
Working time	1 hour
Cure time	24 hours

* defined as time for viscosity to double

c) Cured Material Tested according to ASTM after 7 days at 25 °C	
Tensile Strength	6 MPa
Elongation at break	410 %
Tear Strength, die B.	24 kN/m
Modulus at 100 %	0.7 MPa
Hardness	22 Shore A
Linear Shrinkage	0.5 %

These properties are not affected by heat aging for 24 hours at 150 °C.

These values are not intended for use in preparing specification. Please contact Dow Corning Europe prior to writing specifications.

How to Use

To ensure maximum reliability and performance, the following information should be read carefully.

Preparation

The original from which the mould is to be made should be thoroughly cleaned of dirt and all contaminants. Where solvents are used for the cleaning, care should be taken to ensure they are compatible with the original and sufficient time should be allowed for them to fully evaporate. If required, the original and the holding box should be coated with a release agent. This is particularly important with porous substrates. Suitable release agents are petroleum jelly or soap solutions.

Mixing

The base and the catalyst should be stirred prior to use. They should then be thoroughly mixed together in a ratio of 20 parts base : 1 part catalyst, by weight.

Hand mixing or mechanical mixing are satisfactory but care should be taken to avoid entrapping too much air or splashing the catalyst.

Mixing should be completed in 2-4 minutes and should not generate excessive heat (35 °C maximum).

APPENDIX 2

National Semiconductor Corporation

PRELIMINARY
January 1987

LM607/LM607A/LM607B Precision Operational Amplifier

General Description

The LM607 series of precision operational amplifiers are trimmed at wafer sort to extremely low values of offset voltage. Advanced circuit design and testing techniques allow guaranteed drift specifications as low as 0.3 µV/°C with offsets as low as 25 µV.

Other input parameters are equally impressive. The typical open loop voltage gain of 5 Million yields extremely low error in high-gain applications. CMRR and PSRR are typically 140 dB.

Using Super-Beta transistors in the front end enables the LM607 to operate at high input stage current while maintaining low values of input bias current (1 nA typ.). This gives the part its low input voltage noise: 6.5 nV/√Hz.

High operating currents also help give the LM607 its high gain bandwidth product of 1.8 MHz and slew rate of 0.7 V/µs. Despite its higher speed, the LM607 draws less supply current than OP-07 types: only 1 mA at ±15V supplies.

Features

■ Low V_{OS}	LM607A:	25 µV max
■ Low drift	LM607A:	0.3 µV/°C max
■ Drift *100% tested*: A and B grades		
■ High gain	LM607A:	5 million min
■ High CMRR	LM607A:	124 dB min
■ High PSRR	LM607A:	120 dB min
■ Low noise		6.5 nV/√Hz @ 1 kHz
		9 nV/√Hz @ 10 Hz
■ High speed		1.8 MHz gain-bandwidth
		0.7V/µs slew rate
■ Low supply current		1 mA
■ Wide input common mode		±13V
■ Wide supply range		±3V to ±18V
■ Overcompensation		Allows driving high C_L

Typical Performance Characteristics

Voltage Gain

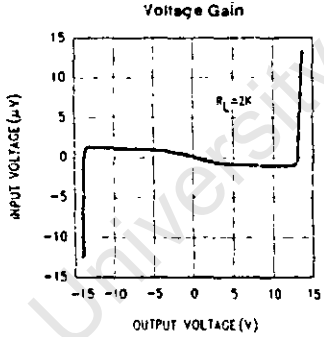

TL/H/8787-1

Input Noise Voltage

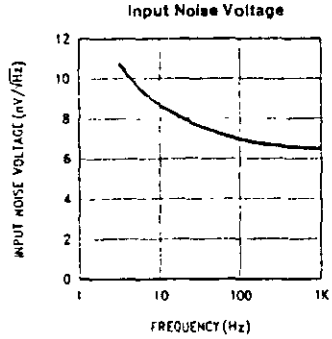

TL/H/8787-2

RRD-B20M115/Printed in U.S.A.

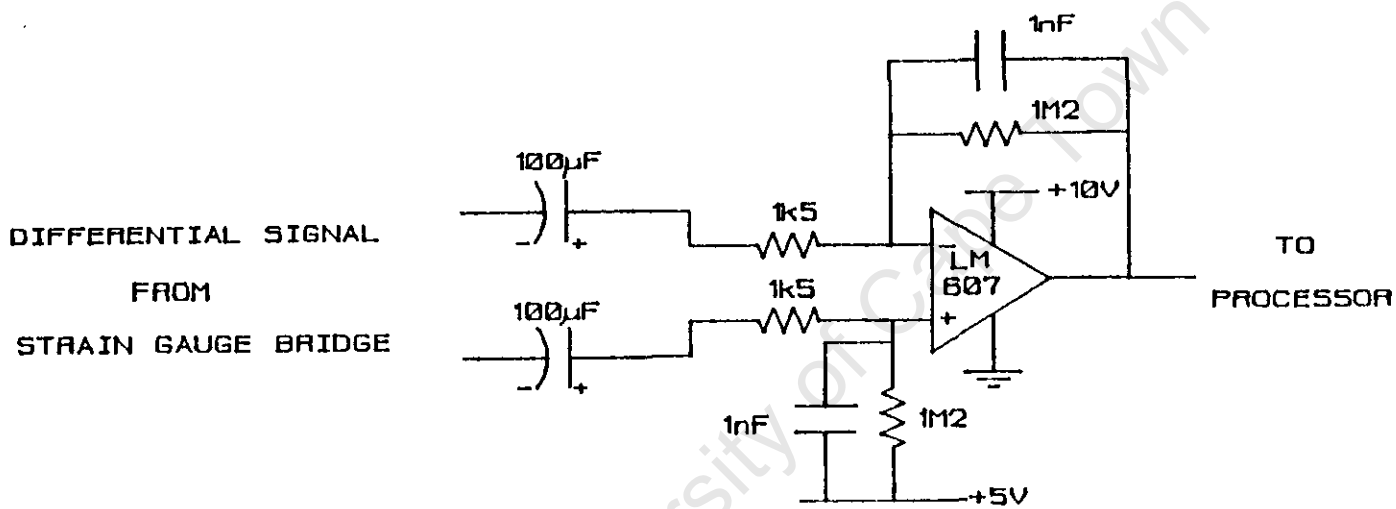

TITLE	DATE
PRE-AMPLIFIER (SEMICONDUCTOR PROBE)	SEPTEMBER 1988

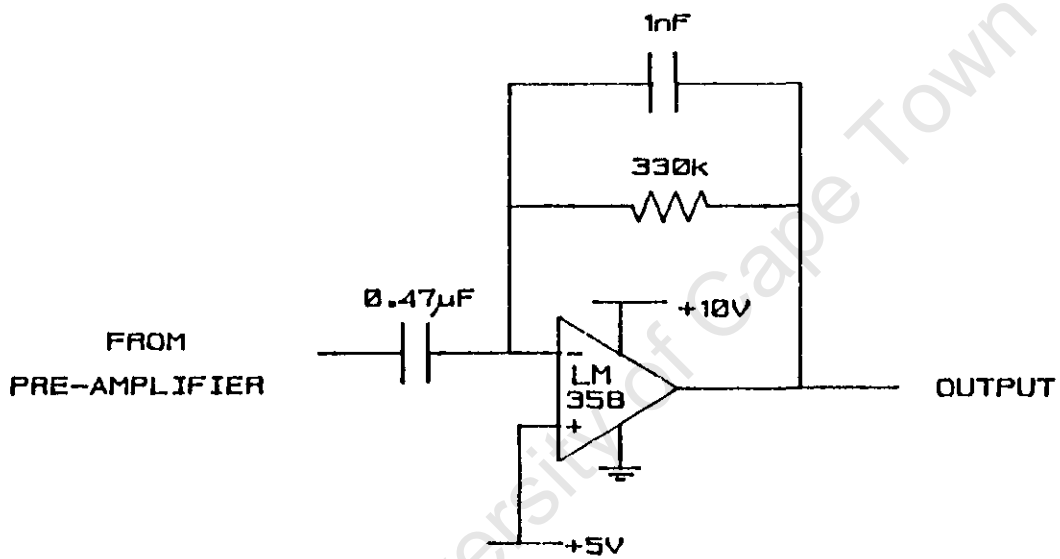

TITLE	DATE
DIFFERENTIATOR	SEPTEMBER 1988

APPENDIX 5

4^{TH} ORDER ELLIPTIC FILTER DESIGN

Specifications: $A_{max} = 0.5dB$
$A_{min} = 50dB$
$f_s/f_c = 2.5$
$H_0 = 1$

From the Nomograph 6.1.3. of the National Semiconductor Handbook, it can be seen that a fourth order filter is required.

Using section 6.46:

$f_{OA} = 0.6322 \times 100Hz = 62.33Hz$
$f_{OB} = 1.0311 \times 100Hz = 103.11Hz$
$f_{ZA} = 2.6893 \times 100Hz = 268.93Hz$
$f_{ZB} = 6.2975 \times 100Hz = 629.75Hz$
$Q_A = 0.7164$
$Q_B = 3.2215$

Arrange in ascending order of Q, i.e. stage B second.

1) Choose $R_{1A} = 20K\Omega$ (Convienient input impedence)

2) Unity gain at D.C. requires $R_4 = R_1$
$R_{4A} = -H_{OLPA} \times R_{1A}$
$= 20K\Omega$

3) $R_{2A} = R_{4A} \times (f_{OA}2/f_c2) = 7.770K\Omega$

4) $R_{3A} = Q_A \times R_{2A}R_{4A} = 8.931K\Omega$

5) Choose $R_{LA} = 20K\Omega$

6) $R_{HA} = R_{LA} \times (f_{nA}2/f_c2) = 144.6K\Omega$

7) $R_{4B} = -H_{OLPB} \times R_{LA} = 20K\Omega$

8) Second Stage centre frequency: $R_{2B} = R_{4B} \times (f_{OB}2/f_c2)$
$= 21.26K\Omega$

9) $R_{3B} = Q_B \times R_2R_4 = 66.43K\Omega$

10) Choose $R_{LB} = 20K\Omega$ for adequate load impendence.

11) $R_{HB} = R_{LB} \times (f_{nB}2/f_c2) = 793.2K\Omega$

12) $R_G = (-R_{LB} \times H_{OLP})/(H_{LPA} \times H_{LPB}) = 20K\Omega$

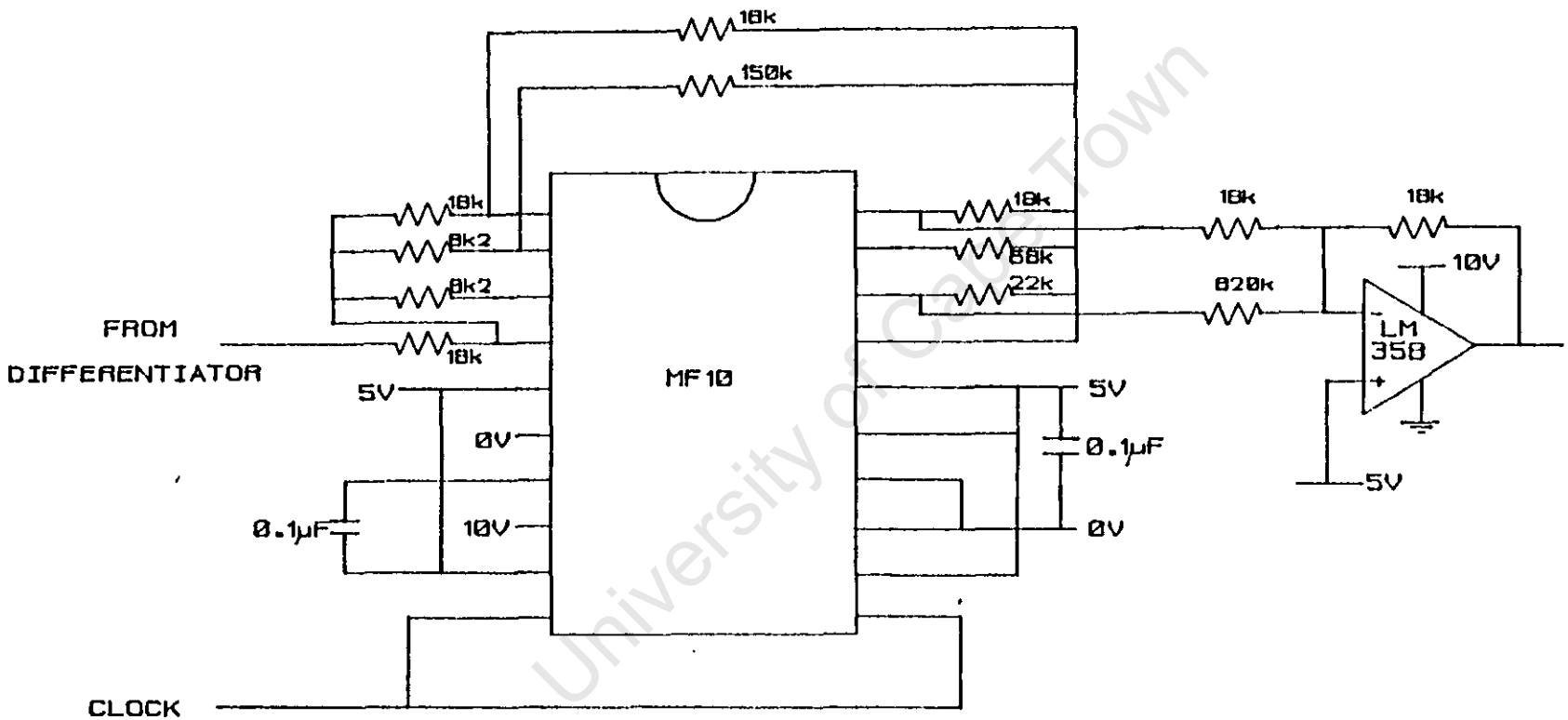

TITLE

SWITCHED CAPACITOR FILTER
(FOURTH ORDER ELLIPTIC)

DATE

SEPTEMBER 1988

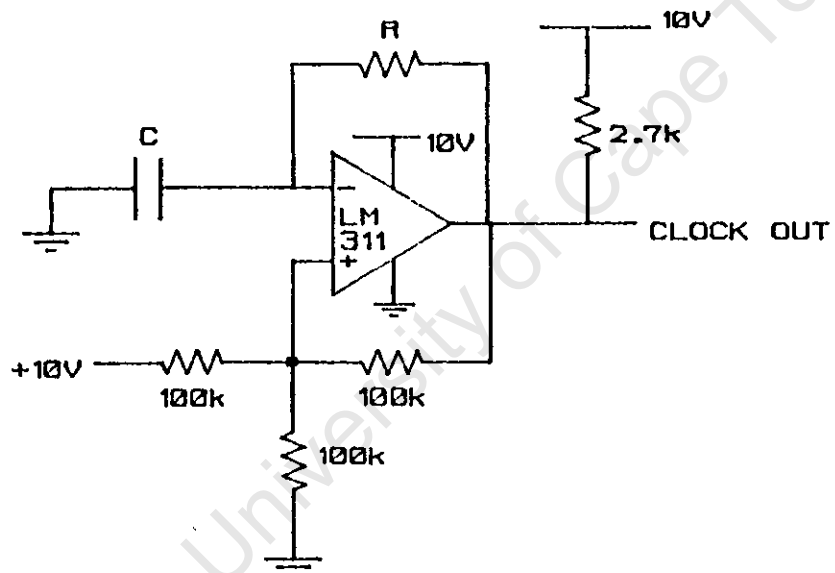

CLOCK FREQUENCY

$$f = \frac{0.56}{RC}$$

R= 94k

C= 1nF

TITLE	DATE
FILTER CLOCK	SEPTEMBER 1988

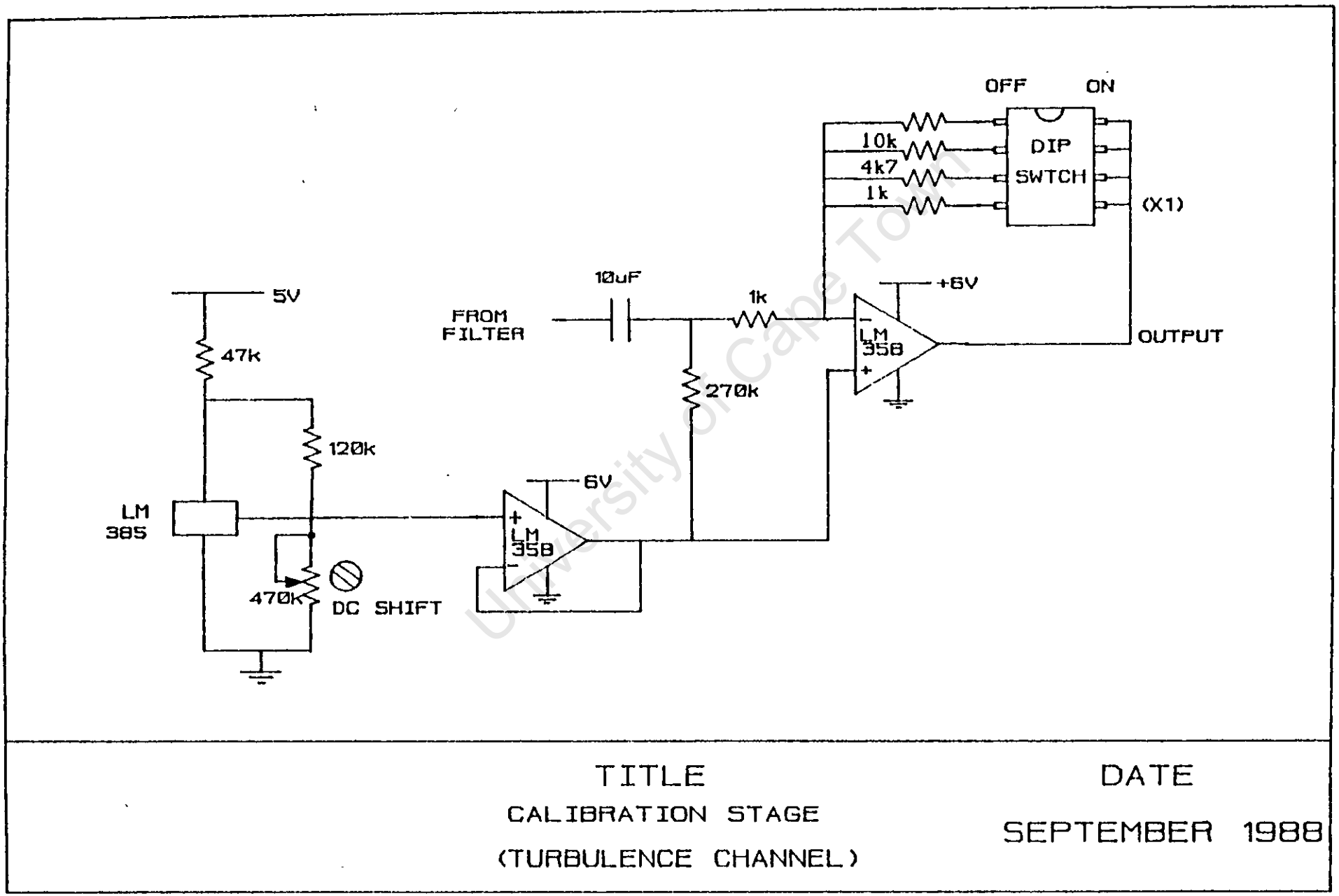

APPENDIX 8

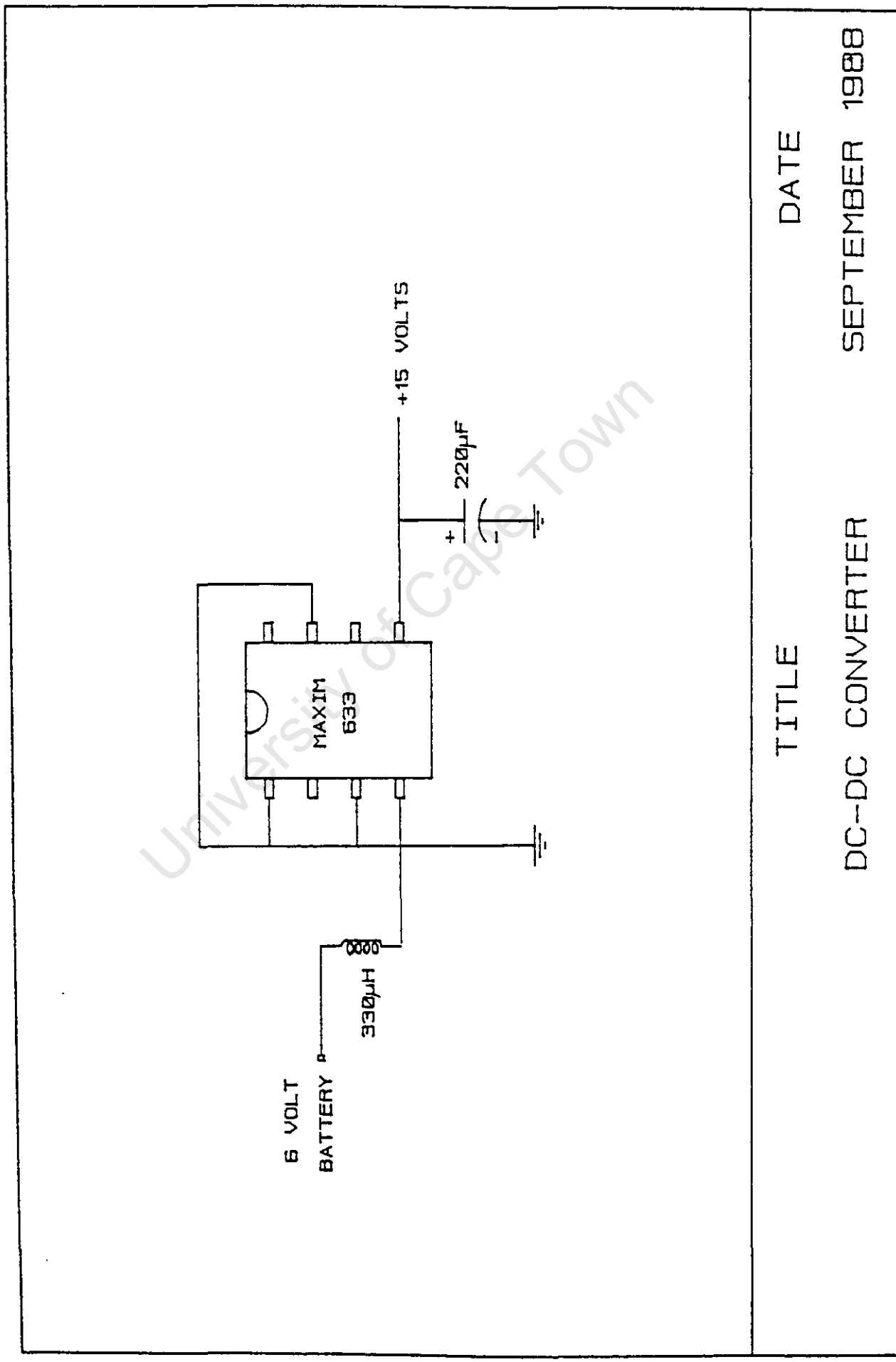

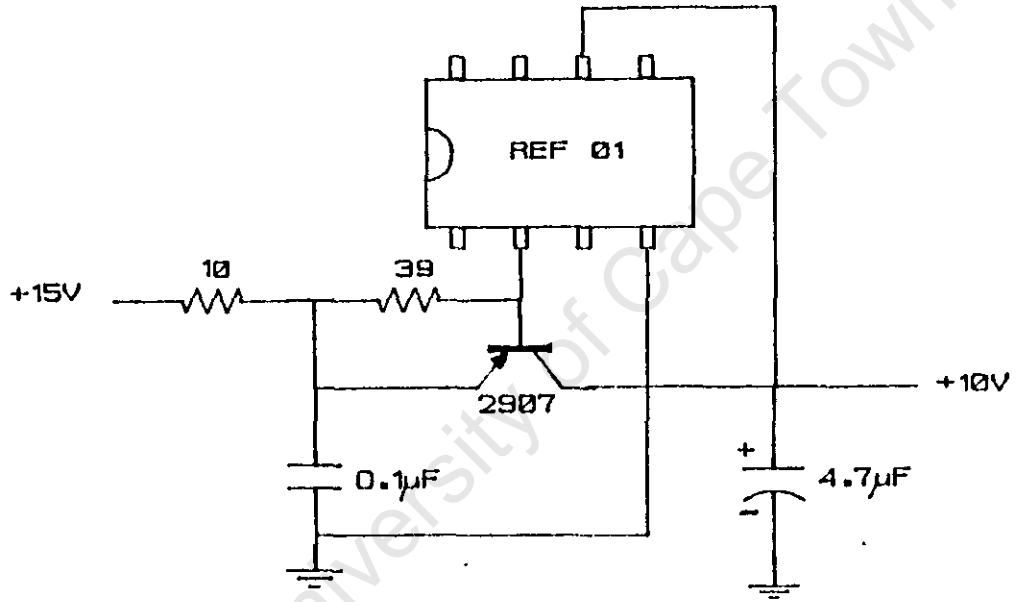

(Resistance values in ohms)

TITLE	DATE
10 VOLT REFERENCE	SEPTEMBER 1988

APPENDIX 10

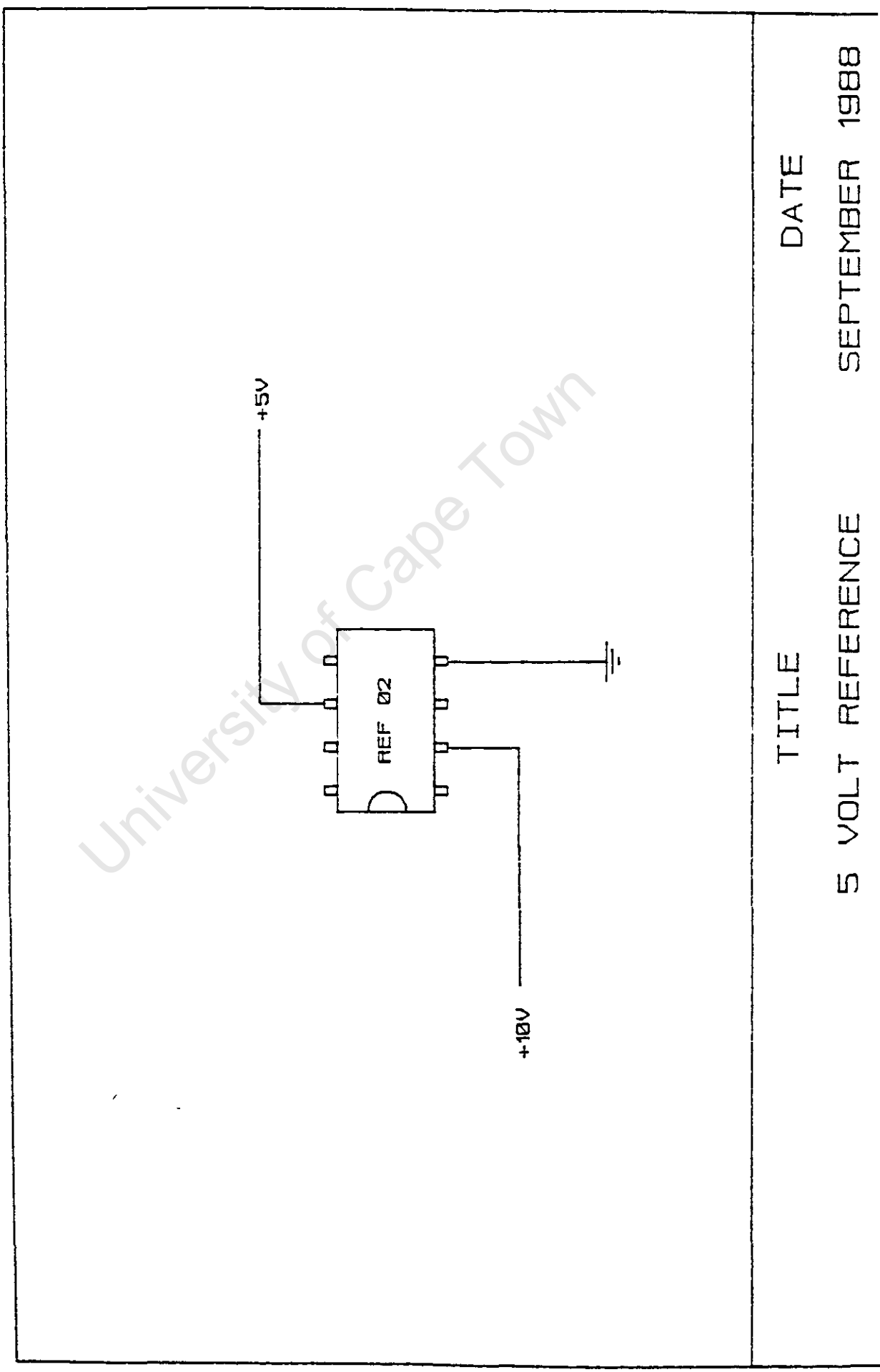

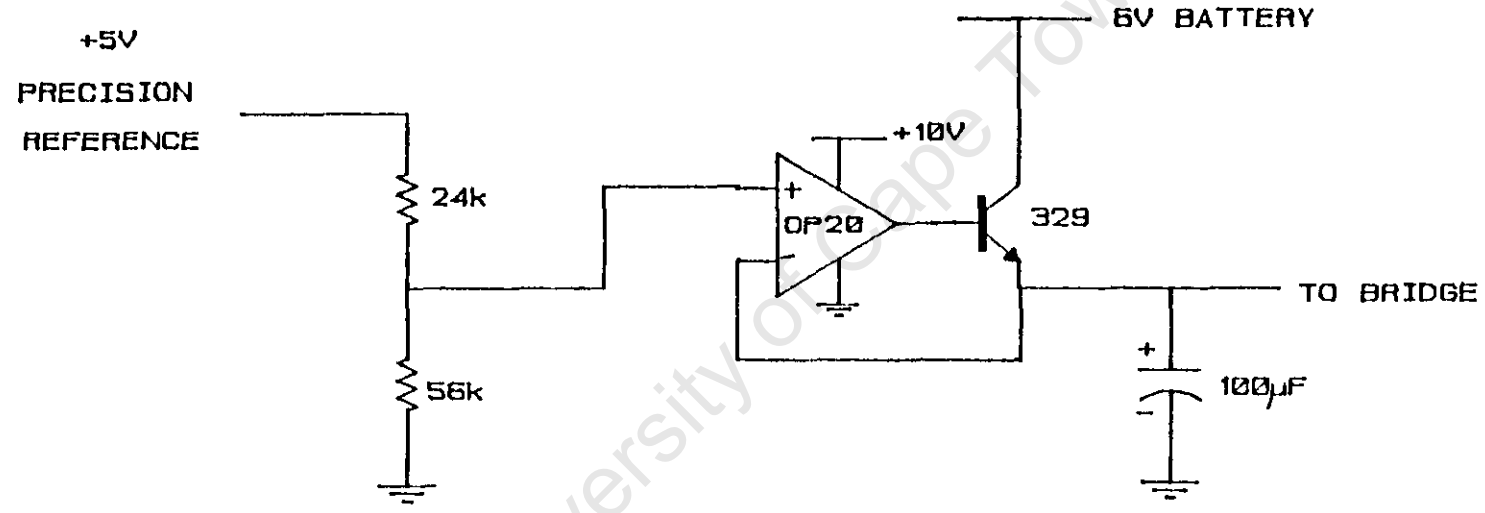

TITLE

STRAIN GAUGE BRIDGE SUPPLY
(TURBULENCE CHANNEL)

DATE

SEPTEMBER 1988

APPENDIX 12

Pressure Transducer Specification Sheet

Miniaturized High Accuracy Gage/Absolute Pressure Transducers

Models MG and MA

New

Small size

0.25% Accuracy

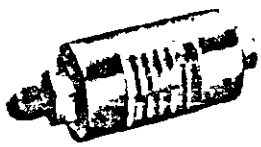

Models MG (Gage) and MA (Absolute) miniaturized, high accuracy pressure transducers are designed for demanding aerospace and industrial applications. These models combine light weight and small size with high accuracy and rugged construction. Pressure ranges from 15 to 10,000 psi are measured within +/-0.25% of full scale. Models MG and MA measure 1.75" in length by 1-1/8" or 1-1/4" in diameter.

		Model MG (Gage) Order Code BP911	Model MA (Absolute) Order Code BP912
PERFORMANCE	Pressure ranges	25 to 500 psig	15 to 10,000 psia
	Accuracy (min)	+/-0 25% F.S.	+/-0.25% F.S.
	Non-Linearity (max)	+/-0.15% F.S.	+/-0.15% F S.
	Hysteresis (max)	+/-0.10% F.S.	+/-0.10% F.S.
	Non-Repeatability (max)	+/-0.05% F.S.	+/-0.05% F.S.
	Output	3mv/v	3mv/v
	Resolution	Infinite	Infinite
ENVIRONMENTAL	Temperature, Operating	-65° F to 300° F	-65° F to 300° F
	Temperature, Compensated	60° F to 160° F	60° F to 160° F
	Temperature Effect		
	- Zero (max)	0 005% F.S./° F	0 005% F.S./° F
	- Span (max)	0.005% Rdg./° F	0.005% Rdg./° F
ELECTRICAL	Strain Gage Type	Bonded foil	Bonded foil
	Excitation (calibration)	10VDC	10VDC
	Bridge Resistance	350 ohm	350 ohm
	Connector Wiring	#2 (See P. 143)	#2 (See P. 143)
	Electrical Termination (std)	PT1H-10-6P or equiv.	PT1H-10-6P or equiv.
	Mating Connector (not incl.)	PT06A-10-6S or equiv.	PT06A-10-6S or equiv.
MECHANICAL	Media	Gas, Liquid	Gas, Liquid
	Overload-Safe	50% Over Capacity	50% Over Capacity
	Pressure Port 15 - 500 psi	1/4-18NPT Male	1/4-18NPT Male
	750 - 1500 psi	N.A.	1/4-18NPT Male
	2000 - 10,000 psi	N.A.	1/4-18NPT Female
	Wetted Parts Material	17-4 PH Stainless	17-4 PH Stainless
	Type (Gage, Abs.)	Gage	Absolute
	Case Material	Stainless	Stainless
	Weight	7 oz.	7 oz.

DIMENSIONS

Model MG (Order Code BP911)

Available Ranges	D"	L"
25; 50; 75; 100; 150 psig	1.25	1.75
200; 300; 500 psig	1.25	1.75

Model MA (Order Code BP912)

Available Ranges	D"	L"
15 psia	1.25	1.75
25; 50; 75; 100; 150; 200; 300 psia	1.125	1.75
500; 750; 1000; 1500; 2000; 3000 psia	1.125	1.75
5000; 7500; 10,000 psia	1.125	1.75

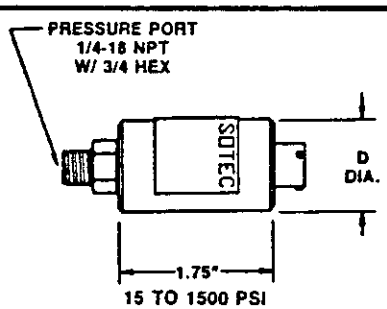

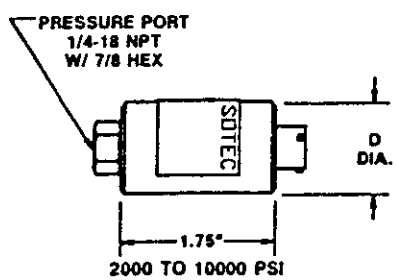

OPTIONS Temperature compensated 1b, 1c, 1d, 1e, 1f; Pressure ports 5a (≤1500 psi only), 5c (≤1500 psi only), 5d (≤1500 psi only); Electrical termination 6e; Precision internal shunt cal 8a (See P. 154)

PREMIUM OPTIONS 1g, 1i; 5c (≥2000 psi only); 6j, 6i; 12a, 12b (See P. 154)

ACCESSORIES Mating connectors and connector/cable assemblies; Pressure port adapters (See P. 138)

APPENDIX 13

SENSOTEC

PRESSURE TRANSDUCER CALIBRATION RECORD

TYPE _____
MODEL NO. MA/5518-09-01
SERIAL NO. 210161
CAPACITY 0-30 PSIA
DATE 11-16-88

Excitation Volts 10 DC/AC RMS
Compensated Temperature Range 30 °F to 130 °F

	% Capacity	Output	
	0	0	Millivolts
Ascending	50	15.041	Millivolts
	100	30.108	Millivolts
Descending	50	15.042	Millivolts
	0	0	Millivolts

RESISTANCE:
Input = 457.9 Ohms
Output = 351.0 Ohms
Leakage = 710 Kmeg Ohms

COLOR CODE
Red = + Input
White = + Output
Green = - Output
Black = - Input

Connector Model C825-10-6F
Non Standard ☐ Standard ☒
Input
+ A&B
- C&D
Output
-E
+F

Pressure Port Fitting 7/16-18 NPT Mating Connector Model PT06A-10-6

Shunt Resistor Value of 59K ohms across
C, D + E = 14.665 Millivolts Output

Accepted & Certified Thomas Drage
Date 11-16-88

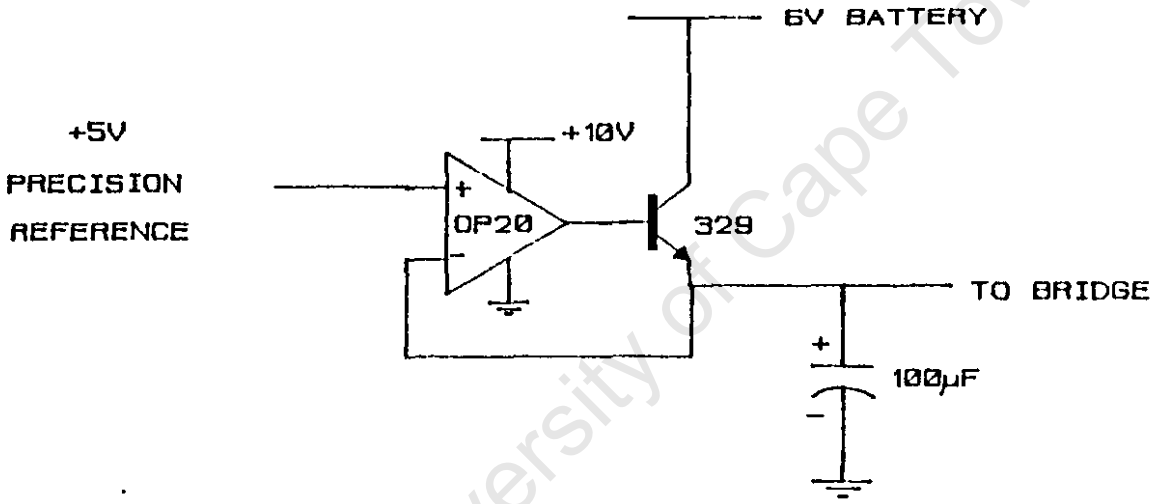

TITLE

STRAIN GAUGE BRIDGE SUPPLY

(PRESSURE CHANNEL)

DATE

SEPTEMBER 1988

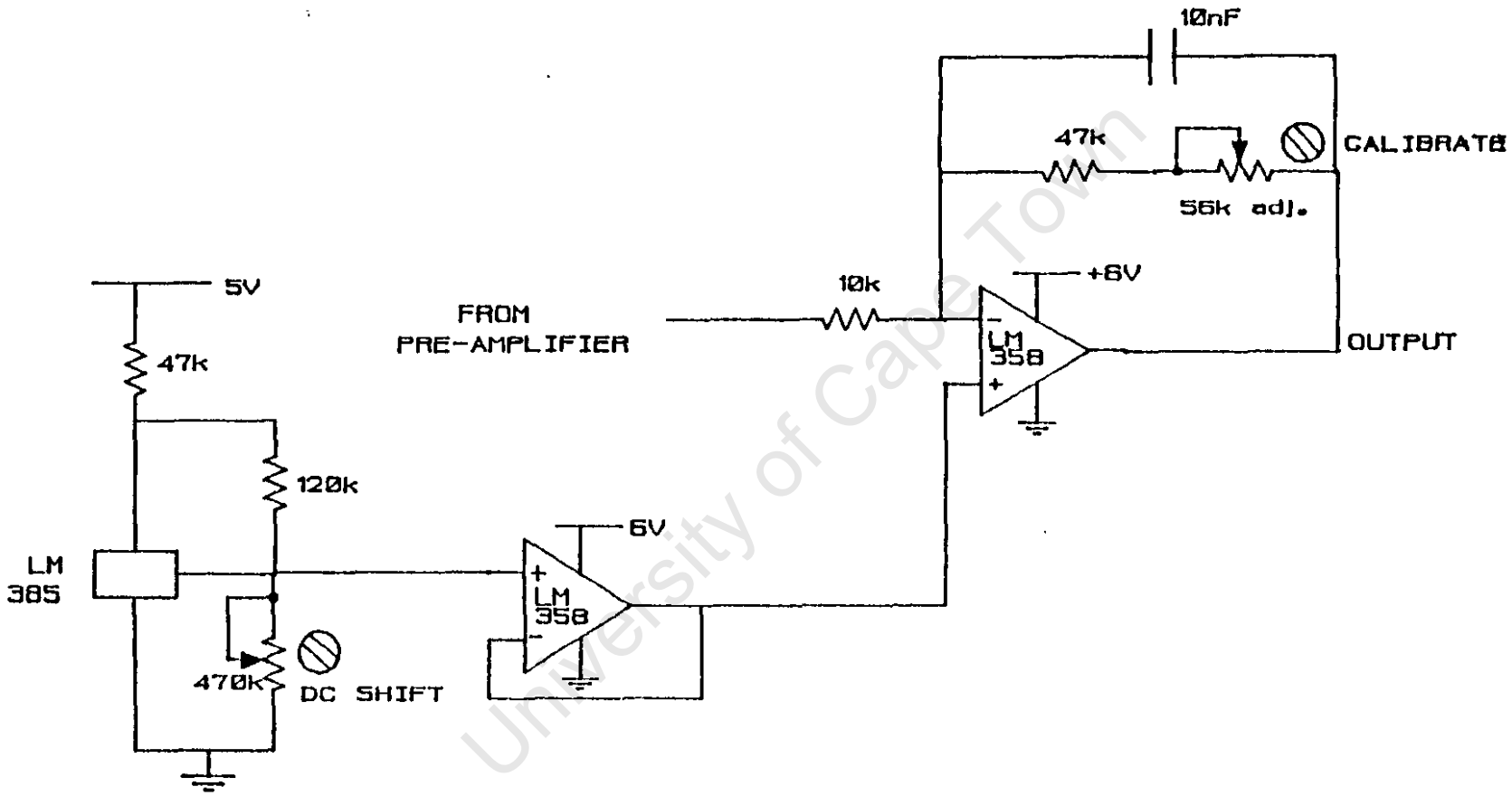

TITLE

CALIBRATION STAGE
(PRESSURE CHANNEL)

DATE

SEPTEMBER 1988

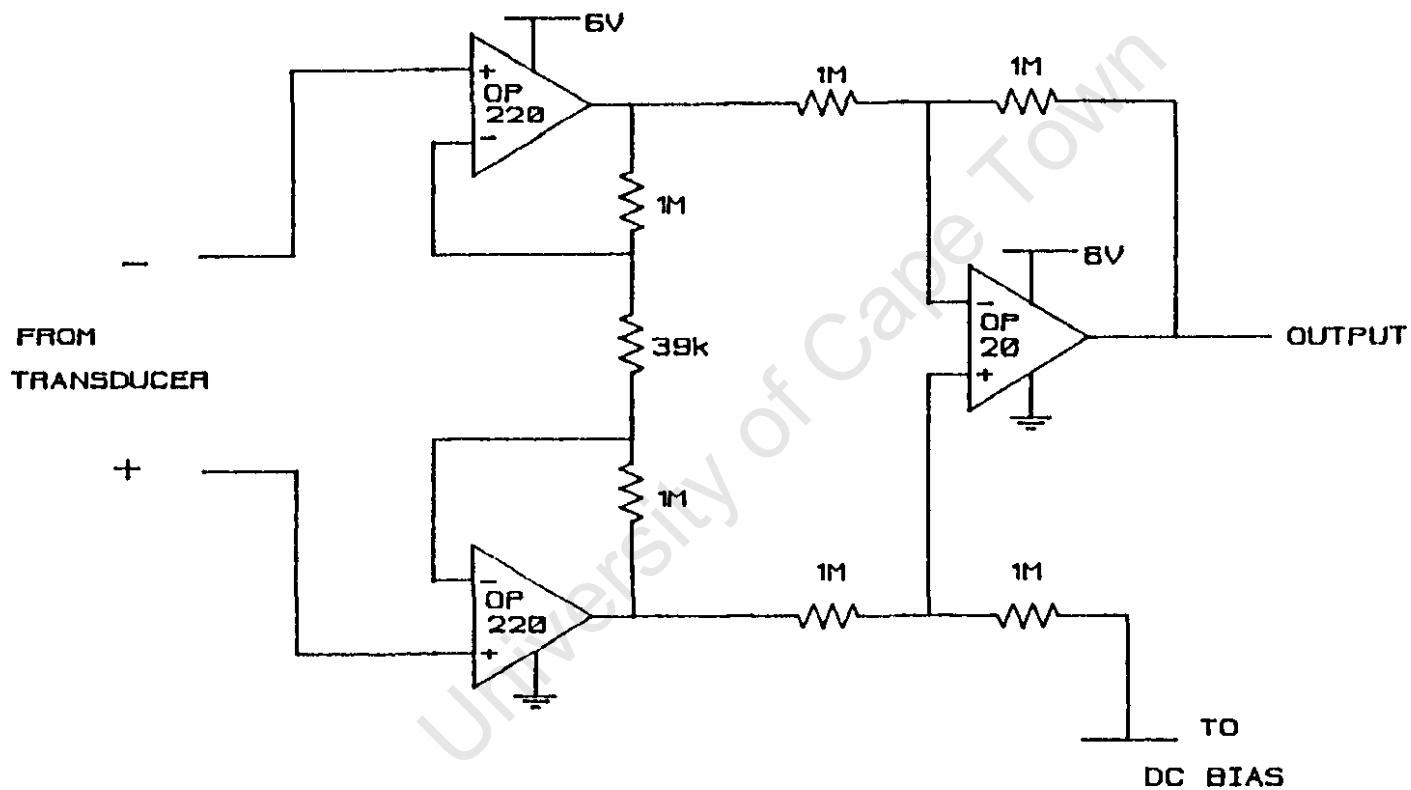

TITLE

PRE-AMPLIFIER
(PRESSURE CHANNEL)

DATE

SEPTEMBER 1988

APPENDIX 17

SOLID STATE DATA-LOGGER

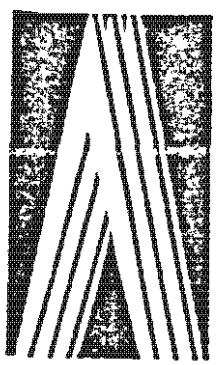

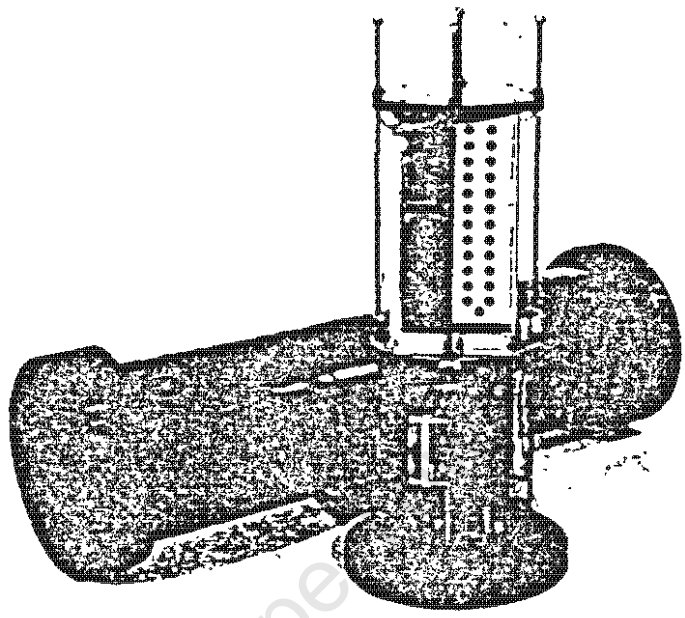

The NRIO solid-state data-logger is used as the heart of most underwater and field instrumentation developed at NRIO. It was designed out of a need for an in situ, large capacity, low powered data-logger and makes use of large CMOS static RAM devices to store data. The CMOS microcomputer which controls the data storage and retrieval can also be programmed to perform control tasks related to any specific instrument. A conventional PC computer is used to recover data from the solid-state memory-module .

DATA STORAGE MODULE

Capacity	* Can be any multiple of 32 k bytes, up to 6+ M bytes. Typically Ø,5 M bytes to 2,2 M byte.
Modules	* Each plug-in module can house sixteen 32 k byte RAMs giving a capacity of Ø,5 M byte/module.
Security	* On-board low-voltage detect circuit prevents false writes to memory under low battery conditions.
Backup	* A standby battery provides backup power to the memory-module for in excess of 9 months.

MICROCOMPUTER

CPU	* The CPU is designed around the Motorola MC146805. User programs can drive i/o to suit requirements of specific instruments.
RTC	* The microcomputer contains an RTC module which can supply full calendar and time information for control, and data indexing.
MEMO	* The skeleton operating system, MEMO, contains a monitor for testing and many routines to support likely data logging tasks.
Data	* Data storage and retrieval are managed by the CPU.

APPENDIX 17(cont.)

DATA RETRIEVAL

Opto link * Communication with the data-logger is done optically. With instruments in underwater housings, data are transmitted via an optical pipe which passes through the lids of the containers. This makes it possible to communicate with instruments after they have been sealed for deployment, or even while they are deployed.

Interface * A simple interface converts the optical signals to RS232 levels for data retrieval by a PC.

Milker * A portable data retrieval (milking) device is available to transport data to a PC. This device also has other useful operational and testing functions.

READALL * READALL is the data retrieval program for the PC. It is written in GWBASIC and provides amongst othe things, routines for data retrieval, data plotting and the generation of calibrated ASCII data files.

POWER SOURCE

Battery * The data-logger is powered by rechargeable sealed lead acid batteries. Battery life varies with the data logging task, but typical life will be 3 to 6 months. Longer times have been obtained.

Standby * A 3 volt standby alkaline-battery is used to support the memory-module should the main battery fail. For longer life and greater security, a lithium battery can be used.

APPLICATIONS

This data-logger has already been used in a variety of instruments developed at NRIO. The more significant of these are:

* Vector Averaging Current Meter
* Electro-magnetic Current Meter
* Wavestaff Water Level Recorder
* Pressure Transducer Water Level Recorder
* Acoustic Water Level Recorder

Reliability has been high and the solid-state memory-module ha proved itself as a safe and convenient data storage medium.

CSIR NRIO
Stellenbosch Ø2231-75101 Contact person: S G Holroy

APPENDIX 18

Effect of 10 Hz Low Pass F.I.R. Filter

Response Before Filtering:

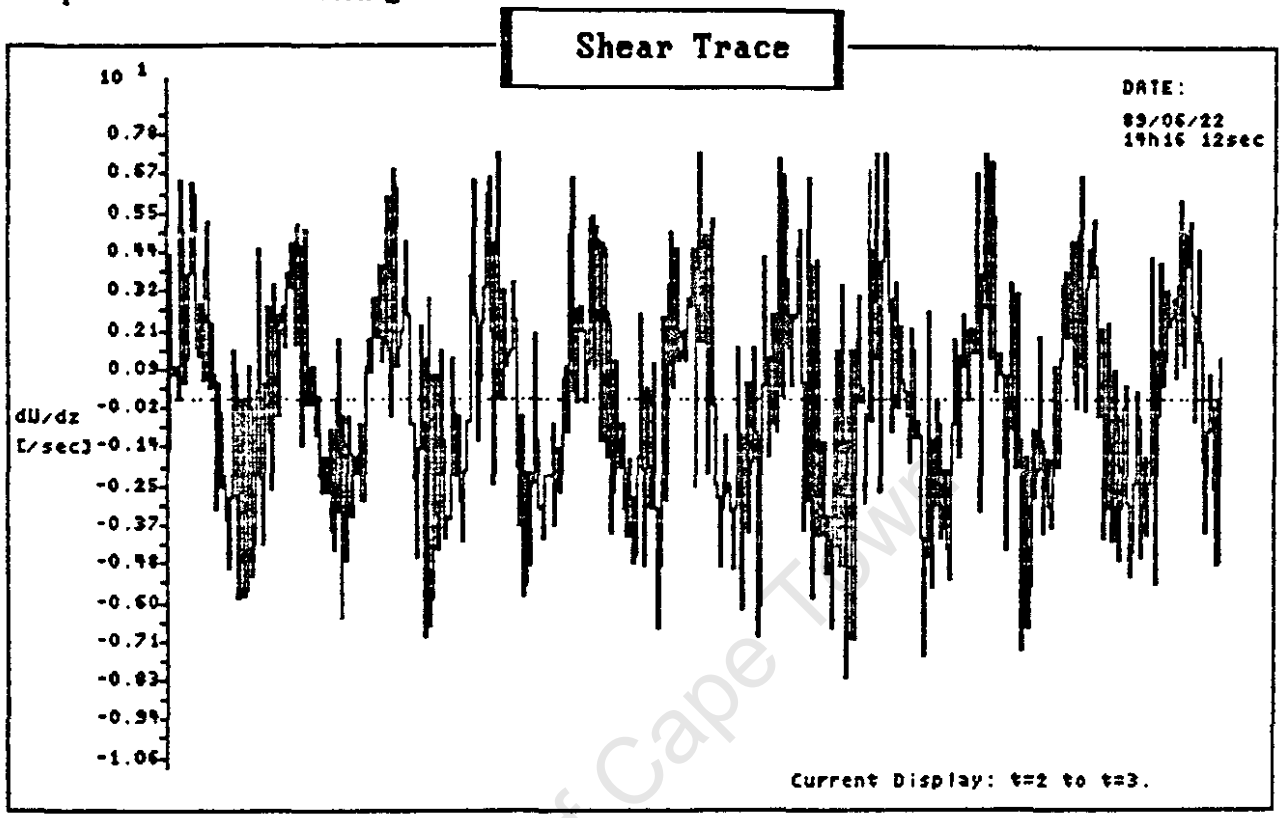

Filtered Response:

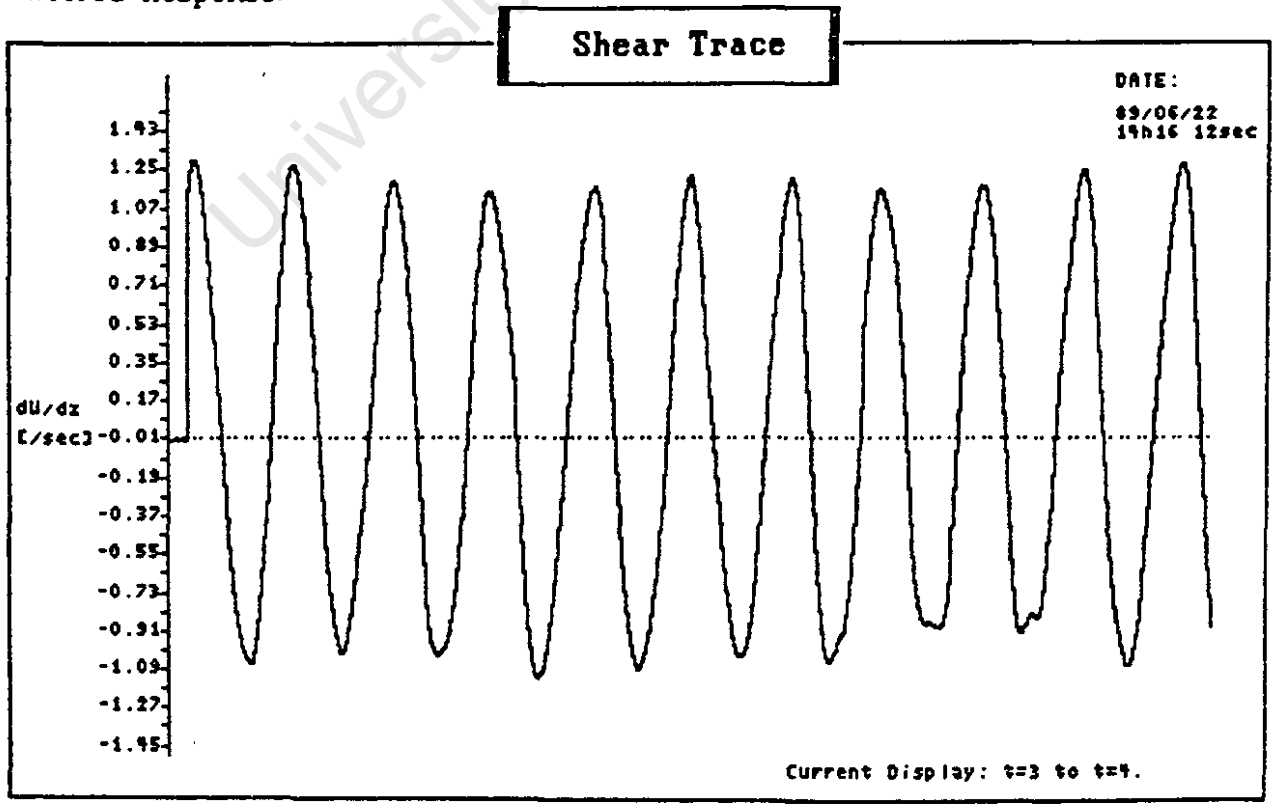

* Excitation Frequency = 10.7 Hz.

APPENDIX 18(cont.)

Effect of 10 Hz Low Pass F.I.R. Filter

Response Before Filtering:

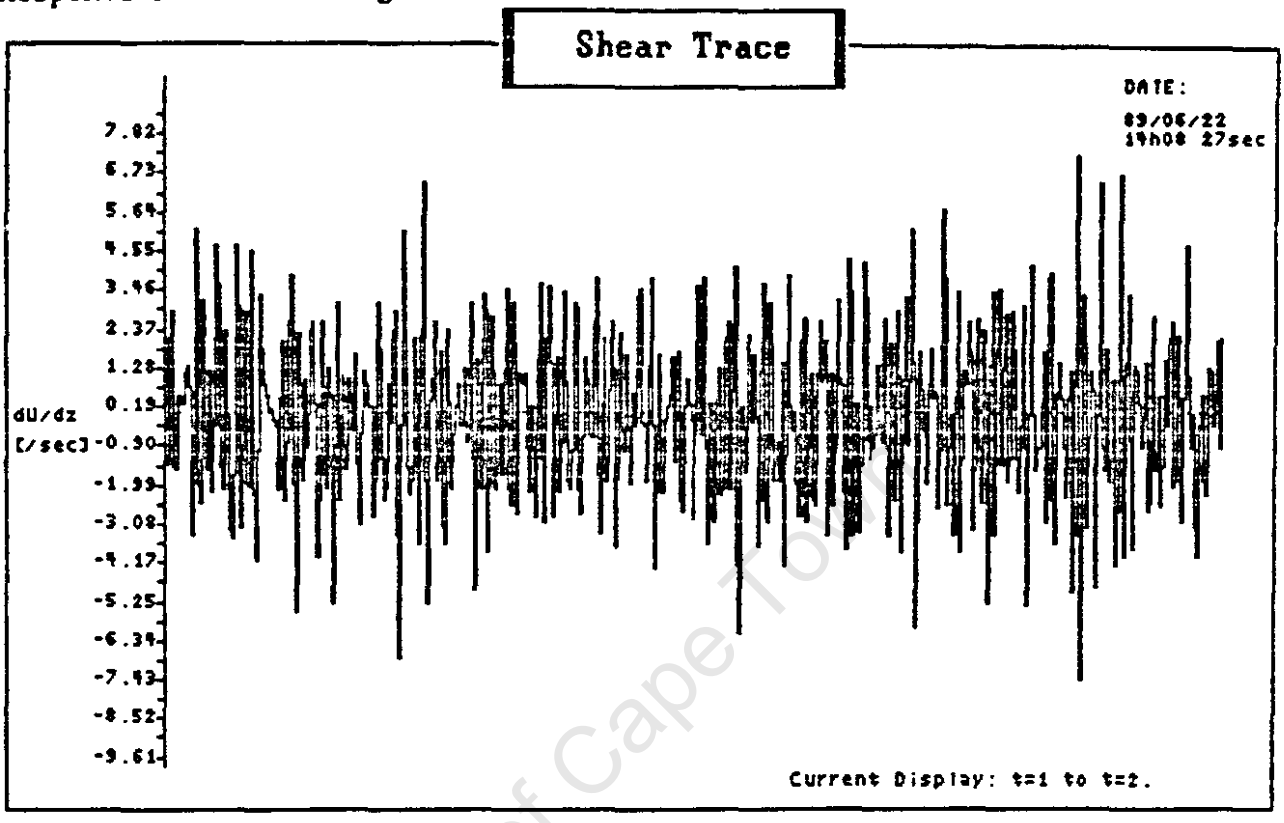

Filtered Response:

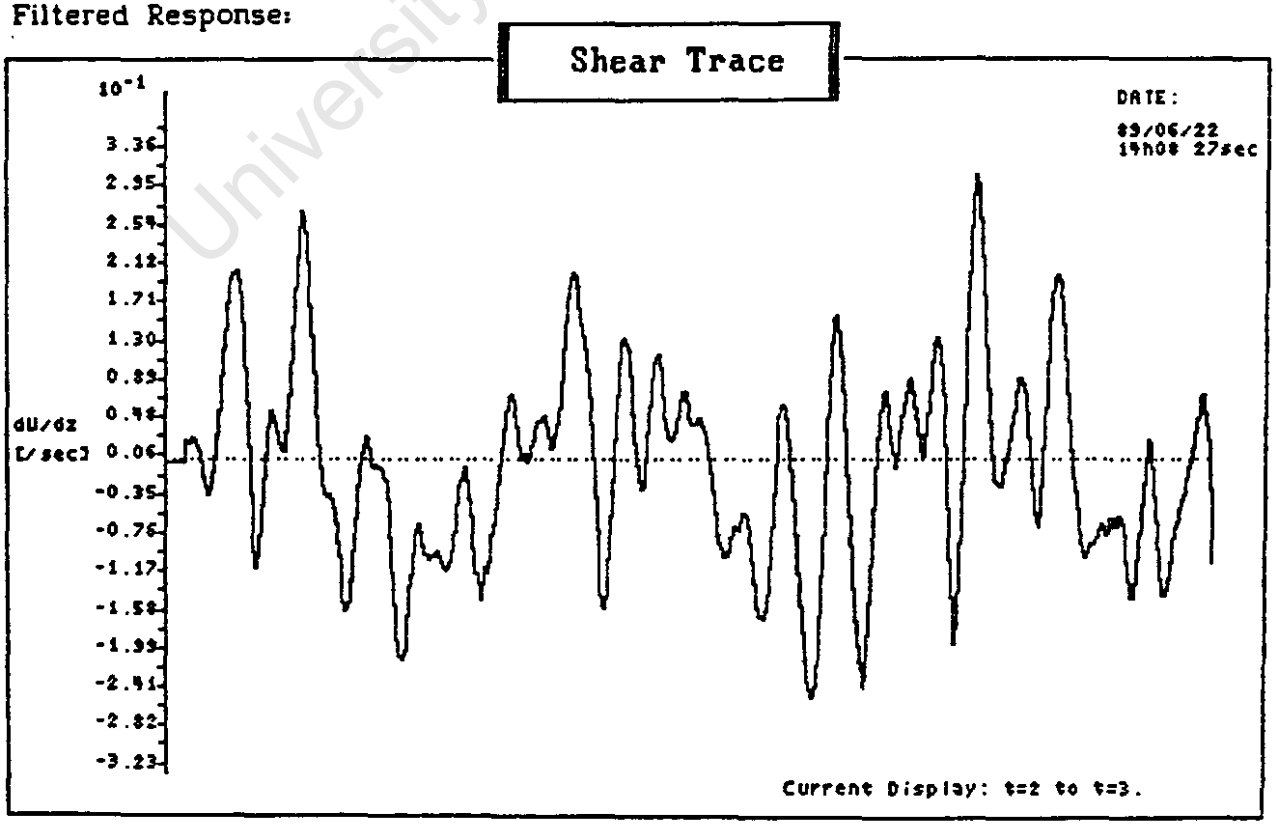

* Excitation Frequency = 2.4 Hz.

APPENDIX 19

Spectra Generated by Calibration Procedure

Spectrum A: Excitation Frequency = 2.4 Hz.
$\alpha_m = 3^\circ$

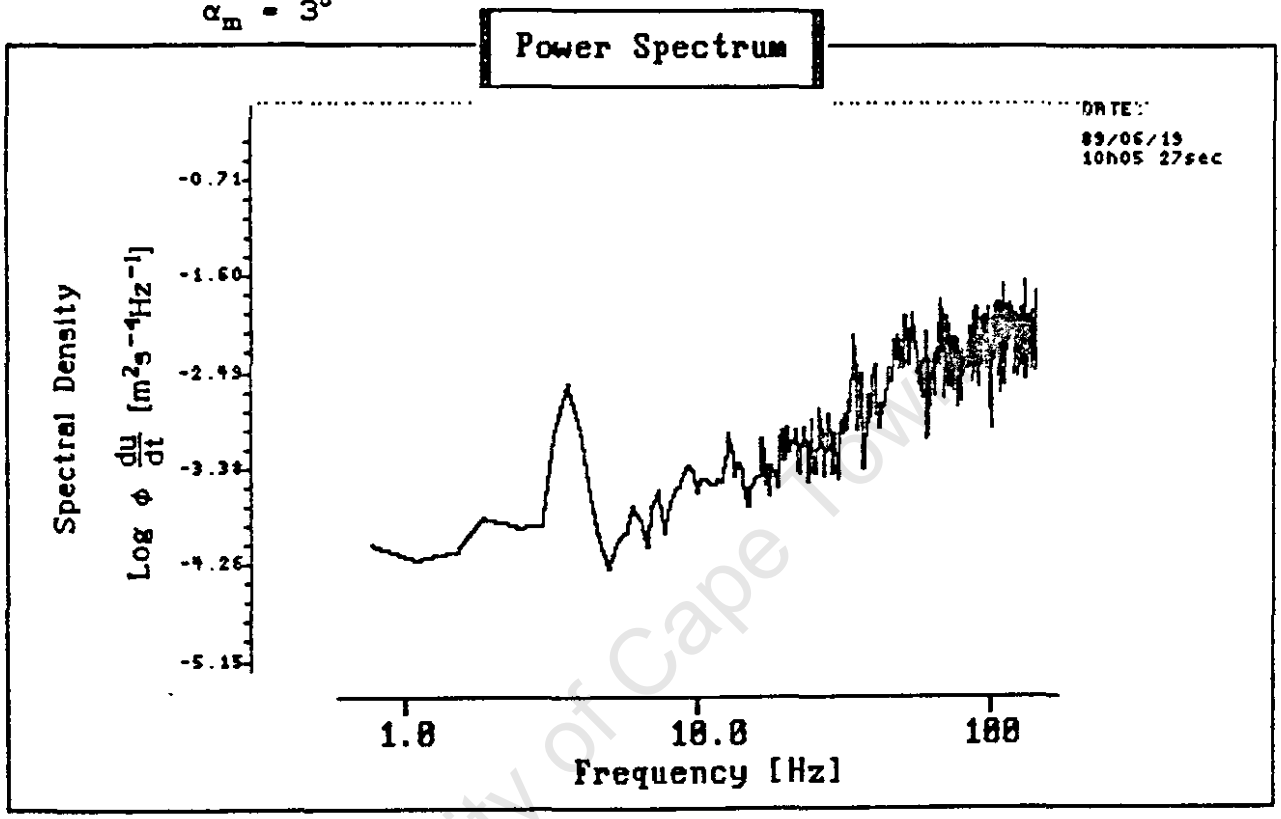

Spectrum B: Excitation Frequency = 9.8 Hz.
$\alpha_m = 3^\circ$

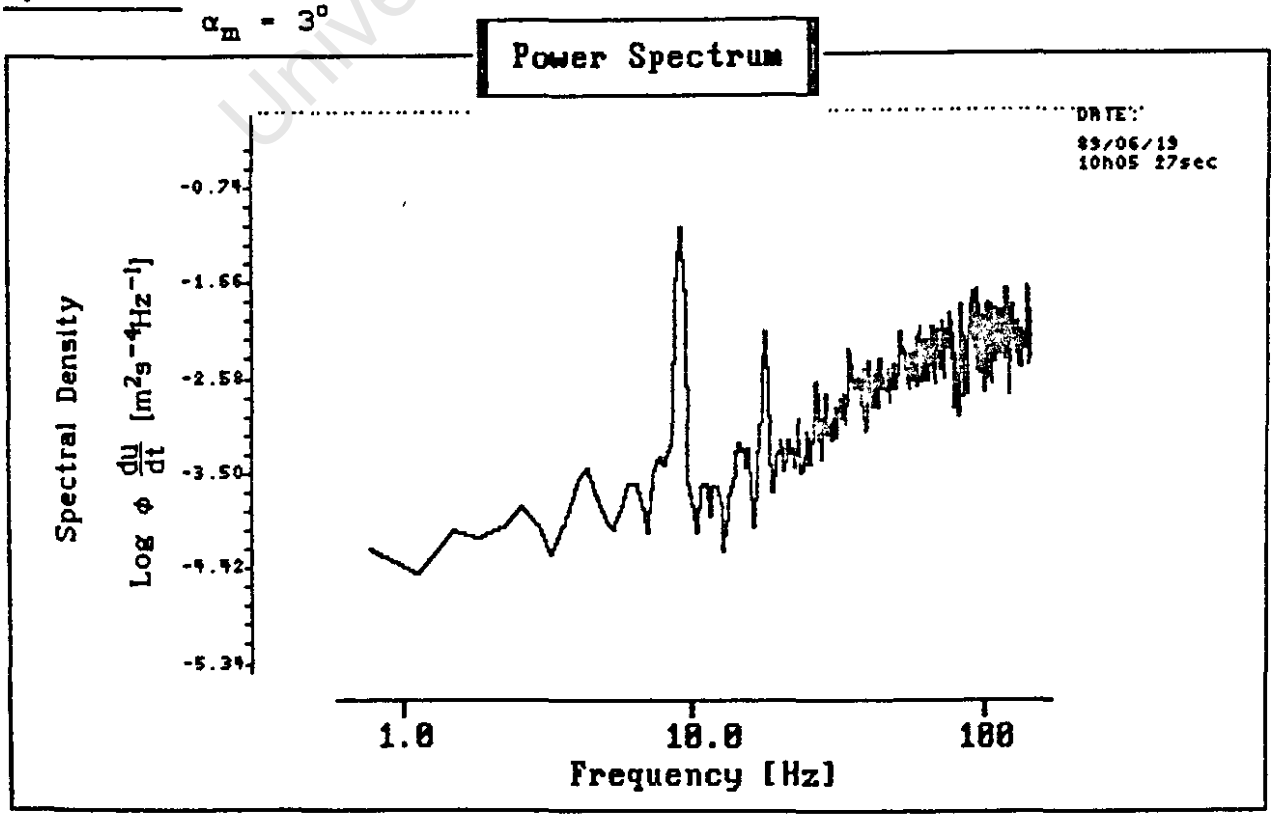

APPENDIX 19(cont.)

Spectra Generated by Calibration Procedure

Spectrum C: Excitation Frequency = 10.0 Hz.

$\alpha_m = 7^0$

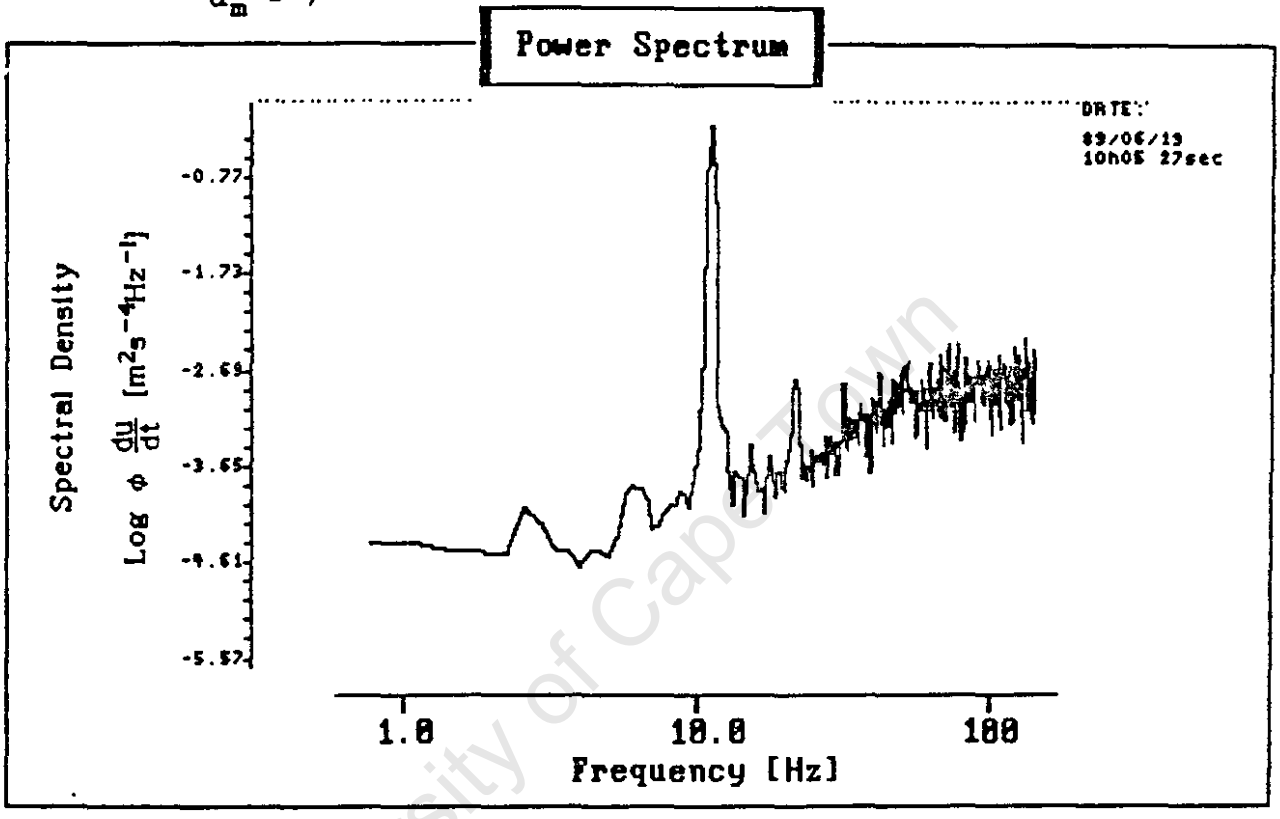

APPENDIX 20

Dynamic Response of Probe (Themocline Simulation)

TEMPERATURE VS TIME:

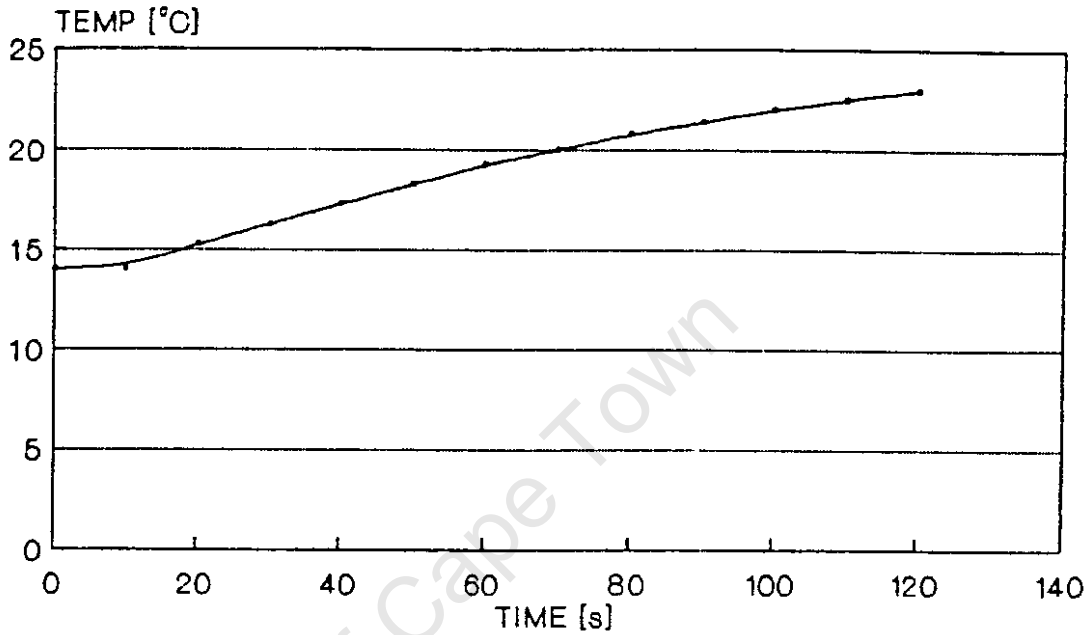

PROBE RESPONSE VS TIME:

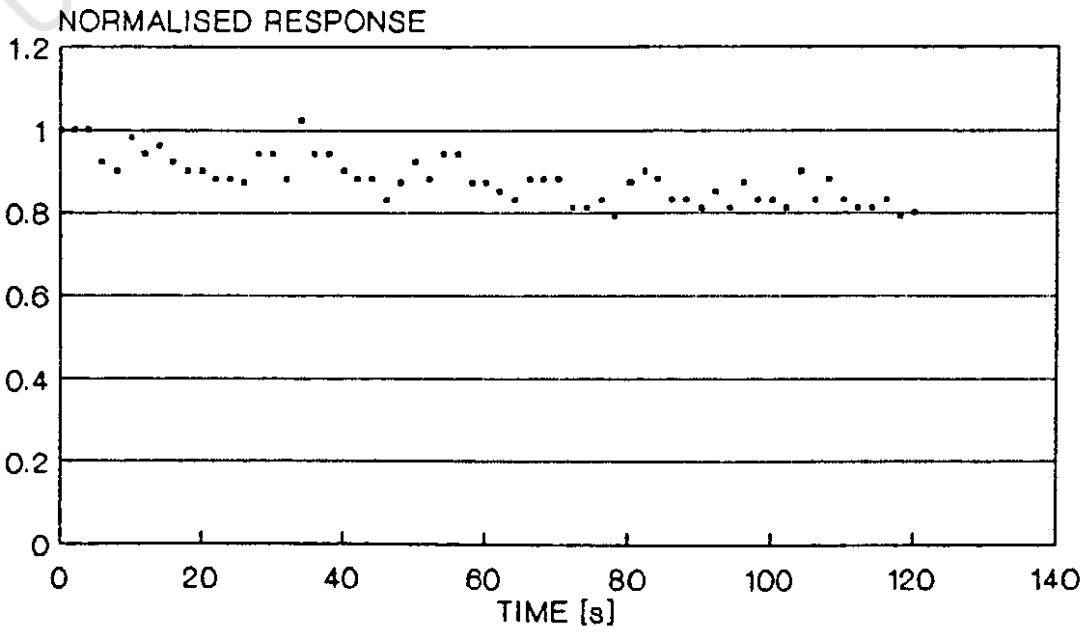

APPENDIX 21

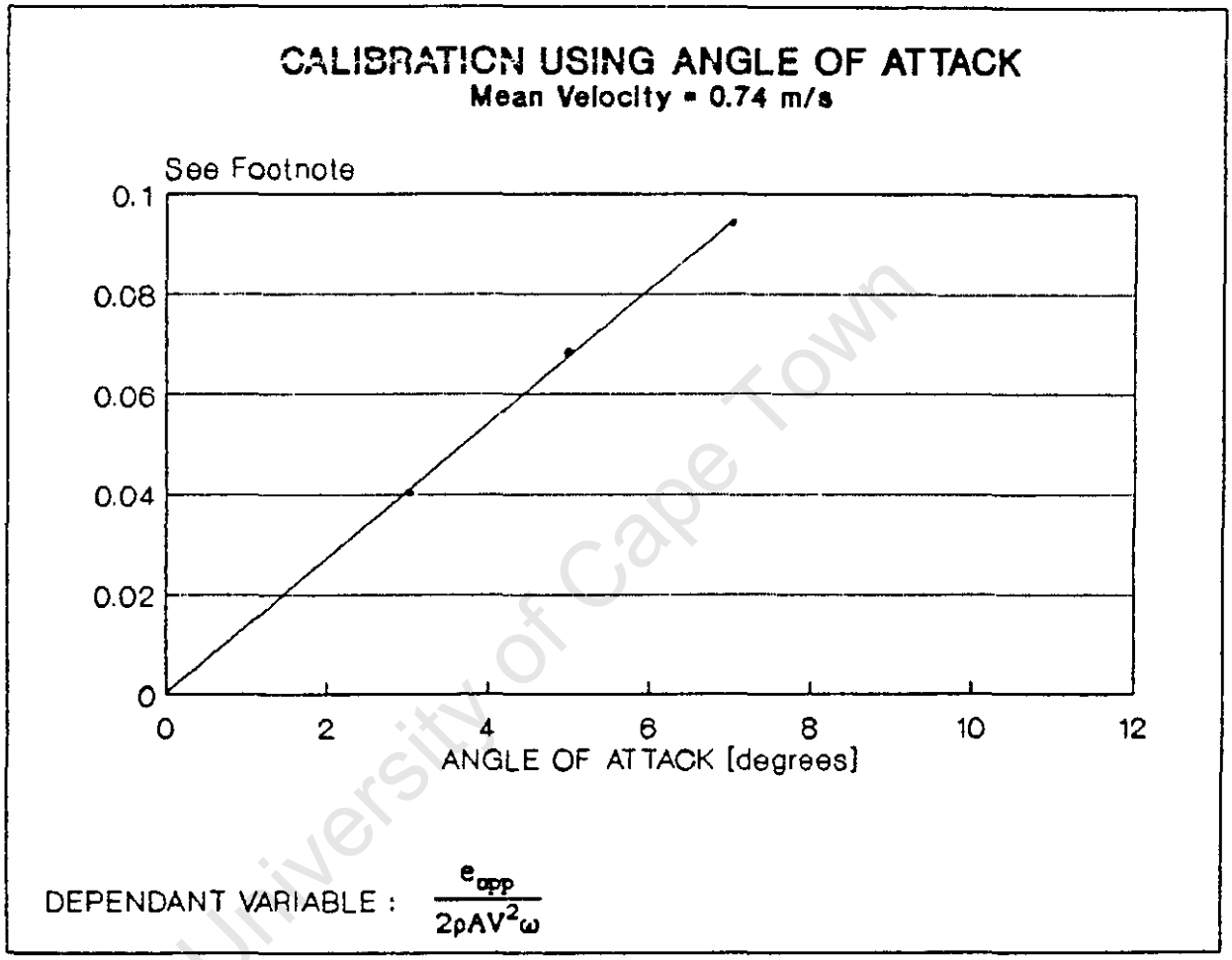

APPENDIX 22

Thermal Impulse Response of Probe
(dT = 31 °C for 6 seconds)

TEMPERATURE RESPONSE:

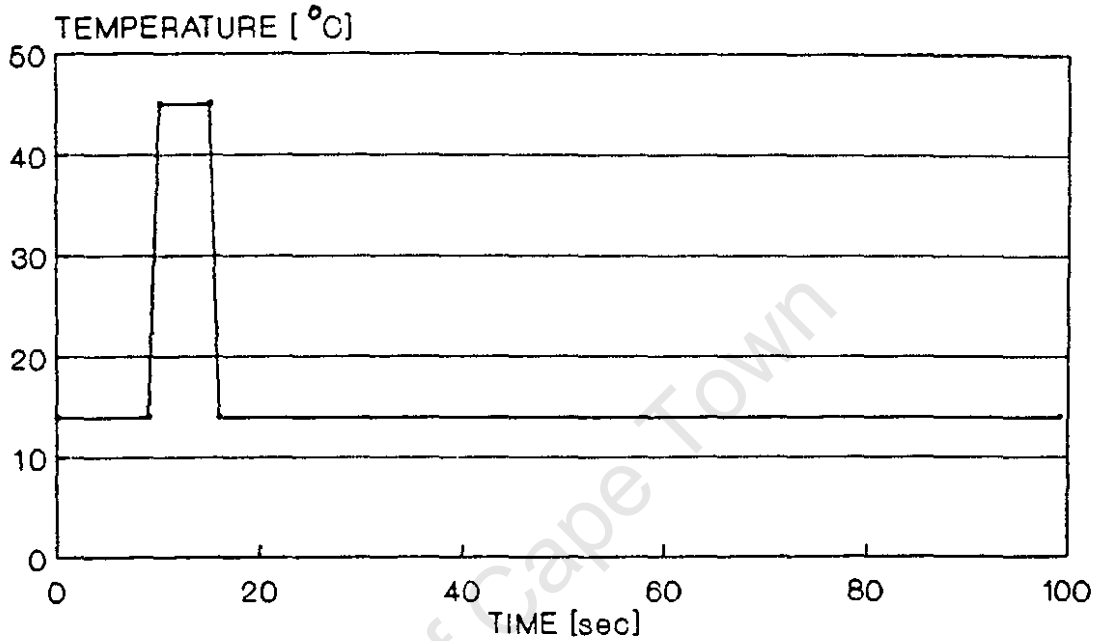

NORMALISED PROBE RESPONSE:

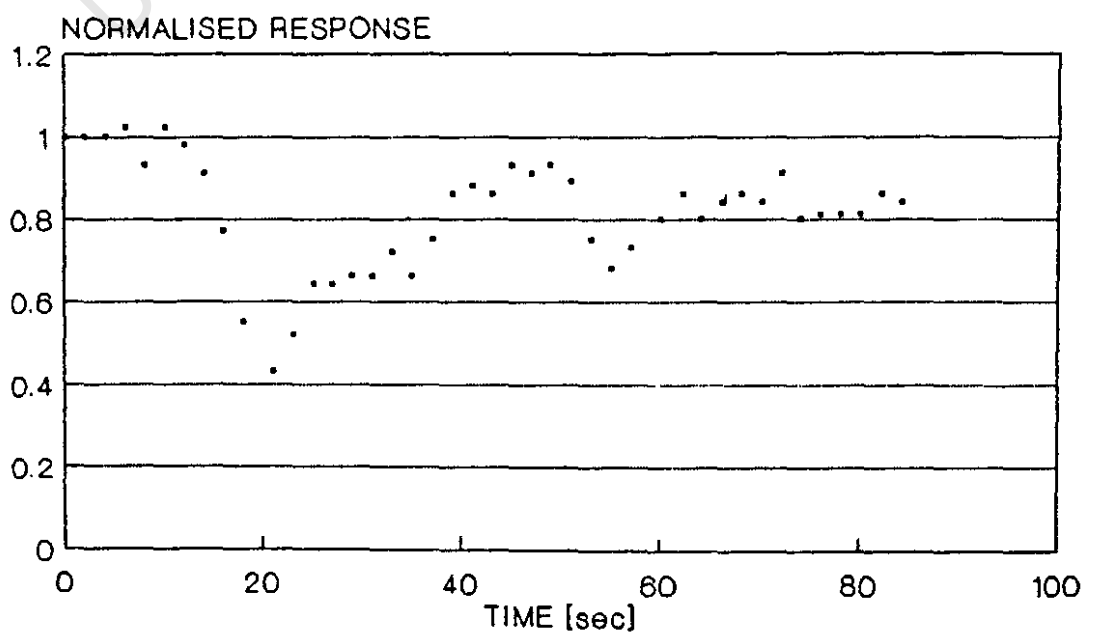

DETAILED VIEW OF STRAIN GAUGE PROBE

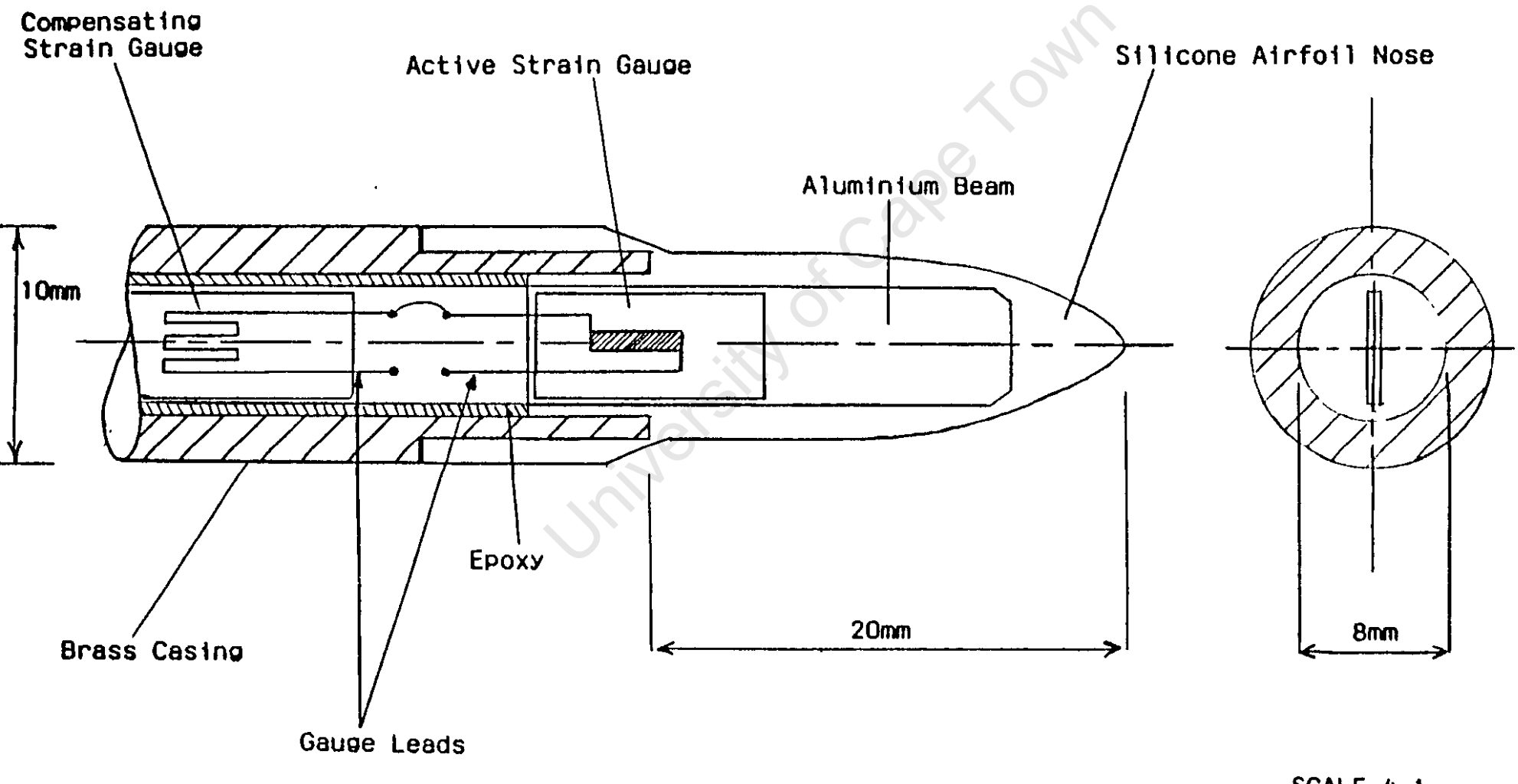

SCALE 4:1

LONGITUDINAL VIEW THROUGH VEHICLE

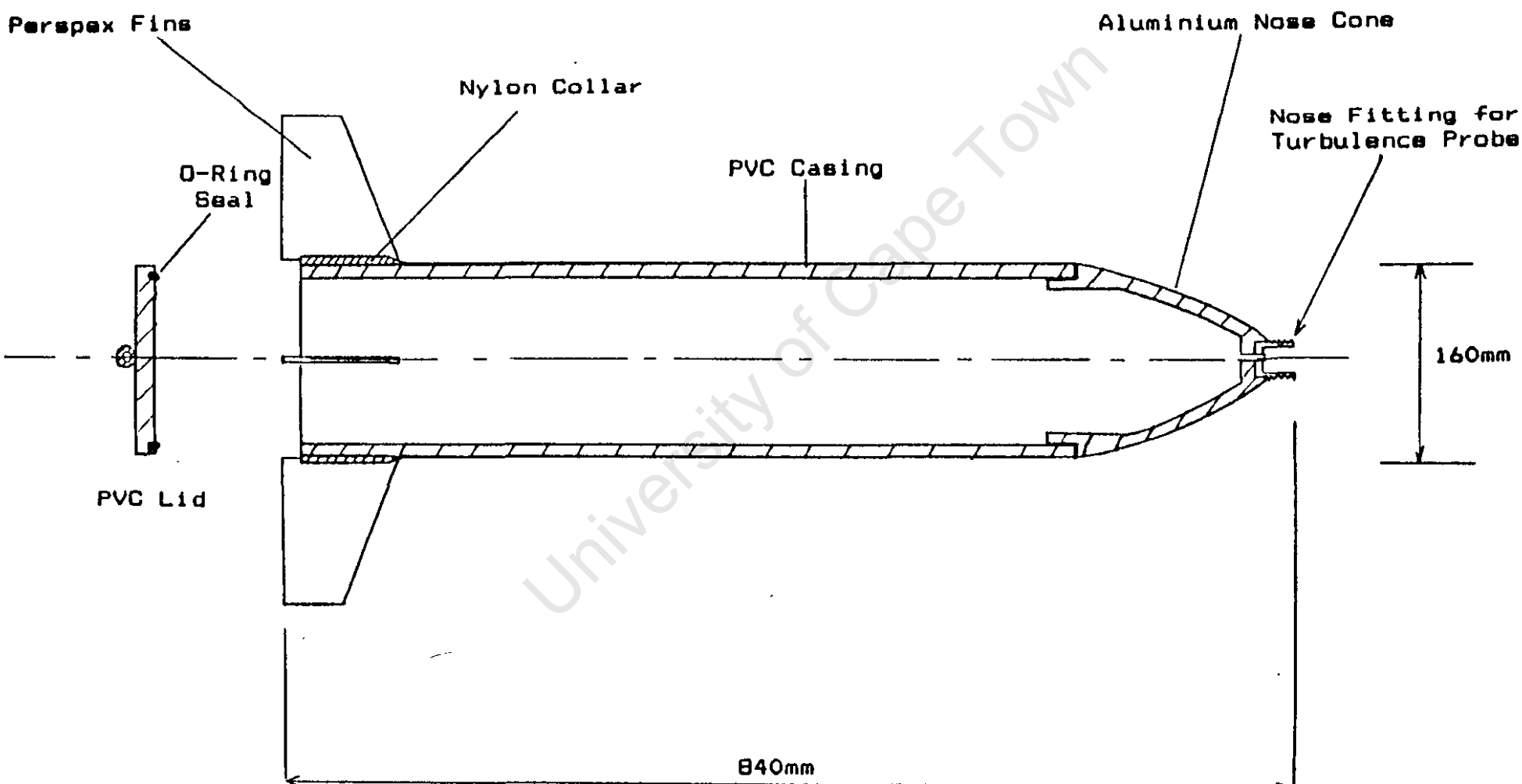

SCALE 1:5

APPENDIX 25

CALCULATION OF WEIGHT OF BALLASTS REQUIRED TO CONTROL VEHICLE FALL SPEED

J.D. Woods (1969), describes the in water weight, W, of a free falling vehicle as

$$W = \frac{1}{2} C_d \rho A U^2$$

where C_d is the drag coefficient of a vehicle with a cross sectional area, A. The vehicle falls freely at a speed U through a fluid of density ρ.

For the vehicle illustrated in Appendix 24, falling through sea water, the following specifications apply:

$A = 0.02\ m^2$
$\rho = 1027\ kg/m^3$
$C_d \approx 0.4$ (Personal communication - A.Sayers, Fluid dynamics department, U.C.T.)

Furthermore, the volume of water displaced by the vehicle is appoximately $0.0148\ m^3$ and has an equivalent mass of 15.2 kg. If the vehicle fall-speed is to be controlled at $1 ms^{-1}$, then using the above equation, the required total vehicle mass is 16 kg.

This mass is comprised of the following components:

Data Logger:	5.39 kg
Vehicle:	6.90 kg
Probes + Vehicle Lid:	1.05 kg
Additional Ballast:	2.66 kg

Due to the approximations used for values of vehicle volume and drag coefficient, the above calculation gives only a rough estimate of the required mass of the ballasting weights.This mass may be fine tuned in the field to give the exact required fall speed.

EXPLODED VIEW OF STING ASSEMBLY

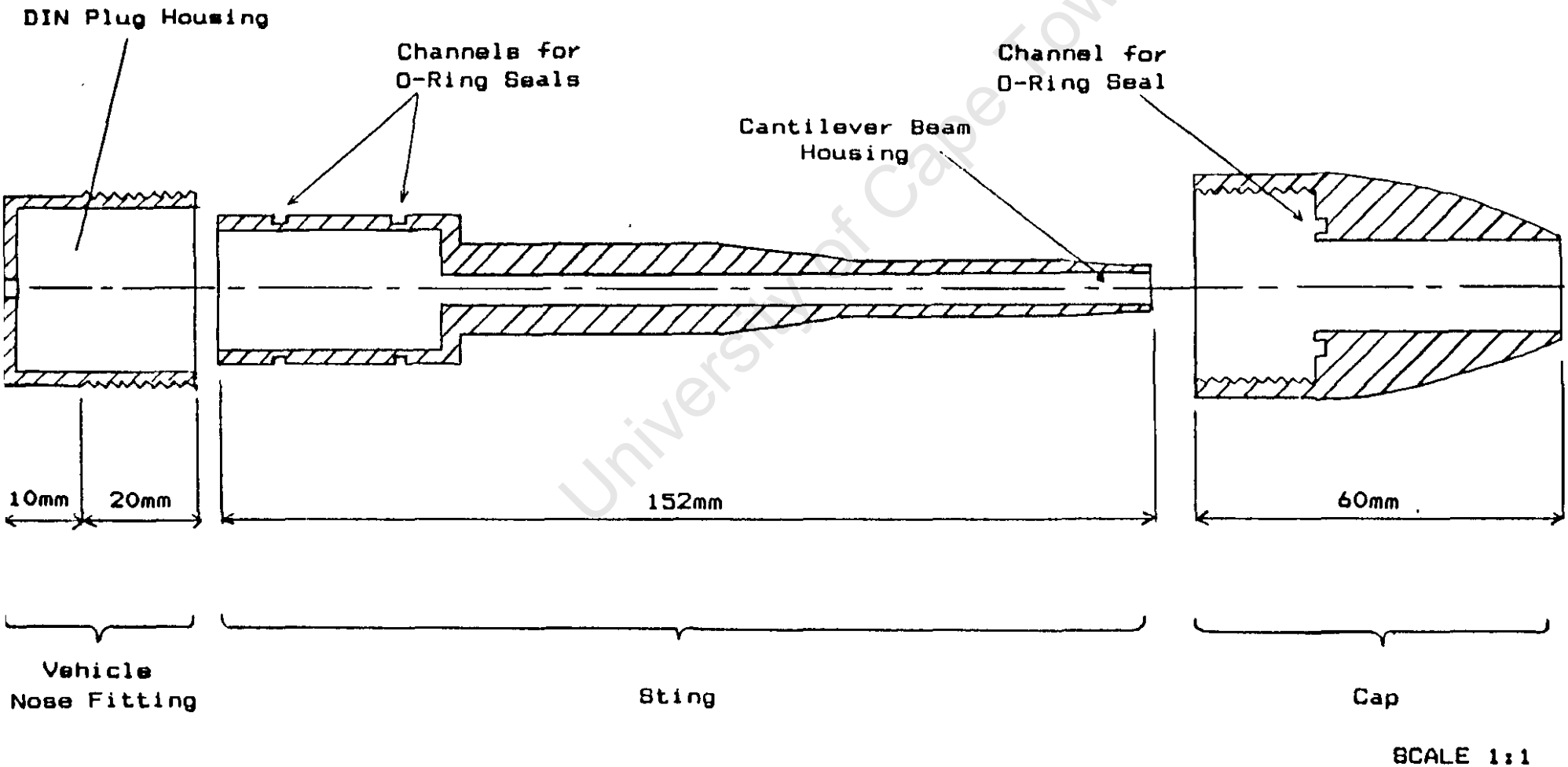

SCALE 1:1

APPENDIX 27

Deployment Simulation used to Calibrate Pressure Transducer

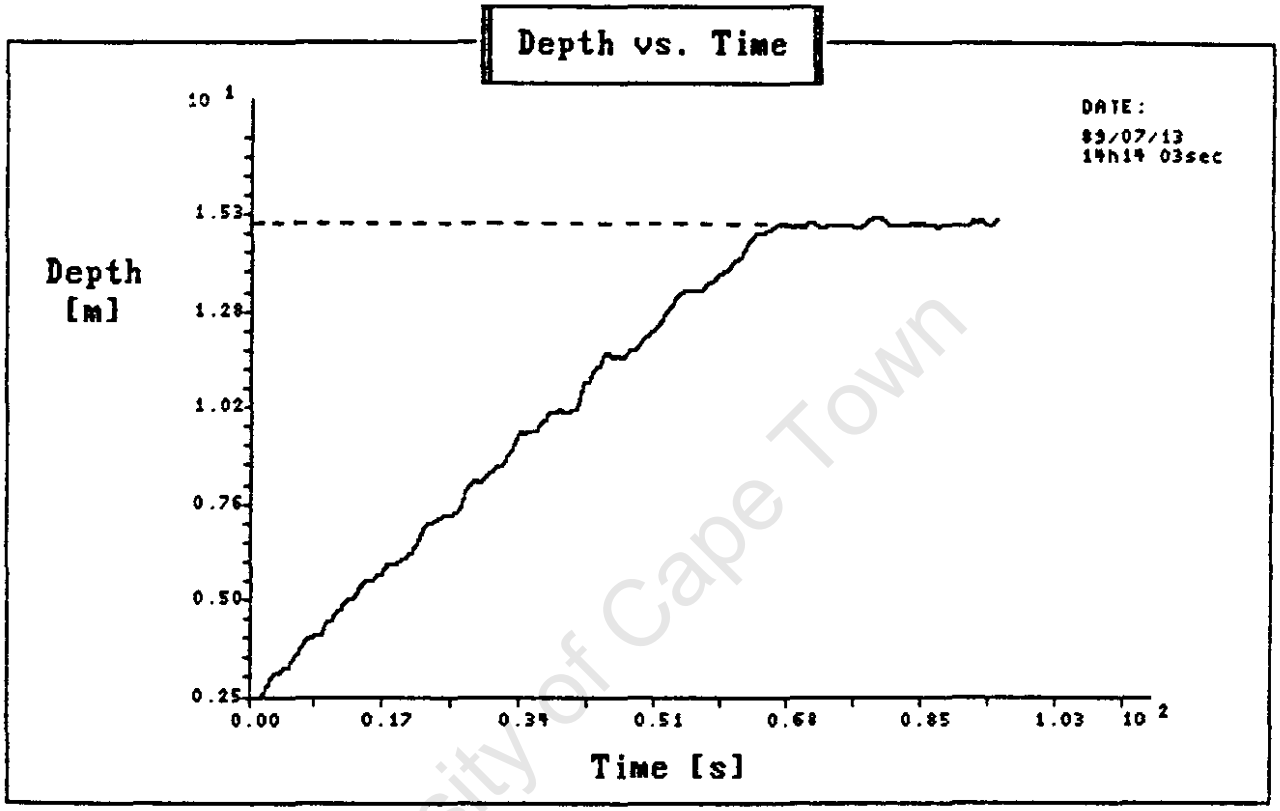

* Simulated deployment to 15m of water.
* Resultant trace for calibration coefficient = 48 dBar.

APPENDIX 28

DATA LOGGER OPERATING INSTRUCTIONS

To Start the Data Logger

1. Connect the "Red lead" connector to red (+) battery terminal and "Black lead" connector to the black (-) terminal on battery.

2. Push "R" on Keyboard and the "=" will be displayed on the left-hand side of the display, indicating that the machine has been reset.

To Check the Sensors

While in the Reset (=) mode, push "L" on the keyboard to start the sensor check mode. Each input channel will sequentially be displayed for a few seconds on the LDC display. Push "R" to terminate the sensor check mode.

To Start the Data Logger for Deployment

1. Connect power to the instrument.

2. Push "R" for reset.

3. Push "P" and "test" or "data" will be displayed. If "data" is displayed it means that the memory module still contains valid data. Push "G" to erase the data, or "S" to retain the existing data by skipping to the end of the valid data and starting recording from the next available memory position.

   On pushing "G", "test" will be displayed.

   The "test" is a memory test. Once the Data Logger has passed the memory test, six zeros will be displayed. Enter the date; first the year then the month and day, eg. 881016.

   Push "ENT" and four zeros will be displayed. Enter the time in 24 hour format; first the hours then the minutes, eg. 1047 for 10h47. Push "ENT" and the date will be repeated on the display before the time is again displayed.

APPENDIX 28(cont.)

Approximately 5 seconds later "A" will be displayed. This indicates that the Data Logger program is running with the power to the sensors switched off. When the reed switch is momentarily triggered (closed) power is supplied to the sensors and "Ab" is displayed.

As soon as the pressure has reached its preset trigger level, the Data Logger will start recording, the display will indicate the starting time of this record. A "F" is displayed to indicate the end of a recording cycle. The operator at this stage may either wish to retrieve the data or trigger another record via the reed switch.

NOTE: The memory can only store 8 records.

Cleaning of the instrument

When cleaning the instrument i.e. scraping off barnacles, etc. after recovery, keep the plate covering the perspex "eyes" in place as scratches on the "eyes" cause "read errors" during the data recovering process.

DATA RECOVERY

1. Connect the optical sensor plug to the Data Logger taking note of the direction of the arrow marked between the 2 perspex "eyes".

2. Connect the RS232 link to the P C computer serial input.

3 Connect the mains.

4. To run the program, type in "Readall" and follow the prompts.

5. The display on the Data Logger will go through a reset phase and end with a "d" on the left-hand side and "00" on the right-hand side.

6. At the end of the data transfer, and "E" will be displayed and "Readall" will end. However, if the Data Logger ran out of memory before ending off the last file, no "E" will be displayed and a "b" will remain indefinitely on the display. In this case it is safe to assume that all the data have been transferred as the PC will continue to wait for the rest of the file.

APPENDIX 28(cont.)

A full memory module can contain up to 8 files for the 512k version.

7. It is recommended that the Data Logger is put on charge to reduce the possibility of errors due to low voltages.

8. After the data have been successfully retrieved, disconnect the AA cells by unplugging the white plug on the mother board.

APPENDIX 29

FORMAT OF MULTIPLEXED DATA RECORDS.

CONTENTS OF EACH RECORD:

Hex data Sequence:	Description
[7 bytes]	Sub-header generated by "READALL".
[01] [01]	SOH (Start of header)
[87 bytes]	Header
[02] [02]	EOH (End of header)
[60 480 bytes]	Data File
[03] [03]	ETX (End of text file)
[1A]	Disk Housekeeping

INFORMATION CONTAINED IN FILE HEADER:

Bytes:		
	73-74:	Date of file (Year).
	75-76:	Date of file (Month).
	77-78:	Date of file (Day).
	79:	Blank space
	80-81:	Time of file generation (hrs.).
	82-83:	Time of file generation (mins.).
	83-84:	Time of file generation (secs.).

FORMAT OF DATA FILE:

[100 bytes]	Data from turbulence channel sampled @ 499.26 Hz.
[1 byte]	Temperature value.
[100 bytes]	Turbulence data.
[1 byte]	Pressure value.
[150 bytes]	Turbulence data.
[1 byte]	Temperature value.
[100 bytes]	Turbulence data.
[1 byte]	Pressure value.
[150 bytes]	Turbulence data.
[1 byte]	Temperature value.

etc.

APPENDIX 30

Software Reference: Program DATASORT

```
Program Datasort(input,output);

{ This program sorts the multiplexed hexidecimal file created by 'READALL' }
{  into four text files, namely: the header file, the turbulence data      }
{      file, the pressure data file and the temperature data file.         }

Type
   Directory = string[35];
   Name = String[5];
   DataFile = File of Byte;
var
   HeadFile,TurbFile,PresFile,TempFile: DataFile;      { Sorted Data }
                                                       {    Files.   }
   Workfile       : Datafile;        { Source Data file name. }
   Destination    : Directory;       { Destination Data file path. }
   Filepath       : Directory;       { Source Data file path. }
   FullfileName   : Directory;       { Source Data file name. }
   FirstDeployment: Integer;         { Stores filenumber of first file }
   Recnum         : Integer;         { Number of probe deployments. }
   I              : Integer;         { Loop variables. }
   Compute        : Boolean;         { Flags program end }
   Hexvalue       : Byte;            { Data file element }
   Cont           : Char;            { Signals termination }
   N1,N2,N3,N4    : Name;            { Dummy file names. }


Procedure DefineWorkFile(var Filepath,Fullfilename:Directory;
                             Recnum,Firstnum:Integer);
var
  Filenum  : String[3];
begin
  Str(Recnum,Filenum);
  FullFilename := Filepath + Filenum + '.bas';
  Assign (Workfile,FullfileName);
  {$I-}
  Reset (Workfile);    { Program terminates if source file does not exist. }
  {$I+}
  if IOresult <> 0 then
  begin
    If Recnum = Firstnum then
    begin
      Writeln('Cannot find ',Filepath,Recnum,'.bas');
      Writeln('Please ensure that the above data file exists.');
      Writeln;Writeln;Writeln;
      Writeln('Datasort terminated.');
      Halt
    end
    else
    begin
      Writeln('All available files have been sorted.');
      Writeln('Datasort complete.');
      Compute := false;
    end
  end
end;

Procedure CreateFilenames(var H_name,Tu_name,P_name,Te_name:Name;
                          var Record_num :Integer);
var
  DeploymentNum : String[1];
begin
  Str(Record_num,DeploymentNum);
  H_name := 'Head' + DeploymentNum;
  Tu_name := 'Turb' + DeploymentNum;
  P_name := 'Pres' + DeploymentNum;
  Te_name := 'Temp' + DeploymentNum
end;

Procedure AssignFiles(var HeadFile,Turbfile,PressFile,Tempfile:Datafile;
                      var Header_name,Turb_name,Press_name,Temp_name:Name;
                      var Outputpath:Directory);
```

APPENDIX 30(cont.)

Program DATASORT (Page 2)

```
var
  ExternalName     : String[40];
begin
  ExternalName := OutputPath + '\' + Header_name + '.pas';
  Assign(Headfile,ExternalName);
  Rewrite(Headfile);
  ExternalName := OutputPath + '\' + Turb_name + '.pas';
  Assign(Turbfile,ExternalName);
  Rewrite(Turbfile);
  ExternalName := OutputPath + '\' + Press_name + '.pas';
  Assign(Pressfile,ExternalName);
  Rewrite(Pressfile);
  ExternalName := OutputPath + '\' + Temp_name + '.pas';
  Assign(Tempfile,ExternalName);
  Rewrite(tempfile)
end;

Procedure Transfer(var DestinationFile:Datafile);
var
  Hexvalue   : Byte;           { Transfers single byte from source }
begin                          {          to destination.          }
  Read(Workfile,Hexvalue);
  Write(DestinationFile,Hexvalue)
end;

Procedure CloseFiles(var Headfile,Turbfile,Presfile,Tempfile:Datafile);
begin
  Close(Headfile);
  Close(Turbfile);
  Close(Presfile);
  Close(tempfile)
end;

Procedure Quit(var F1,F2,F3,F4:Datafile); { User triggered 'quit' routine. }
var
  Keyvalue : Char;
begin
  Read(Kbd,Keyvalue);
  if Keyvalue = 'Q' then
  begin
    Writeln;
    Writeln('Datasort terminated.');
    CloseFiles(F1,F2,F3,F4);
    Close(Workfile);
    Halt
  end
end;

Procedure Initdatafiles(var Record_num:Integer;var HFile,TuFile,PFile,TeFile:
                        DatafiTe;var Compute:Boolean);
var
  N1,N2,N3,N4 : Name;            { Dummy file names. }
begin
  CreateFilenames(N1,N2,N3,N4,Record_num);
  AssignFiles(HFile,TuFile,PFile,TeFile,N1,N2,N3,N4,Destination);
end;


Procedure Recordread(var Record_num:Integer;var Headx,Turbx,Presx,Tempx:
                                                Datafile);
var
  I,J   :Integer;
begin
  Writeln;
  Writeln('Sorting deployment No.',Record_num,' ...');
  Writeln;Writeln;Writeln('Press " Q " to quit.');
  Writeln;
  for I:=1 to 9 do Read(Workfile,Hexvalue);  { Advances pointer beyond SOH }
  for I := 1 to 87 do Transfer(Headx);       { Reads File header. }
  for I := 1 to 2 do Read(Workfile,Hexvalue);
  for I := 1 to 100 do Transfer(Turbx);
```

APPENDIX 30(cont.)

Program DATASORT (Page 3)

```
 Transfer(Tempx);
  for I := 1 to 100 do Transfer(Turbx);
  Transfer(Presx);
  for J := 1 to 239 do                { Sorts multiplexed source data file. }
  begin
    for I := 1 to 150 do Transfer(Turbx);
    Transfer(Tempx);
    for I := 1 to 100 do Transfer(Turbx);
    Transfer(Presx);
    if Keypressed then Quit(Headx,Turbx,Presx,Tempx);
  end;
  for I := 1 to 50 do Transfer(Turbx);
  Writeln;Writeln;
  Writeln('Deployment No.',Record_num,' sorted.');
  CloseFiles(Headx,Turbx,Presx,Tempx);
end;

                              { MAIN PROGRAM }
begin
  Clrscr;
  Writeln('Enter path and generic filename of source Data.');
  Writeln('e.g. A:\ Directory\ Filename');
  Writeln;
  Readln (Filepath);
  Writeln;
  Writeln('Enter the number of the first file:');
  Writeln;
  Readln (Recnum);
  Writeln;Writeln;
  Writeln('Enter path and name of new directory where ');
  Writeln('sorted files are to be stored.');
  Writeln('e.g. A:\ NewDirectoryName');
  Writeln;
  Readln (Destination);
  {$I-}
  MKdir(Destination);
  {$I+}
  if IOresult <> 0 then
  begin
    Writeln('Directory ',Destination,' already exists.');
    Writeln('Please select a path and a NEW directory:');
    Readln(Destination);
    MKdir(Destination);
  end;
  Compute := True;
  FirstDeployment := Recnum;
  for I := FirstDeployment to (FirstDeployment + 7) do
  begin
    if compute then
    begin
      if I = (Recnum + 5) then
      begin
        Writeln;
        Writeln('If you are using a 360K floppy disk, it will be full.');
        Writeln('Replace it with a new formatted disk and ');
        Writeln('press " R " when ready to continue...');
        Writeln;
        Writeln('If you are using a Hard-drive, ignore the above');
        Writeln('and press " C " to continue...');
        Repeat until Keypressed;
        Read(Kbd,Cont);
        If Cont = 'R' then MKdir(Destination);{Creates directory on new disk}
        If Cont = 'r' then MKdir(Destination);
      end;
      DefineWorkFile(Filepath,FullFileName,Recnum,FirstDeployment);
      Initdatafiles(Recnum,HeadFile,TurbFile,PresFile,TempFile,Compute);
      If Compute then
      begin
        Recordread(Recnum,HeadFile,TurbFile,PresFile,TempFile);
      end
      else
```

APPENDIX 30(cont.)

Program DATASORT (Page 4)

```
      begin
        Erase(Headfile);Erase(Turbfile);
        Erase(Presfile);Erase(Tempfile);
      end;
      Close(workfile);
      Recnum := Recnum + 1
    end
  end;
  if Recnum = (Firstdeployment + 7) then Writeln('Datasort completed.')
End.
```

APPENDIX 31

Software Reference: Program TROUT

```
Program TROUT(input,output);

{ $I typedef.sys }
{ $I graphix.sys }
{ $I Kernel.sys }
{ $I windows.sys }          (* Graphics include files *)
{ $I findgrid.hgh }
{ $I axis.hgh }
{ $I polygon.hgh }
{ $I Deriv.inc }

type
  Datafile  = File of Byte; { File type for source data }
  Directory = String[35];   { Path for input and output Data }
  Date      = String[30];   { Record of Date for Graph identification }
  Datearray = Array[1..8] of Date;

var
  Print       :Boolean;     { Print Option }
  Option      :Char;        { Defines selected deployment option }
  Header      :Datearray;
  Filepath    :Directory;   { Path of Source data }
  Complete    :Boolean;     { Flag to validify file existance }
  Finished    :Boolean;     { Flag to detect termination }
  Routine     :Char;        { Defines user selected analysis option }
  HeadX       :DataFile;
  Screenline  :String[80];  { Reads line of text from screen }
  Headerfile  :Text;        { Temp. file for storage of deployment stats }
  Pathfile    :Text;


{*************************************************************}
{*      Procedure Mainmenu asks the user to select the appropriate    *}
{*      analysis routine.The user may choose:                         *}
{*              - To display dates and times of deployments           *}
{*              - To analyse pressure data                            *}
{*              - To analyse turbulence data                          *}
{*              - To quit                                             *}
{*************************************************************}

Procedure MainMenu(var SelectedFunction:Char);
var
  Firstbyte   :Char;
begin
  While Firstbyte <> #27 do
  begin
    Clrscr;
    Writeln;Writeln;
    Writeln('MAIN MENU':42);
    Writeln('----------':43);
    Writeln;
    Writeln('Please select one of the following functions:');
    Writeln;Writeln;
    Writeln('[F1]   Display of the date and time of each probe deployment.');
    Writeln;
    Writeln('[F2]   Analysis of probe fall speed and deployment depth.');
    Writeln;
    Writeln('[F3]   Analysis of turbulence Data.');
    Writeln;
    Writeln('[F4]   Quit.');
    Writeln;Writeln;
    Read(kbd,Firstbyte);
    Read(Kbd,SelectedFunction);
  end
end;


{*************************************************************}
{*            The following procedures create a text file containing   *}
{*            all information relating to deployment times.This data   *}
{*              is then listed on the corresponding graphs for I.D.    *}
```

APPENDIX 31(cont.)

Program TROUT (Page 2)

```
{**********************************************************************}

Procedure ReadDate(var Datefile:Datafile);
var
  Hexnum :Byte;          { File Element }
  I      :Integer;       { Loop variable }
begin
  for I := 1 to 2 do
  begin
    Read(Datefile,Hexnum);
    Write(Headerfile,Chr(Hexnum))
  end
end;

Procedure WritetoHeadfile(var Deploynum:Integer);
var
  Firstnum:Integer;      { Records number of first deployment }
  Intfile :DataFile;     { Internal assignment for 'HEAD' files }
  Extname :String[40];   { External assignment for 'HEAD' files }
  Number  :String[1];
begin
  Firstnum := Deploynum;
  repeat
    Str(Deploynum,Number);
    Extname := Filepath + '\ Head' + Number + '.pas';
    Assign(Intfile,Extname);
    {$I-}
    Reset(Intfile)
    {$I+};
    Complete := (IOresult <> 0);
    If not Complete then
    begin
      Seek(Intfile,73);          { Sets File Pointer }
      Write(Headerfile,'                ',Deploynum,'              ');
      ReadDate(Intfile);         { Reads Year }
      Write(Headerfile,'/ ');
      ReadDate(Intfile);         { Reads Month }
      Write(Headerfile,'/ ');
      ReadDate(Intfile);         { Reads Day }
      Seek(Intfile,80);          { Sets File Pointer }
      Write(Headerfile,'  ');
      ReadDate(Intfile);         { Reads Time[Hrs.] }
      Write(Headerfile,'h');
      ReadDate(Intfile);         { Reads Time[mins.] }
      Write(Headerfile,' ');
      ReadDate(Intfile);         { Reads Time[secs.] }
      Write(Headerfile,'secs.                ');
      Close(Intfile);
      Writeln(Headerfile);
    end
    else if complete and (firstnum=deploynum) then
    begin
      Writeln('Cannot find ',Extname,'.');
      Writeln('Program TROUT terminated.');
      Halt;
    end;
    Deploynum := Deploynum + 1;
  until complete;
end;

Procedure DeploymentDates;
var
  Error     : Boolean;   { Detects incorrect source path }
  I,J       : Integer;   { I Represents deployment number }
begin
  Writeln;
  Writeln('Input number assigned to first Deployment:');
  Readln(I);
  Assign(Headerfile,Filepath + '\ Header.pas');
  {$I-}
  Rewrite(Headerfile)
```

APPENDIX 31(cont.)

Program TROUT (Page 3)

```
  {$I+};
  Error := (IOresult <> 0);
  If Error then
  begin
    Writeln('Cannot find Directory ',Filepath);
    Writeln;
    Writeln('Please check that the above Directory containing ');
    Writeln('the Data files generated by "DATASORT" exists.');
    Writeln;
    Writeln('Program TROUT aborted.');
    Halt;
  end;
  WriteToHeadfile(1);
  Reset(Headerfile);
  for J := 1 to (I-1) do
  begin
    Readln(Headerfile,screenline);
    Header[J] := Copy(Screenline,37,28);    { Sets up array for Graph ID }
  end;
  Close(Headerfile);
  Assign(Pathfile,'DataPath.pas');
  Rewrite(Pathfile);
  Write(Pathfile,Filepath);
  Close(Pathfile);
end;


Procedure DisplayHeadfile;       { Displays times of all deployments }
begin
  Clrscr;
  Writeln;
  Writeln('DEPLOYMENT':27,'DATE':15,'TIME':17);
  Writeln;
  Assign(Headerfile,Filepath + '\ Header.pas');
  Reset(Headerfile);
  While not EOF(Headerfile) do
  begin
    Readln(Headerfile,Screenline);
    Writeln(Screenline);              { Displays Text file on screen }
  end;
  Close(Headerfile);
  Writeln;Writeln;
  Writeln('Press <SHIFT> and <PrtSc> to get a Hardcopy.');
  Writeln;Writeln('Press any Key to return to Main Menu');
  Repeat Until KeyPressed
end;


{**********************************************************************}
{       The following procedures are related to the analysis of data     }
{       from the pressure transducer.These include graphing routines     }
{       used to plot depth and fall-speed vs. time, as well as a 5pt.    }
{       differentiation algorithm to derive the speed characteristic.    }
{**********************************************************************}

Procedure ChoosePresfile(var Presfile:Datafile;var InvalidFile:Boolean);
var
  Extfile  :String[40];    { Path and name of external pressure file }
begin
  Clrscr;
  Writeln;Writeln;
  Writeln('Please select deployment number to be analysed.');
  Writeln('Enter number (1-8)');
  Writeln;Writeln;
  Readln(Option);
  Extfile := Filepath + '\ Pres' + Option + '.pas';
  Assign(Presfile,Extfile);
  {$I-}
  Reset(Presfile);
  {$I+};
  InvalidFile := (IOresult <> 0);   { Error if no external file found }
```

APPENDIX 31(cont.)

Program TROUT (Page 4)

```
  If InvalidFile then
  begin
    Writeln;
    Writeln('Cannot find Data file PRES',Option,'.PAS.');
    Writeln('Press any Key to return to Main Menu.');
    Repeat until Keypressed
  end
end;

Procedure GraphPlot(var Graphvalues:Plotarray;var T1:Integer;
                    var Title,YTitle,Unit:Wrkstring;Print:Boolean);
var
  Num,R   :Integer;   { Num is Integer derived from deployment selection }
  Day,Time:String[12];{ Graph Identification }
begin
  EnterGraphic;
  DefineWindow(1,trunc(Xmaxglb/10),trunc(Ymaxglb/10),
                 trunc((Xmaxglb*9)/10),trunc((Ymaxglb*9)/10));
  DefineWindow(2,trunc(Xmaxglb/10),trunc(Ymaxglb/10),
                 trunc((Xmaxglb*9)/10),trunc((Ymaxglb*9)/10));
  Defineworld(1,0,1000,1000,0);
  Selectwindow(2);
  SetHeaderoff;
  Findworld(2,Graphvalues,(trunc((T1)/0.6)),1.2,1.2);
  Selectwindow(2);
  DrawBorder;
  GotoXY(32,2);Write('┌──────────────┐');
  GotoXY(32,3);Write('│ ',Title,' │');
  GotoXY(32,4);Write('└──────────────┘');
  SetLinestyle(0);
  DrawAxis(0,5,10,15,5,25,9,0,false);
  DrawPolygon(Graphvalues,1,-trunc(T1/0.6),0,1,0);
  Selectworld(1);
  Selectwindow(1);
  GotoXY(10,9);Write(YTitle);          { Labels Y-Axis }
  GotoXY(10,10);Write(Unit);
  GotoXY(38,22);Write('Time [s]');     { Labels X-Axis }
  Val(option,Num,R);
  Day := Copy(Header[num],1,8);
  Time := Copy(Header[num],16,12);
  DrawTextW(850,80,1,'DATE:');
  DrawTextW(850,120,1,Day);            { Graph Identification : Date }
  DrawTextW(840,145,1,Time);           { Graph Identification : Time }
  if Print then Hardcopy(false,6);
  Repeat Until KeyPressed;
  LeaveGraphic
end;

Procedure LowpassFilter(var Data:Plotarray);
var
  I      : Integer;  { Loop variable }
begin
  for I := 3 to 198 do
  begin
    Data[I,2]:=(Data[I-2,2]+Data[I-1,2]+Data[I,2]+Data[I+1,2]+Data[I+2,2])/5;
  end
end;

Procedure Speedcalc(var Pressure,Speed:Plotarray);
const
Numpts   = 200;  { Specifies number of data points }
Numderiv = 200;  { Number of points at which derivative is evaluated }
var
Timeaxis   :TDvector;  { Array of sample time for numerical differentiation }
Presvector :TDvector;  { Array of pressure values for differentiation }
Speedvector:TDvector;  { Resultant array from numerical diffentiation }
Error      :Byte;      { Returns error status after differentiation }
I          :Integer;   { Loop variable }

begin
  for I:= 1 to 200 do
```

APPENDIX 31(cont.)

Program TROUT (Page 5)

```
  begin
    Timeaxis[I] := Pressure[I,1];          { Creates vector for time axis }
    Presvector[I] := Pressure[I,2]         { Vector of displacement values }
  end;
  First_Derivative(Numpts,Timeaxis,Presvector,5,Numderiv,
                   Timeaxis,Speedvector,Error);
  if Error = 0 then
  begin
    for I := 1 to 200 do
    begin
      Speed[I,1] := Timeaxis[I];           { Copies time axis for speed graph }
      Speed[I,2] := Speedvector[I];        { Copies speed points calculated }
    end;
    Lowpassfilter(Speed);
  end
  else
  begin
    Writeln('Error ',Error,' detected in speed calculation.');
    Writeln('Program TROUT aborted.');
    halt;
  end
end;

Procedure CreatePlotArrays(var Presfile:Datafile;var Pressure,Speed:PlotArray;
                           var Calibrate:Real);
var
hexnum      :Byte;       { Data file element }
I           :Integer;    { Loop counter }
Pressureval :Real;       { Plot array element }
Time        :Real;       { Sampling Period }

begin
  Writeln('Calculating curves...');
  for I := 1 to 200 do                   {Pressure file contains 200 bytes }
  begin
    Read(Presfile,Hexnum);               { Reads data point from ext. file }
    Pressureval := Hexnum * Calibrate;   { Calibrates data point }
    Pressure[I,2] := Pressureval         { Writes datapoint to plot array }
  end;
  time := 0;
  for I := 1 to 200 do
  begin
    Pressure[I,1] := time;
    time := time + 0.6012                { Sampling period is 0.6012secs. }
  end;
  Close(Presfile);
  {* LowpassFilter(Pressure);  *}           { Filters data }
  Speedcalc(Pressure,Speed);             { Calculates array for speed curve }
end;

Procedure PressureMenu(var PressureArray,Speedarray:Plotarray;
                       var  AnotherFile:Boolean;var TI:Integer);
var
  Print      :Boolean;   { Print option }
  FirstByte  :Char;      { First byte of escape sequence }
  PlotOption :Char;      { User selected graph }
  A,B,I      :Integer;   { Used to compute average speed }
  Rate       :Real;      { Used to compute average speed }
  tA,tB      :Real;      { Used to compute average speed }
  Title      :Wrkstring; { Graph heading }
  YTitle     :Wrkstring; { Dependent variable }
  Unit       :Wrkstring; { Units of dependent variable }
begin
  Clrscr;
  Writeln;
  Writeln('SUB-MENU':44);
  Writeln('--------':44);
  Writeln('Pressure Derived Graph Selection':56);
  Writeln('(Deployment No.':47,Option,'.)');
  Writeln;Writeln;
  Writeln('Please select one of the following functions:');
```

APPENDIX 31(cont.)

Program TROUT (Page 6)

```
Writeln;Writeln;
Writeln('[F1]    Plot of Vehicle Depth vs. Time.');Writeln;
Writeln('[F2]    Plot of Vehicle Fall-Speed vs. Time.');Writeln;
Writeln('[F3]    Compute Fall-Speed over specified time interval');Writeln;
Writeln('[F4]    Hardcopy of present depth characteristic.');Writeln;
Writeln('[F5]    Hardcopy of present speed characteristic.');Writeln;
Writeln('[F6]    Select Pressure Data from another deployment.');Writeln;
Writeln('[F7]    Return to Main Menu.');
Read(Kbd,FirstByte);
Read(Kbd,PlotOption);
CASE PlotOption OF
    $59: begin
           Title := 'Depth vs. Time';YTitle := 'Depth';Unit := ' [m]';
           Print := false;
           GraphPlot(PressureArray,T1,Title,YTitle,Unit,Print);
           PressureMenu(PressureArray,SpeedArray,Anotherfile,T1);
         end;
    $60: begin
           Title := 'Speed vs. Time';YTitle := 'Speed';Unit := '[m/s]';
           Print := false;
           GraphPlot(SpeedArray,T1,Title,YTitle,Unit,Print);
           PressureMenu(PressureArray,SpeedArray,Anotherfile,T1);
         end;
    $61: begin
           Clrscr;Writeln;
           Writeln('Enter start-time of interval:');
           Read(tA);Writeln;
           Writeln('Enter end-time of interval (t[max] = 120 secs.):');
           Read(tB);Writeln;Writeln;
           A := Round(tA/0.6012);    { Sample period is 0.6012 seconds }
           B := Round(tB/0.6012);
           If A = 0 then A := 1;
           Rate := 0;
           for I := A to B do
           begin
             Rate := Rate + Speedarray[I,2];
           end;
           Rate := Rate/(B-A);
           Writeln('Average fall-speed over selected interval');
           Writeln('is ',Rate:4:2,' m/s.');
           Writeln;
           Writeln('Press <RETURN> to continue...');
           Repeat until keypressed;
           PressureMenu(PressureArray,SpeedArray,Anotherfile,T1);
         end;
    $62: begin
           Clrscr;
           Writeln;Writeln;
           Writeln('Please ensure printer is on-line.');
           Writeln('Hit any key to start print.');
           Writeln;
           Repeat Until Keypressed;
           Title := 'Depth vs. Time';YTitle := 'Depth';Unit :=' [m]';
           Print := true;
           GraphPlot(PressureArray,T1,Title,YTitle,Unit,Print);
           PressureMenu(PressureArray,SpeedArray,Anotherfile,T1)
         end;
    $63: begin
           Clrscr;
           Writeln;Writeln;
           Writeln('Please ensure printer is on-line.');
           Writeln('Hit any Key to start print.');
           Writeln;
           Repeat Until Keypressed;
           Title := 'Speed vs. Time';YTitle := 'Speed';Unit := '[m/s]';
           Print := true;
           GraphPlot(SpeedArray,T1,Title,YTitle,Unit,Print);
           PressureMenu(PressureArray,SpeedArray,Anotherfile,T1)
         end;
    $64: AnotherFile := True;
    $65: AnotherFile := False;
```

APPENDIX 31(cont.)

Program TROUT (Page 7)

```
  end
end;

Procedure PressureAnalyse;
var
Error      :Boolean;      { Detects invalid external file name }
Moredata   :Boolean;      { Flag for user termination }
dBar       :Integer;      { Full-Scale transducer output }
T1         :Integer;      { Scale output data to maximise resolution }
Calibrate  :Real;         { Calibration coefficient }
Pressure   :PlotArray;    { Pressure values from file }
Speed      :PlotArray;    { Differentiated pressure values }
Presfile   :Datafile;     { Input data file }

begin
  Clrscr;
  Writeln;Writeln;
  Writeln('Please enter the calibrated full-scale pressure for the');
  Writeln('         pressure transducer in [dBars].');
  Writeln;
  Readln(dBar);
  Writeln;Writeln;Writeln;Writeln;
  Writeln('Please enter the time range to be analysed.');
  Writeln('Analysis begins from t=0 when probe is deployed.');
  Writeln;
  Writeln('Enter time when deployment is complete:');
  Writeln('(t[max] = 120 secs.)');
  Writeln;
  Readln(T1);
  While T1 > 120 do
  begin
    Writeln;
    Writeln('Sorry,t[max] is 120 seconds.');
    Writeln('Please enter a value less than or equal to this.');
    Readln(T1)
  end;
  Calibrate := dBar/256.0;
  Error := False;
  MoreData := True;
  ChoosePresfile(Presfile,error);
  If not Error then
  begin
    CreatePlotArrays(Presfile,Pressure,Speed,Calibrate);
  end;
  While MoreData and not Error do
  begin
    PressureMenu(Pressure,Speed,Moredata,T1);
    if MoreData then
    begin
      ChoosePresfile(Presfile,Error);
      if not error then
        begin
          CreatePlotArrays(Presfile,Pressure,Speed,Calibrate);
          PressureMenu(Pressure,Speed,Moredata,T1)
        end
    end
  end
end;

Procedure TurbulenceAnalyse;
begin
  Clrscr;
  Writeln;Writeln;
  Finished := true;
end;


{*****************************************************************}
{*     Procedure SELECTROUTINE controls the program by selecting the      *}
{*       the appropriate algorithm chosen by the user in MAINMENU.        *}
{*****************************************************************}
```

APPENDIX 31(cont.)

Program TROUT (Page 8)

```
Procedure SelectRoutine;
begin
  MainMenu(Routine);
  CASE Routine OF
    $59: DisplayHeadfile;
    $60: PressureAnalyse;
    $61: Begin
         TurbulenceAnalyse
         end;
    $62: Finished := True
  end
end;


{**************************************************************************}
{*                          Main Program                                  *}
{**************************************************************************}

begin
  Initgraphic;        { Initialises the graphics system for graphs }
  Leavegraphic;       { Temporerily leaves the graphic system }
  Clrscr;
  Writeln;Writeln;
  Writeln('Enter path and sub-directory of input Data.');
  Writeln('e.g.   C:\ Filepath\ Subdirectory');
  Writeln;
  Readln(Filepath);
  DeploymentDates;            { Sets up file with dates for graph ID }
  Finished := False;
  While not Finished do SelectRoutine;
  Writeln('Program TROUT terminated.');
  Writeln('Type ' Trace ' to analyse turbulence in time domain ');
  Writeln('OR');
  Writeln('Type ' Spectrum ' to perform Power Spectral analysis.');
end.
```

APPENDIX 32

Software Reference: Program TRACE

```
program Trace(input,output);

type
  Directory = String[35];
  Date = String[30];
  Datearray = Array[1..8] of Date;
  Tapweight = Array[-10..10] of Real;
  Turbdatafile = file;
  TMvector = Array[0..2047] of real;
  Turbarray = Array[1..464,0..127] of byte;
  Arrayptr = ^Turbarray;
{ $I typedef.sys }
{ $I graphix.sys }
{ $I Kernel.sys }
{ $I windows.sys }          (* Graphics include files *)
{ $I findworld.hgh }
{ $I axis.hgh }
{ $I polygon.hgh }
var
  Buffer     :Arrayptr;        { Segmented array of turbulence data }
  Err        :Boolean;         { Assigned to validity of selected filename }
  LPF        :Boolean;         { Turns low pass filter ON/OFF }
  Moredata   :Boolean;         { Flag for User termination }
  Print      :Boolean;         { Print option }
  FilterType :Char;            { User selected filter characteristic }
  Option     :Char;            { User selected input file }
  Header     :DateArray;       { Array of deployment statistics }
  Filepath   :Directory;       { Directory of source data }
  Maxshear   :Real;            { Sets graphics scaling for shear trace }
  Turbdata   :Turbdatafile;    { Hex file with turbulence data }


Procedure SetupHeader;
var
  I          :Integer;
  Path       :Text;
  Headerfile :Text;
  Screenline :String[80];
begin
  Assign(Path,'DataPath.pas');
  Reset(Path);
  Read(Path,Filepath);
  Close(Path);
  Assign(Headerfile,Filepath + '\ Header.pas');
  Reset(Headerfile);
  I :=1;
  Repeat
    Readln(Headerfile,Screenline);
    Header[I] := Copy(Screenline,37,28);  { Sets up array for Graph ID }
    I := I+1;
  Until EOF(Headerfile);
  Close(Headerfile);
(*  Erase(Path);     *)
(*  Erase(Headerfile) *)
end;

Procedure ChooseTurbfile(var Turbfile:Turbdatafile;var InvalidFile:Boolean);
var
  Extfile  :String[40];    { Path and name of external pressure file }
begin
  Clrscr;
  Writeln;Writeln;
  Writeln('Please select deployment number to be analysed.');
  Writeln('Enter number (1-8)');
  Writeln;Writeln;
  Read(Kbd,Option);
  Extfile := Filepath + '\ Turb' + Option + '.pas';
  Assign(Turbfile,Extfile);
  {$I-}
  Reset(Turbfile);
  {$I+};
```

APPENDIX 32(cont.)

Program TRACE (Page 2)

```
  InvalidFile := (IOresult <> 0);   { Error if no external file found }
  If InvalidFile then
  begin
    Writeln;
    Writeln('Cannot find Data file TURB',Option,'.PAS.');
    Writeln('Press any Key to return to Main Menu.');
    Repeat until Keypressed
  end
end;

Procedure ReadTurbfile(var Turbfile:Turbdatafile;
                       var A:Arrayptr;var Filesize:Integer);
begin
  Reset(Turbfile);
  Filesize := Filesize(Turbfile);
  Blockread(Turbfile,A^,Filesize);
  Close(Turbfile);
end;

Procedure FlushBuffer(var A:Arrayptr;var Length:Integer);
var
  J,K     :Integer;       { Loop variables }
begin
  Writeln;Writeln;
  Writeln('Clearing Memory...');
  for J := 1 to Length do
  begin
    for K := 0 to 127 do A^[J,K] := 0;
  end
end;

Procedure CalcOffset(Localmem:Arrayptr;var Offset:Integer);
var                                 { Calculates d.c. offset of sampled data }
  Runave :Real;
  I,J    :Integer;
begin
  Runave := 0;
  for J := 1 to 4 do
  begin
    for I:= 0 to 127 do Runave := Runave + (Localmem^[J,I]/512);
  end;
  Offset := Round(Runave);
end;

{**************************************************************************}
{*    Procedure Filter is used to filter data (LPF with 25Hz cut-off),    *}
{*    before it is plotted.The tap weights are calculated from an FIR     *}
{*    LPF truncated to 11 points and windowed through a Hamming window.   *}
{**************************************************************************}

Procedure LPFmenu;
begin
  LPF := true;
  Clrscr;Writeln;Writeln('Select filter characteristic:');
  Writeln;Writeln;
  Writeln('         [F1]     Cut-off frequency : 5 Hz.');Writeln;
  Writeln('         [F2]     Cut-off frequency : 10 Hz.');Writeln;
  Writeln('         [F3]     Cut-off frequency : 25 Hz.');Writeln;
  Writeln('         [F4]     Cut-off frequency : 50 Hz.');Writeln;
  Writeln('         [F5]     Turn filter off.');
  Read(Kbd,FilterType);
  Read(Kbd,FilterType);
end;

Procedure SelectWeights(var H:Tapweight);
var
  I :Integer;
begin
  Case FilterType of                { Initialises array with filter weights }
  $59: begin
         H[-10]:= 0.001497; H[-9]:= 0.001943;
```

APPENDIX 32(cont.)

Program TRACE (Page 3)

```
        H[-8] := 0.003218; H[-7]:= 0.005220;
        H[-6] := 0.007770; H[-5]:= 0.010622;{ Tap weights for F(LP) : 5 Hz }
        H[-4] := 0.013500; H[-3]:= 0.016110;
        H[-2] := 0.018197; H[-1]:= 0.019540;
        H[0]  := 0.02;
      end;
  $60: begin
        H[-10]:= 0.002422; H[-9]:= 0.003280;
        H[-8] := 0.005638; H[-7]:= 0.009447;
        H[-6] := 0.014450; H[-5]:= 0.020206;{ Tap weights for F(LP): 10 Hz }
        H[-4] := 0.026154; H[-3]:= 0.031653;
        H[-2] := 0.036103; H[-1]:= 0.038992;
        H[0]  := 0.04;
      end;
  $61: begin
        H[-10]:= 0.000000; H[-9]:= 0.001120;
        H[-8] := 0.003926; H[-7]:= 0.009919;
        H[-6] := 0.020076; H[-5]:= 0.034376;{ Tap weights for F(LP): 25 Hz }
        H[-4] := 0.051625; H[-3]:= 0.069563;
        H[-2] := 0.085331; H[-1]:= 0.095146;
        H[0]  := 0.1;
      end;
  $62: begin
        H[-10]:= 0.000000; H[-9]:=-0.002131;
        H[-8] :=-0.006351; H[-7]:=-0.011661;
        H[-6] :=-0.012404; H[-5]:= 0.00000 ;{ Tap weights for F(LP): 50 Hz }
        H[-4] := 0.003190; H[-3]:= 0.081775;
        H[-2] := 0.038072; H[-1]:= 0.182888;
        H[0]  := 0.2;
      end;
  $63: LPF := false;
  end;
  For I := 1 to 10 do H[I] := H[-I];  { Filter is symmetric }
end;

Procedure Filter(var U:Plotarray);
var
  H         :Tapweight;              { Storage array for tap weights }
  I,K       :Integer;                          { Loop variable }
  Y         :Array[1..1024] of real;   { Output array from filter }
begin
  SelectWeights(H);
  If LPF then
  begin
    For I := 1 to 10 do Y[I] := 0;
    For I := 11 to 1014 do             { Neccesary to preserve causality }
    begin
      Y[I] := 0;
      For K := -10 to 10 do
      begin                              { Convolution of FIR filter and  }
        Y[I] := (Y[I]+U[I+K,2]*H[K]);    {      and input sequence.       }
      end;
    end;
    For I := 1015 to 1024 do Y[I] := 0;
    For I := 1 to 1024 do U[I,2] := Y[I];
  end
end;

{**************************************************************************}
{*  The following procedures calculate and plot the shear trace over a    *}
{*            1 second period selected by the User.                       *}
{**************************************************************************}

Procedure CalcRMS(Signal:Plotarray;var RMS:Real);
var
  I    :Integer;     { Loop variable }
begin
  RMS := 0;
  for I := 1 to 500 do Signal[I,2] := sqr(Signal[I,2]);
  for I := 1 to 500 do RMS := RMS + Signal[I,2]/500; { Calculates RMS value }
  RMS := sqrt(RMS);
```

APPENDIX 32(cont.)

Program TRACE (Page 4)

```
end;

Procedure SetupGraphics1;
begin
  Intergraphic;
  DefineWindow(1,trunc(Xmaxglb/10),trunc(Ymaxglb/10),
               trunc((Xmaxglb*9)/10),trunc((Ymaxglb*9)/10));
  DefineWindow(2,trunc(Xmaxglb/10),trunc(Ymaxglb/10),
               trunc((Xmaxglb*9)/10),trunc((Ymaxglb*9)/10));
  Defineworld(1,0,1000,1000,0);
  Selectworld(1);
  Selectwindow(1);
  SetBackground(0);
  DrawBorder;
  GotoXY(33,2);Write('┌──────────────┐');
  GotoXY(33,3);Write('│ Shear Trace  │');
  GotoXY(33,4);Write('└──────────────┘')
end;

Procedure PlotTrace1(ShearArray:plotarray);
begin
  Findworld(2,Sheararray,500,1,1.3);
  Selectwindow(2);
  DrawAxis(0,8,5,5,1,5,9,1,false);
  DrawPolygon(ShearArray,1,500,0,1,0)
end;

Procedure DisplayLabels1(var L:Integer);
var
  T1,T2          :Integer;       { Start and finish times of current trace }
  Num,R          :Integer;
  I,J            :Integer;       { Loop variables for repetitive labels }
  Day,Time       :String[12];    { Date and time for deployment }
  Timestring     :String[40];
  T1ch,T2ch      :String[3];     { Character equivalents of T1 and T2 }
begin
  Selectworld(1);
  Selectwindow(1);
  DrawTextW(7,480,1,'dU/dz');
  DrawTextW(7,520,1,'[/sec]');
  val(Option,num,R);
  Day := Copy(Header[num],1,8);
  Time := Copy(Header[num],16,12);
  DrawTextW(880,50,1,'DATE:');
  DrawTextW(880,90,1,Day);       { Graph identification : Date }
  DrawTextW(870,115,1,Time);     { Graph identification : Time }
  T2 := trunc(L*128/499.26);     { Sample frequency is 499.26 Hz}
  T1 := T2 - 1;
  Str(T1,T1ch);                  { Converts times into characters }
  Str(T2,T2ch);
  Timestring := 'Current Display: t:'+ T1ch + ' to t:'+ T2ch +'.';
  DrawTextW(620,960,1,Timestring)
end;

Procedure ShearMenu1(var MoreShears:Boolean;var TotalTime,AccumTime,
                     Calibrate,RMS:Real;var Localmem:Arrayptr;J,K,L:integer);
var
  Choice         :Char;          { Denotes user menu option  }
  dc             :Integer;       { Subtract dc component from running average }
  OutputArray    :PlotArray;     { Passes Array for plotting }
begin
  ClrScr;
  Writeln;Writeln;
  Writeln('Total Deployment time is ',Totaltime:4:1,' seconds.');
  Writeln('Currently: ',AccumTime:4:1,' seconds have been displayed.');
  Writeln('Last RMS value :',RMS:8:5,' m/s per metre.');
  Writeln;
  Writeln('Please select one of the following options :');
  Writeln;Writeln;
  Writeln('    [F1]      Hardcopy of previous 1 second trace.');Writeln;
  Writeln('    [F2]      Display of next 1 second period.');Writeln;
```

APPENDIX 32(cont.)

Program TRACE (Page 5)

```
  Writeln('    [F3]      Change filter characteristic.');Writeln;
  Writeln('    [F4]      Return to Turbulence sub-Menu.');Writeln;
  Read(Kbd,Choice);
  Read(Kbd,Choice);
  Case Choice of
    $59: begin
           CalcOffset(Localmem,dc);
           Clrscr;
           Writeln;Writeln;
           Writeln('Please ensure printer is on-line.');
           Writeln('Hit <RETURN> to start plot');
           Repeat until keypressed;
           K := 0;          { Sets parameters back 1 seconds }
           L := L-4;        { L is value parameter - does'nt effect globals }
           for J := 1 to 512 do
           begin
             OutputArray[J,1] := J*(1/500);
             OutputArray[J,2] := Calibrate*(0.75/128)*(Localmem^[L,K] - dc);
             K := K+1;
             If K = 128 then
             begin
               K := 0;
               L := L + 1
             end
           end;
           If LPF then
           begin
             Writeln;Writeln('Filtering...');
             Filter(OutputArray);
           end;
           SetupGraphics1;
           PlotTrace1(OutputArray);
           DisplayLabels1(L);
           Hardcopy(false,6);
           Leavegraphic;
           ShearMenu1(Moreshears,TotalTime,AccumTime,
                      Calibrate,RMS,Localmem,J,K,L)
         end;
    $60: MoreShears := true;
    $61: begin
           LPFmenu;
           ShearMenu1(MoreShears,TotalTime,AccumTime,Calibrate,RMS,
                      Localmem,J,K,L);
         end;
    $62: begin
           MoreShears := false;
         end;
  end
end;

Procedure calcShearArray1(var Localmem:Arrayptr;
                          var Calibrate,TotalTime:Real);
var
  ShearArray :Plotarray;  { Array of 1024 vertices (2 seconds) }
  MoreShears :Boolean;    { Flags user selected termination }
  Abort      :Char;       { Flags user selected termination }
  dc         :Integer;    { Subtract dc component from running average }
  J,K,L      :Integer;    { Loop variables }
  AccumTime  :Real;       { Returns accumulated time }
  RMS        :Real;       { Used to calculate RMS value }
begin
  CalcOffset(Localmem,dc);
  K := 0;
  L := 1;
  Clrscr;
  Writeln;Writeln;
  MoreShears := true;
  AccumTime := 0;
  Writeln;
  Writeln('Total deployment time is ',TotalTime:4:1,' seconds.');
  Writeln;
```

APPENDIX 32(cont.)

Program TRACE (Page 6)

```
  Writeln('Press <RETURN> to commence trace of first 1 second');
  Writeln('   or  " Q "   to return to Menu.');
  Readln(Abort);
  If Abort = 'Q' then MoreShears := false;
  While MoreShears do
  Begin
    AccumTime := Accumtime + 1.0255;  { Sample frequency is 499.26 Hz }
    for J := 1 to 512 do              { 1/F x 512 = 1.0255 secs. }
    begin
      ShearArray[J,1] := J*(1/500);
      ShearArray[J,2] := Calibrate * (Localmem^[L,K] - dc) * (0.00586);
      K := K+1;                         { Subtract DC component of 127,   }
      If K = 128 then                   { 0.75 Volts = byte value of 128  }
      begin                             { so 0.00586 = .75/128 }
        K := 0;
        L := L + 1;
      end
    end;
    If LPF then
    begin
      Writeln;Writeln('Filtering...');
      Filter(ShearArray);
    end;
    CalcRMS(ShearArray,RMS);
    SetupGraphics1;
    PlotTrace1(ShearArray);
    DisplayLabels1(L);
    Repeat Until Keypressed;
    Leavegraphic;
    ShearMenu1(Moreshears,TotalTime,AccumTime,Calibrate,RMS,Localmem,J,K,L)
  end;
end;

{*****************************************************************}
{*   The following procedures calculate and plot the shear trace over a   *}
{*            10 second period selected by the User.                       *}
{*****************************************************************}

Procedure SetupGraphics10;
begin
  Entergraphic;
  DefineWindow(1,trunc(Xmaxglb/5),trunc(Ymaxglb/12),
                 trunc((Xmaxglb*4)/5),trunc((Ymaxglb*3)/12));
  DefineWindow(2,trunc(Xmaxglb/5),trunc(Ymaxglb*3/12),
                 trunc((Xmaxglb*4)/5),trunc((Ymaxglb*5)/12));
  DefineWindow(3,trunc(Xmaxglb/5),trunc(Ymaxglb*5/12),
                 trunc((Xmaxglb*4)/5),trunc((Ymaxglb*7)/12));
  DefineWindow(4,trunc(Xmaxglb/5),trunc(Ymaxglb*7/12),
                 trunc((Xmaxglb*4)/5),trunc((Ymaxglb*9)/12));
  DefineWindow(5,trunc(Xmaxglb/5),trunc(Ymaxglb*9/12),
                 trunc((Xmaxglb*4)/5),trunc((Ymaxglb*11)/12));
  DefineWindow(6,trunc(Xmaxglb/10),trunc(Ymaxglb/14),
                 trunc((Xmaxglb*9)/10),trunc((Ymaxglb*13)/14));
  Defineworld(2,0,1000,1000,0);
  Selectworld(2);
  SelectWindow(6);
  SetBackground(0);
  Drawborder;
  GotoXY(33,1);Write('┌──────────────┐');
  GotoXY(33,2);Write('│ Shear Trace  │');
  GotoXY(33,3);Write('└──────────────┘')
end;

Procedure PlotTrace10(var ShearArray:plotarray;var Tracenum:Integer);
begin
  { FindWorld(1,Sheararray,1024,1,1.2); } { Used for automatic scaling }
  Defineworld(1,0,-maxshear,2.05,maxshear);
  Selectworld(1);
  SelectWindow(Tracenum);
  SetLinestyle(0);
  DrawAxis(0,5,1,1,0,1,9,1,false);
```

APPENDIX 32(cont.)

Program TRACE (Page 7)

```
  DrawPolygon(ShearArray,1,1024,0,1,0)
end;

Procedure DisplayLabels10(var L:Integer);
var
  T1,T2          :Integer;       { Start and finish times of current trace }
  Num,R          :Integer;
  I,J            :Integer;       { Loop variables for repetitive labels }
  Day,Time       :String[12];    { Date and time for deployment }
  Timestring     :String[40];
  T1ch,T2ch      :String[3];     { Character equivalents of T1 and T2 }
begin
  Selectworld(2);
  Selectwindow(6);
  val(Option,num,R);
  Day := Copy(Header[num],1,8);
  Time := Copy(Header[num],16,12);
  DrawTextW(880,50,1,'DATE:');
  DrawTextW(880,90,1,Day);       { Graph identification : Date }
  DrawTextW(870,115,1,Time);     { Graph identification : Time }
  J := 80;
  DrawTextW(75,J,1,'dU/dz');
  DrawTextW(75,(J+25),1,'[/sec]');
  for I := 1 to 4 do
  begin
    J := J + 200;
    DrawTextW(70,J,1,'dU/dz');          { Labels shear axes }
    DrawTextW(70,(J+25),1,'[/sec]');
    DrawTextW(880,J,1,'Time [s]');      { Labels time axes }
  end;
  T2 := trunc(Lx128/499.26);
  T1 := T2 - 10;
  Str(T1,T1ch);                         { Converts times into characters }
  Str(T2,T2ch);
  Timestring := 'Current Display: t='+ T1ch + ' to t='+ T2ch +'.';
  DrawTextW(620,960,1,Timestring)
end;

Procedure ShearMenu10(var MoreShears:Boolean;var TotalTime,AccumTime,
                      Calibrate:Real;var Localmem:Arraypir;I,J,K,L:Integer);
var
  Choice      :Char;       { Denotes user menu option  }
  dc          :Integer;
  OutputArray :PlotArray;  { Passes Array for plotting }
begin
  CalcOffset(Localmem,dc);
  ClrScr;
  Writeln;Writeln;
  Writeln('Total Deployment time is ',Totaltime:4:1,' seconds.');
  Writeln('Currently: ',AccumTime:4:1,' seconds have been displayed.');
  Writeln;
  Writeln('Please select one of the following options :');
  Writeln;Writeln;
  Writeln('    [F1]      Hardcopy of previous 10 second trace.');Writeln;
  Writeln('    [F2]      Display of next 10 second period.');Writeln;
  Writeln('    [F3]      Change filter characteristic');Writeln;
  Writeln('    [F4]      Change full scale shear value');Writeln;
  Writeln('    [F5]      Return to Turbulence sub-Menu.');Writeln;
  Read(Kbd,Choice);
  Read(Kbd,Choice);
  Case Choice of
    #59: begin
           ClrScr;
           Writeln;Writeln;
           Writeln('Please ensure printer is on-line.');
           Writeln('Hit <RETURN> to start plot');
           Repeat until keypressed;
           K := 0;                  { Sets parameters back 10 seconds }
           L := L-40;     { L is value parameter - does'nt effect globals }
           SetupGraphics10;
           For I := 1 to 5 do
```

APPENDIX 32(cont.)

Program TRACE (Page 8)

```
          begin
            for J := 1 to 1024 do
            begin
              OutputArray[J,1] := J*(1/500);
              OutputArray[J,2] := Calibrate*(0.75/128)*(Localmem^[L,K] - dc);
              K := K+1;
              If K = 128 then
              begin
                K := 0;
                L := L + 1
              end
            end;
            If LPF then Filter(OutputArray);
            PlotTrace10(OutputArray,1)
          end;
          DisplayLabels10(L);
          Hardcopy(false,6);
          Leavegraphic;
          ShearMenu10(Moreshears,TotalTime,AccumTime,
                      Calibrate,Localmem,1,J,K,L)
        end;
    '60': MoreShears := true;
    '61': begin
            LPFmenu;
            ShearMenu10(MoreShears,TotalTime,AccumTime,
                        Calibrate,Localmem,1,J,K,L);
          end;
    '62': begin
            Writeln('Enter maximum value for shears expected:');
            Readln(maxshear);
            maxshear := maxshear * 2;   { Calculates p-p value }
            ShearMenu10(MoreShears,TotalTime,AccumTime,
                        Calibrate,Localmem,1,J,K,L);
          end;
    '63': MoreShears := false
  end
end;

Procedure calcShearArray10(var Localmem:Arrayptr;
                           var Calibrate,TotalTime:Real);
var
  ShearArray :Plotarray;  { Array of 1024 vertices (2 seconds) }
  MoreShears :Boolean;    { Flags user selected termination }
  Abort      :Char;       { Flags user selected termination }
  dc         :Integer;
  I,J,K,L    :Integer;    { Loop variables }
  AccumTime  :Real;       { Returns accumulated time }
begin
  CalcOffset(Localmem,dc);{ Calculates dc component }
  K := 0;
  L := 1;
  Clrscr;
  Writeln;Writeln;
  MoreShears := true;
  AccumTime := 0;
  Writeln;
  Writeln('Total deployment time is ',TotalTime:4:1,' seconds.');
  Writeln;
  Writeln('Press <RETURN> to commence trace of first 10 seconds');
  Writeln('   or  ' Q '   to return to Menu.');
  Readln(Abort);
  If Abort = 'Q' then MoreShears := false;
  While MoreShears do
  begin
    SetupGraphics10;
    for I := 1 to 5 do
    begin
      AccumTime := Accumtime + 2.0;
      for J := 1 to 1024 do
      begin
        ShearArray[J,1] := J*(1/500);
```

APPENDIX 32(cont.)

Program TRACE (Page 9)

```
      ShearArray[J,2] := Calibrate*(0.75/128)*(Localmem^[L,K] - dc);
      K := K+1;
      If K = 128 then
      begin
        K := 0;
        L := L + 1;
      end
    end;
    If LPF then Filter(ShearArray);
    PlotTrace10(ShearArray,1)
  end;
  DisplayLabels10(L);
  Repeat Until Keypressed;
  Leavegraphic;
  ShearMenu10(Noreshears,TotalTime,AccumTime,Calibrate,Localmem,I,J,K,L)
 end
end;

Procedure calcShearTrace(var Turbfile:Turbdatafile);
const
  p = 1027;     { Density of sea water in kg per cubic metre. }
  A = 5.025E-5; { Probe X-sectional area in square metres. }
var
  Localmem    :Arrayptr;    { Internal array to maximise plot speed }
  Keyval      :Char;        { Value returned from user input }
  Plotoption  :Char;        { Significant byte of ecsape sequence }
  Calibrate   :Real;        { Calibration coefficient is function of speed }
  Speed       :Real;        { Fall speed for calibration purposes }
  Size        :Integer;     { Number of 128 byte records in datafile }
  Time        :Real;        { Returns total deployment time }
begin
  Clrscr;
  Writeln;
  Writeln('Please enter the average fall-speed ');
  Writeln('of the vehicle in [m/s]:');
  Writeln;
  Readln(Speed);
  Writeln('Please enter the calibration coefficient of the probe:');
  Writeln;
  Readln(Calibrate);
  Writeln;Writeln;Writeln;Writeln;
  Calibrate := 1/(Calibrate*p*A*sqr(Speed)); { Defines cal. coefficient }
  Writeln;
  Writeln('Please enter maximum expected shear value:');
  Readln(maxshear);
  New(Localmem);
  ReadTurbfile(Turbfile,Localmem,Size);       { Reads file into array }
  Time := Size * 0.256;
  LPF := false;                              { Low Pass filter off by default }
  Clrscr;Writeln;
  Writeln('Please select one of the following options:');
  Writeln;Writeln;Writeln;
  Writeln('       [F1]      Display trace in 1 second segments.');Writeln;
  Writeln('       [F2]      Display trace in 10 second segments.');Writeln;
  Read(Kbd,PlotOption);
  Read(Kbd,Plotoption);
  Writeln;Writeln('Do you wish to filter the data ? (Y/N):');
  Read(Kbd,Keyval);
  If Keyval = 'Y' then LPF := true;
  If Keyval = 'y' then LPF := true;
  If LPF then LPFmenu;
  CASE PlotOption OF
      #59: calcShearArray1(Localmem,Calibrate,Time);
      #60: calcShearArray10(Localmem,Calibrate,Time);
  end;
  FlushBuffer(Localmem,Size);
  Dispose(Localmem);
end;

Procedure TurbMenu(var AnotherFile:Boolean);
var
```

APPENDIX 32(cont.)

Program TRACE (Page 10)

```
  Plotoption :Char;      { Significant byte of ecsape sequence }
begin
  Clrscr;
  Writeln;
  Writeln('SUB-MENU':44);
  Writeln('--------':44);
  Writeln('Turbulence derived Graph Selection':57);
  Writeln('(Deployment No.':47,Option,'.)');
  Writeln;Writeln;
  Writeln('Please select one of the following functions:');
  Writeln;Writeln;
  Writeln('     [F1]      Trace of shear magnitude vs time.');
  Writeln;
  Writeln('     [F2]      Select Turbulence Data from another deployment.');
  Writeln;
  Writeln('     [F3]      Quit.');
  Read(Kbd,Plotoption);
  Read(Kbd,Plotoption);
  CASE PlotOption OF
      $59: begin
             calcShearTrace(TurbData);
             TurbMenu(Anotherfile)
           end;
      $60: AnotherFile := True;
      $61: AnotherFile := False;
  end
end;

{*****************************************************************}
{                          Main program                           }
{*****************************************************************}

begin
  InitGraphic;
  LeaveGraphic;
  Err := False;                  { Initialises Error flag }
  MoreData := True;
  SetupHeader;
  ChooseTurbfile(Turbdata,err);
  While MoreData and not Err do    { Error occurs at EOF }
  begin
    TurbMenu(Moredata);
    if MoreData then
    begin
      ChooseTurbfile(Turbdata,Err);
      if not err then
      begin
        TurbMenu(Moredata)
      end
    end
  end;
  Writeln;Writeln('Program TRACE terminated.');
end.
```

APPENDIX 33

Software Reference: Program SPECTRUM

```
program Spectrum(input,output);

type
Directory = String[35];
Date = String[30];
Datearray = Array[1..8] of Date;
Storage = Array[0..2047] of real;
FFTFile = file of Storage;
Turbdatafile = file;
TNvector = Array[0..2047] of real;
Turbarray = Array[1..464,0..127] of byte;
Arrayptr = ^Turbarray;
TNvectorptr = ^TNvector;

{ $I typedef.sys }
{ $I graphix.sys }
{ $I Kernel.sys }
{ $I windows.sys }            (* Graphics include files *)
{ $I findwrld.hgh }
{ $I axis.hgh }
{ $I polygon.hgh }
{ $I FFTB4.INC }               (* Numerical methods *)
{ $I REALFFT.INC }             (*   include files.  *)

var
Buffer     :Arrayptr;        { Segmented array of turbulence data }
Err        :Boolean;         { Assigned to validity of selected filename }
Noredata   :Boolean;         { Flag for User termination }
Print      :Boolean;         { Print option }
Suppress   :Boolean;         { Interference suppression of shear data }
Option     :Char;            { User selected input file }
Header     :DateArray;       { Array of deployment statistics }
Filepath   :Directory;       { Directory of source data }
Turbdata   :Turbdatafile;    { Hex file with turbulence data }

Overlay Procedure SetupHeader;
var
I :Integer;
Path       :Text;
Headerfle  :Text;
Screenline :String[80];
begin
  Assign(Path,'DataPath.pas');
  Reset(Path);
  Read(Path,Filepath);
  Close(Path);
  Assign(Headerfle,Filepath + '\ Header.pas');
  Reset(Headerfle);
  I :=1;
  Repeat
    Readln(Headerfle,Screenline);
    Header[I] := Copy(Screenline,37,28);  { Sets up array for Graph ID }
    I := I+1;
  Until EOF(Headerfle);
  Close(Headerfle);
  Erase(Path);
  Erase(Headerfle)
end;

Overlay Procedure ChooseTurbfile(var Turbfile:Turbdatafile;
                                 var InvalidFile:Boolean);
var
  Extfile  :String[40];    { Path and name of external pressure file }
begin
  Clrscr;
  Writeln;Writeln;
  Writeln('Please select deployment number to be analysed.');
  Writeln('Enter number (1-8)');
  Writeln;Writeln;
  Read(Kbd,Option);
```

APPENDIX 33(cont.)

Program SPECTRUM (Page 2)

```
  Extfile := Filepath + '\ Turb' + Option + '.pas';
  Assign(Turbfile,Extfile);
  {$I-}
  Reset(Turbfile);
  {$I+};
  InvalidFile := (IOresult <> 0);   { Error if no external file found }
  If InvalidFile then
  begin
    Writeln;
    Writeln('Cannot find Data file TURB',Option,'.PAS.');
    Writeln('Press any key to return to Main Menu.');
    Repeat until Keypressed
  end
end;

Overlay Procedure ReadTurbfile(var Turbfile:Turbdatafile;
                               var A:Arrayptr;var Filesize:Integer);
begin
  Reset(Turbfile);
  Filesize := Filesize(Turbfile);
  Blockread(Turbfile,A^,Filesize);
  Close(Turbfile);
end;

Overlay Procedure FlushBuffer(var A:Arrayptr;var Length:Integer);
var
J,K     :Integer;       { Loop variables }
begin
 Writeln;Writeln;
 Writeln('Clearing Memory...');
  for J := 1 to Length do
  begin
    for K := 0 to 127 do A^[J,K] := 0;
  end
end;


{*****************************************************************}
{*   The following procedures produce a plot of the time averaged Power    *}
{*   Spectrum of the segmented turbulence data file.The segment length     *}
{*   is fixed at 2048 bytes (4 second sections).Each segment is windowed,  *}
{*   transformed using a 1024 radix4 FFT, converted to a power spectrum    *}
{*   using the direct Welch method and finally added to the array holding  *}
{*   the accumulated average spectrum.                                     *}
{*****************************************************************}

Function Log(x:Real) :Real;
begin
  Log := Ln(abs(x))/Ln(10);
end;

Overlay Procedure Saveplot(FFT:Storage);
var
  SavedFFT   : FFTfile;       { Storage for FFT }
  I          : Integer;        { Loop variable }
  Name       : String[8];
begin
  Writeln('Input name of storage file (8 letters max.):');
  Readln(Name);
  Assign(SavedFFT,Filepath + '\' + Name + '.fft');
  Rewrite(SavedFFT);
  Write(SavedFFT,FFT);
  Close(SavedFFT);
  Writeln('File saved.');
end;

Overlay Procedure CalcRMS(FFT:Storage);
var
  Cmax     : Integer;       { Number of components within band }
  I        : Integer;       { Loop variable }
  Fmax     : Real;          { Band limiting frequency }
```

APPENDIX 33(cont.)

Program SPECTRUM (Page 3)

```
  MS      : Real;         { Intergrated spectrum }
begin
  ClrScr;Writeln;
  Writeln('Enter band-limit frequency:');
  Writeln('f[max] = 200Hz.');
  Readln(Fmax);
  Fmax := Fmax/0.2438;        { Components spaced at .2438 Hz }
  Cmax := Round(Fmax);
  MS := 0;
  for I := 0 to Cmax do MS := MS + FFT[I];
  MS := 0.2438 * MS;
  Writeln;
  Writeln('Mean Square shear over given band is ',MS:6:4,' per second.');
  Writeln;Writeln('Press any Key to continue...');
  Repeat until Keypressed;
end;

Overlay Procedure ComponentTable(FFT:Storage);
var
  Moretables :Boolean;
  Keyval     :Char;
  I,J,K      :Integer;
  First,Freq :Real;
begin
  Moretables := true;
  Clrscr;Writeln;Writeln;
  Writeln('Enter lowest component of interest:');
  Readln(First);
  Writeln;
  I := Round(First/0.2438);
  Freq := I * 0.2438;
  While Moretables do
  begin
    Clrscr;
    For J := 1 to 5 do Write('F[Hz]   [#]    ');
    Writeln;
    For J := 1 to 5 do Write('------ ------  ');
    Writeln;
    For J := 1 to 20 do
    begin
      For K := 1 to 5 do
      begin
        Write(Freq:5:1,' ',FFT[I]:6,'  ');
        I := I + 1;
        Freq := Freq + 0.2438;
      end;
      Writeln
    end;
    Writeln;
    Writeln('Press <RETURN> to display next page or * Q * to quit.');
    Repeat until Keypressed;
    Read(Kbd,Keyval);
    If Keyval = 'Q' then Moretables := false;
    If Keyval = 'q' then Moretables := false;
  end
end;

Procedure AxisMenu(var Linear,Quit:Boolean;var FFTresults:Storage);
var
  FirstByte  :Char;       { First byte of escape sequence }
  Axisoption :Char;       { Significant byte of ecsape sequence }
begin
ClrScr;
  Writeln;
  Writeln;
  Writeln('Please select one of the following options:');
  Writeln;Writeln;
  Writeln('                [F1] :   Display Spectrum (Linear Scale)');Writeln;
  Writeln('                [F2] :   Display Spectrum (Log Scale)');Writeln;
  Writeln('                [F3] :   Printout of previous display.');Writeln;
  Writeln('                [F4] :   Tabulate amplitude components.');Writeln;
```

APPENDIX 33(cont.)

Program SPECTRUM (Page 4)

```
  Writeln('              [F5] :   Save current Spectrum');Writeln;
  Writeln('              [F6] :   Calculate Mean Square shear.');Writeln;
  Writeln('              [F7] :   Return to Main Menu.');
  Writeln;Writeln;
  Read(Kbd,FirstByte);
  Read(Kbd,AxisOption);
  While (Axisoption<#59) or (Axisoption>#65) do
  begin
    Writeln('Invalid Option.');
    Writeln('Please select appropriate function:');
    Read(Kbd,Firstbyte);
    Read(Kbd,Axisoption);
  end;
  Case AxisOption of
     #59 : Linear := true;
     #60 : Linear := false;
     #61 : begin
             Print := true;
             Writeln;Writeln;
             Writeln('Please ensure printer is on-line.');
             Writeln('Press any key when ready to continue.');
             Repeat until Keypressed
           end;
     #62 : begin
             ComponentTable(FFTresults);
             AxisMenu(Linear,Quit,FFTresults);
           end;
     #63 : begin
             Saveplot(FFTResults);
             AxisMenu(Linear,Quit,FFTresults);
           end;
     #64 : begin
             CalcRMS(FFTResults);
             AxisMenu(Linear,Quit,FFTresults);
           end;
     #65 : Quit := true;
  end
end;

Procedure Interpolate(I:Integer;var DataArray:Storage);
begin
   DataArray[I-1] := DataArray[I-2];
   DataArray[I+1] := DataArray[I+2];
   DataArray[I] := DataArray[I-1]+ (DataArray[I+1]-DataArray[I-1])/2;
end;

Procedure Findnoise(DataArray:Storage;var Biggest:Integer);
var
  J             :Integer;
  Frequency     :Real;
begin
  Biggest := 5;
  for J := 6 to 900 do
  begin
    If DataArray[J] > DataArray[Biggest] then Biggest := J;
  end;
  Frequency := Biggest * 0.2438;
  Writeln;Writeln('Largest component is at ',Frequency:5:1,' Hz.');
end;

Procedure Filternoise(var DataArray:Storage);
var
  I,Biggest   :Integer;   { Loop variable }
  F           :Real;
  Suppress    :Char;
begin
  Suppress := 'Y';
  While Suppress = 'Y' do
  begin
    Findnoise(DataArray,Biggest);
    Writeln('Suppress this component ? (Y/N):');
```

APPENDIX 33(cont.)

Program SPECTRUM (Page 5)

```
    Read(Kbd,Suppress);
    If Suppress = 'Y' then Interpolate(Biggest,DataArray);
  end;
  Writeln;
  Writeln('Enter value of any other frequency to be suppressed ');
  Writeln('or press " 0 " to continue:');
  Readln(F);
  While F <> 0 do
  begin
    F := F/0.2438;
    I := Round(F);
    Interpolate(I,DataArray);
    Writeln;Writeln;
    Writeln('Enter next frequency to be suppressed or press 0 to continue:');
    Readln(F)
  end
end;


Overlay Procedure Plotspectrum(var FFTresults:Storage);
const
  deltaF = 0.2438;
var
  Component   :Plotarray;     { Array to be plotted }
  Linear      :Boolean;       { Denotes Scaling choice }
  Quit        :Boolean;       { Indicates end of routine }
  SuppressCHR :Char;          { User selected suppression }
  I,J         :Integer;       { Loop variables }
  Code        :Integer;       { Used in "val" procedure }
  Num         :Integer;       { Derived from deployment selected }
  Frequency   :Real;          { Frequency value for each power component }
  Day,Time    :String[12];    { Identification of Spectrum plot }
begin
  Quit := false;        { Initialises loop conditions }
  Print := false;
  Suppress := false;
  Axismenu(Linear,Quit,FFTresults);
  While not Quit do
  begin
    Writeln;Writeln('Do you wish to suppress interference?');
    Writeln('Input (Y/N):');Read(Kbd,SuppressCHR);
    If SuppressCHR = 'Y' then Suppress := true;
    If Suppress then Filternoise(FFTResults);
    Writeln;
    Writeln('Drawing...');
    Frequency := 0;
    Component[1,1] := Frequency;
    Component[1,2] := 0;                { Supress d.c. component  }
    for I := 2 to 900 do                { 900 iterations = 220Hz  }
    begin
      Frequency := Frequency + deltaF;
      Component[I,1] := Log(Frequency);
      if Linear then
      begin
        Component[I,2] := FFTresults[I-1];
      end
      else
      begin
        Component[I,2] := Log (FFTresults[I-1]);
      end
    end;
    EnterGraphic;
    DefineWindow(1,trunc(Xmaxgib/10),trunc(Ymaxgib/10),
                   trunc((Xmaxgib*9)/10),trunc((Ymaxgib*9)/10));
    DefineWindow(2,trunc(Xmaxgib/10),trunc(Ymaxgib/10),
                   trunc((Xmaxgib*9)/10),trunc((Ymaxgib*9)/10));
    Defineworld(1,0,1000,1000,0);
    SelectWindow(2);
    SetBackground(0);
    Findworld(2,Component,460,1.2,1.2);
    Selectwindow(2);
```

APPENDIX 33(cont.)

Program SPECTRUM (Page 6)

```
    DrawBorder;
    SetLinestyle(0);
    DrawAxis(1,5,10,15,5,40,9,-1,false);
    DrawPolygon(Component,3,-460,0,1,0);
    Selectworld(1);
    Selectwindow(1);
    GotoXY(32,2);Write('┌──────────────┐');
    GotoXY(32,3);Write('│ Power Spectrum │');
    GotoXY(32,4);Write('└──────────────┘');
    GotoXY(9,8); Write('Spectral');              { Labels Y-Axis }
    GotoXY(9,9); Write('Density');
    if Linear then
    begin
      GotoXY(9,11);Write('ϕ dU/dz');
    end
    else                                  { ϕ represents Spectral density }
    begin
      GotoXY(10,11);Write('Log ϕ');
      GotoXY(10,12);Write('dU/dz');
    end;
    Val(option,Num,Code);
    Day := Copy(Header[num],1,8);
    Time := Copy(Header[num],16,12);
    DrawTextW(850,80,1,'DATE:');
    GotoXY(25,20);Write('──────────┬──────────┬──────────┐');
    GotoXY(27,21);Write('1.0       10.0       100');
    GotoXY(37,22);Write('Frequency [Hz]');
    DrawTextW(850,120,1,Day);               { Graph Identification : Date }
    DrawTextW(840,145,1,Time);              { Graph Identification : Time }
    if Print then Hardcopy(false,6);
    Print := false;
    Repeat Until KeyPressed;
    LeaveGraphic;
    AxisMenu(Linear,Quit,FFTresults);
  end
end;

Overlay Procedure Init_FFTstore(var AverageFFT:Storage);
var
  I :Integer;   { Loop variable }
begin
  for I := 0 to 2047 do
  begin
    AverageFFT[I] := 0;     { Initialises storage array }
  end
end;

Overlay Procedure Windowdata(FFTdata:TNvectorptr);
var
Wn       :Real;      { Hanning Window coefficient for each data point }
I,J      :Integer;   { Loop variable }
begin
  Writeln('Windowing...');
  J := 0;
  for I := 0 to 2047 do     { Significant data points of 2048pt array }
  begin
    Wn := (0.5 * (1 - cos( 2*pi*J/2047 ))); { Hanning window function }
    FFTdata^[I] := Wn * FFTdata^[J];
    J := J + 1;
  end
end;

Overlay Procedure calcModulusSquared(var ReResult,ImResult:TNvectorptr);
var
  I     :Integer;     { Loop variable }
begin
  for I := 0 to 2047 do
  begin
    ReResult^[I] := Sqr(ReResult^[I]) + Sqr(ImResult^[I])
  end
end;
```

APPENDIX 33(cont.)

Program SPECTRUM (Page 7)

```
Overlay Procedure AverageSpectrum(var FFToutput:TNvectorptr;var AverageFFT:
                                  Storage;var Factor:Integer);
var
I   :Integer;      { Loop variable }
begin
  Writeln('Averaging...');          { Average is maintained by multipling }
  for I := 0 to 2048 do             {  each term by the number of segments }
  begin
    AverageFFT[I] := AverageFFT[I] + (1/Factor * FFToutput^[I])
  end
end;

Procedure FFTransformdata(var Segmentnum:Integer;var AverageFFT:Storage;
                          var Buffer:Arrayptr;var Calibrate:Real);
var
Inverse     :Boolean;      { Declares transform type;(Inverse or Foreward) }
Error       :Byte;         { Returns Error status after FFT }
Quitoption  :Char;         { Flag to detect termination }
I,J,K,L     :Integer;      { Loop variables }
Offset      :Integer;      { Used to enter correct row of buffer array }
FFTdata     :TNvectorptr;  { Passes data to Radix4 FFT algorithm }
ImResult    :TNvectorptr;  { Array for Im values of FFT input }
begin
  INverse := false;
  Writeln;
  Writeln('Press "Q" if you wish to abort transform.');
  for I := 1 to Segmentnum do
  begin
    if keypressed then
    begin
      Read(Kbd,quitoption);
      if Quitoption = 'Q' then halt
    end;
    Writeln;
    Writeln('Transforming segment ',I);
    New(FFTdata);
    New(Imresult);
    K := 0;
    L := 1;
    Offset := (16 * (I - 1));        { Finds relevent row in buffer array }
    for J := 0 to 2047 do
    begin                                                    { Normalise with }
      FFTdata^[J] := ((1/255)*(Buffer [ (L+offset) ,K]-128));{  1/255 factor, }
      K := K+1;                                              {  128 is d.c.   }
      If K = 128 then
      begin
        K := 0;
        L := L + 1;
      end
    end;
    Windowdata(FFTdata);
    Writeln('Performing FFT...');
    RealFFT(2048,Inverse,FFTdata,Imresult,Error);
    calcModulussquared(FFTdata,Imresult);
    Dispose(Imresult);
    AverageSpectrum(FFTdata,AverageFFT,Segmentnum);
    Dispose(FFTdata)
  end
end;

Procedure calcSpectrum(var Turbfile:Turbdatafile);
const
  p = 1027;     { Water density in kg per cubic metre }
  A = 5.027E-5; { Cross sectional area of probe }
var
  Segmentnum :Integer;       { Number of segments depends on deployment time}
  Size       :Integer;       { Number of 128 byte records in datafile }
  Ti         :Integer;       { User selected segment number }
  Calibrate  :Real;          { Calibration coefficient is function of speed }
  Speed      :Real;          { Fall-speed for calibration }
```

APPENDIX 33(cont.)

Program SPECTRUM (Page 8)

```
  AverageFFT :Storage;       { Array of summated FFT's }
  FFTdata    :TNvectorptr;   { Input/Output array for FFT procedure }
begin
  Clrscr;
  Writeln;Writeln;
  Writeln('The following input values of fall-speed and deployment time');
  Writeln('must be obtained from the pressure characteristics.');
  Writeln;
  Writeln('Please enter the average fall-speed ');
  Writeln('of the vehicle in [m/s]:');
  Readln(Speed);
  Writeln;
  Writeln('Please enter the Calibration coefficient');
  Writeln('of the turbulence probe: ');
  Readln(Calibrate);
  Writeln;Writeln;
  Calibrate := 1/(Calibrate*pi*sqr(speed));
  New(Buffer);
  ReadTurbfile(Turbfile,Buffer,Size);  { Reads file into array }
  Segmentnum := trunc(size/16);        { Determines number of 2048 byte }
                                       {     segments available.        }
  If Segmentnum < 1 then
  begin
    Writeln('There is insufficient data to perform a transform.');
    Writeln('Minimum data size is 2048 bytes.');
    Writeln;
    Writeln('Press any key to return to menu.');
    Repeat Until Keypressed
  end
  else
  begin
    Writeln('Enter number of segments to be analysed:');
    Writeln('(1 Segment = 4 secs of data.)');
    Writeln('[Maximum is ',Segmentnum,' segments.]');
    Writeln;
    Readln(T1);
    while (T1<0) or (T1>segmentnum) do
    begin
      Writeln;Writeln('Invalid selection.');
      Writeln('Enter number of segments:');
      Readln(T1);
    end;
    Segmentnum := T1;
    Init_FFTStore(AverageFFT);
    FFTransformdata(Segmentnum,averageFFT,Buffer,Calibrate);
    FlushBuffer(Buffer,Size);
    Dispose(Buffer);
    Plotspectrum(averageFFT)
  end
end;

Procedure TurbMenu(var AnotherFile:Boolean);
var
FirstByte   :Char;      { First byte of escape sequence }
Plotoption  :Char;      { Significant byte of ecsape sequence }
FFTfilename :Directory; { Path and name of external array to be plotted }
FFTspectrum :Storage;   { Internal name of array }
SavedFFT    :File of Storage; { Internal name of file }
begin
  Clrscr;
  Writeln;
  Writeln('SUB-MENU':44);
  Writeln('--------':44);
  Writeln('Turbulence derived Graph Selection':57);
  Writeln('(Deployment No.':47,Option,'.)');
  Writeln;Writeln;
  Writeln('Please select one of the following functions:');
  Writeln;Writeln;
  Writeln('     [F1]      Plot of time averaged Power Spectrum.');Writeln;
  Writeln('     [F2]      Select Turbulence Data from another deployment.');
  Writeln;
```

APPENDIX 33(cont.)

Program SPECTRUM (Page 9)

```
  Writeln('     [F3]      Plot spectrum of previously processed data.');
  Writeln;
  Writeln('     [F4]      Quit.');
  Read(Kbd,Firstbyte);
  Read(Kbd,Ploteption);
  CASE PlotOption OF
      #59: begin
             calcSpectrum(Turbdata);
             TurbMenu(Anotherfile)
           end;
      #60: AnotherFile := True;
      #61: begin                  { Plots spectrum of previously saved FFT }
             Writeln;Writeln;
             Writeln('Enter path and name of file to be plotted :');
             Writeln('(File must have suffix .fft)');
             Readln(FFTfilenme);
             Assign(SavedFFT,FFTfilenme);
             {$I-}
             Reset(SavedFFT);
             {$I+}
             If IOresult = 0 then
             begin
               Read(SavedFFT,FFTspectrum);
               Close(SavedFFT);
               PlotSpectrum(FFTspectrum);
             end
             else
             begin
                Writeln('Cannot find Data file ',FFTfilenme);
                Writeln('Press any Key to continue.');
                Repeat until Keypressed;
             end;
             TurbMenu(Anotherfile)
           end;
      #62: AnotherFile := False;
  end
end;

{*************************************************************}
{*                        Main program                       *}
{*************************************************************}

begin
  InitGraphic;                { Initialises graphics }
  LeaveGraphic;               { Temporarily leaves graphics }
  Err := False;
  MoreData := True;
  SetupHeader;                { Sets up array for graph identification }
  ChooseTurbfile(Turbdata,err); { User selects input data file }
  While MoreData and not Err do
  begin
    TurbMenu(Moredata);       { Select analysis routine }
    if MoreData then
    begin
      ChooseTurbfile(Turbdata,Err);
      if not err then
      begin
        TurbMenu(Moredata)
      end
    end
  end;
  Writeln;Writeln('Program SPECTRUM terminated');
end.
```

APPENDIX 34

SHEAR TRACE GENERATED DURING FIELD TRIALS
(ST. HELENA BAY)

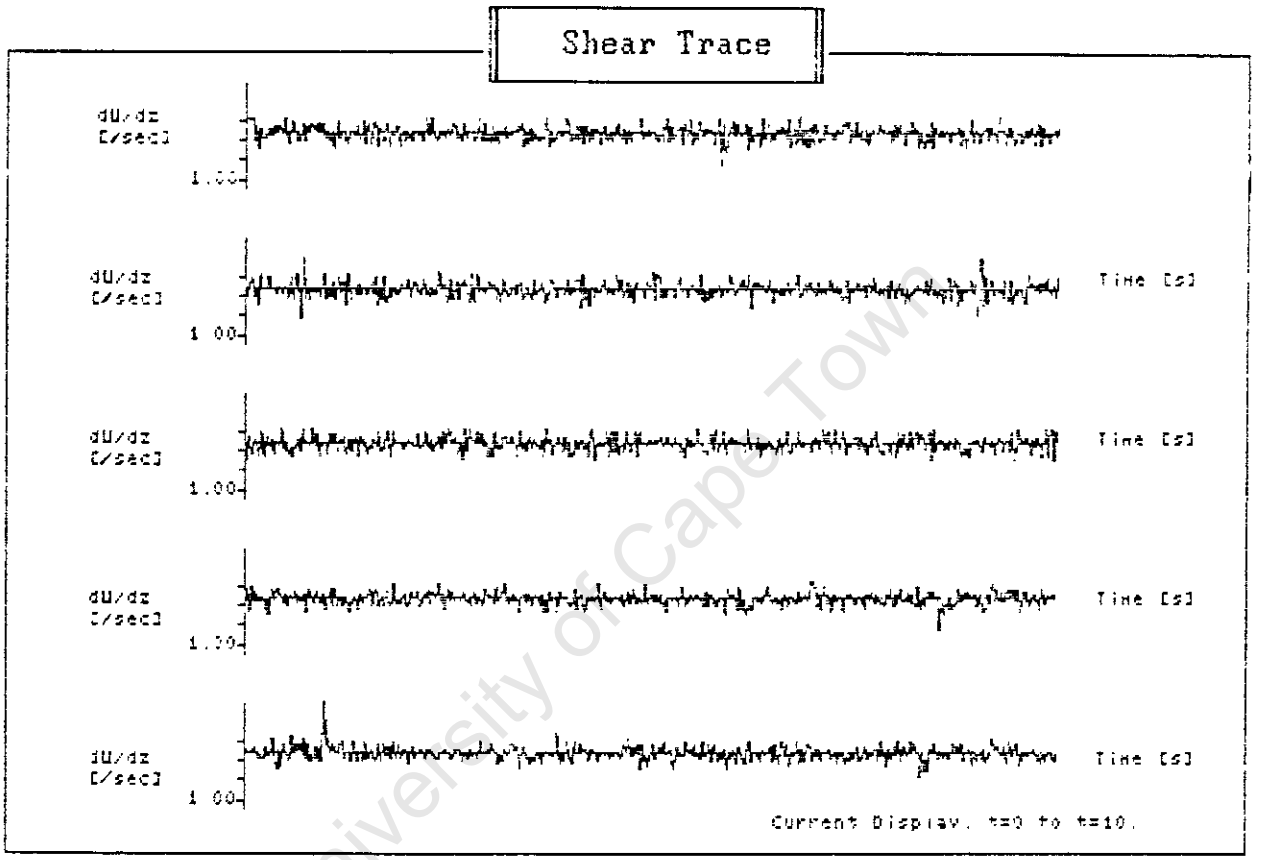

* The above trace represents 5 x 2 second consecutive time intervals, corresponding to 5 x 1.6 metre depth intervals. (Vehicle fall speed is 0.8 ms^{-1})
* Trace commences at a depth of 3 metres.

APPENDIX 35(a)

TEMPERATURE PROFILE : HOUT BAY

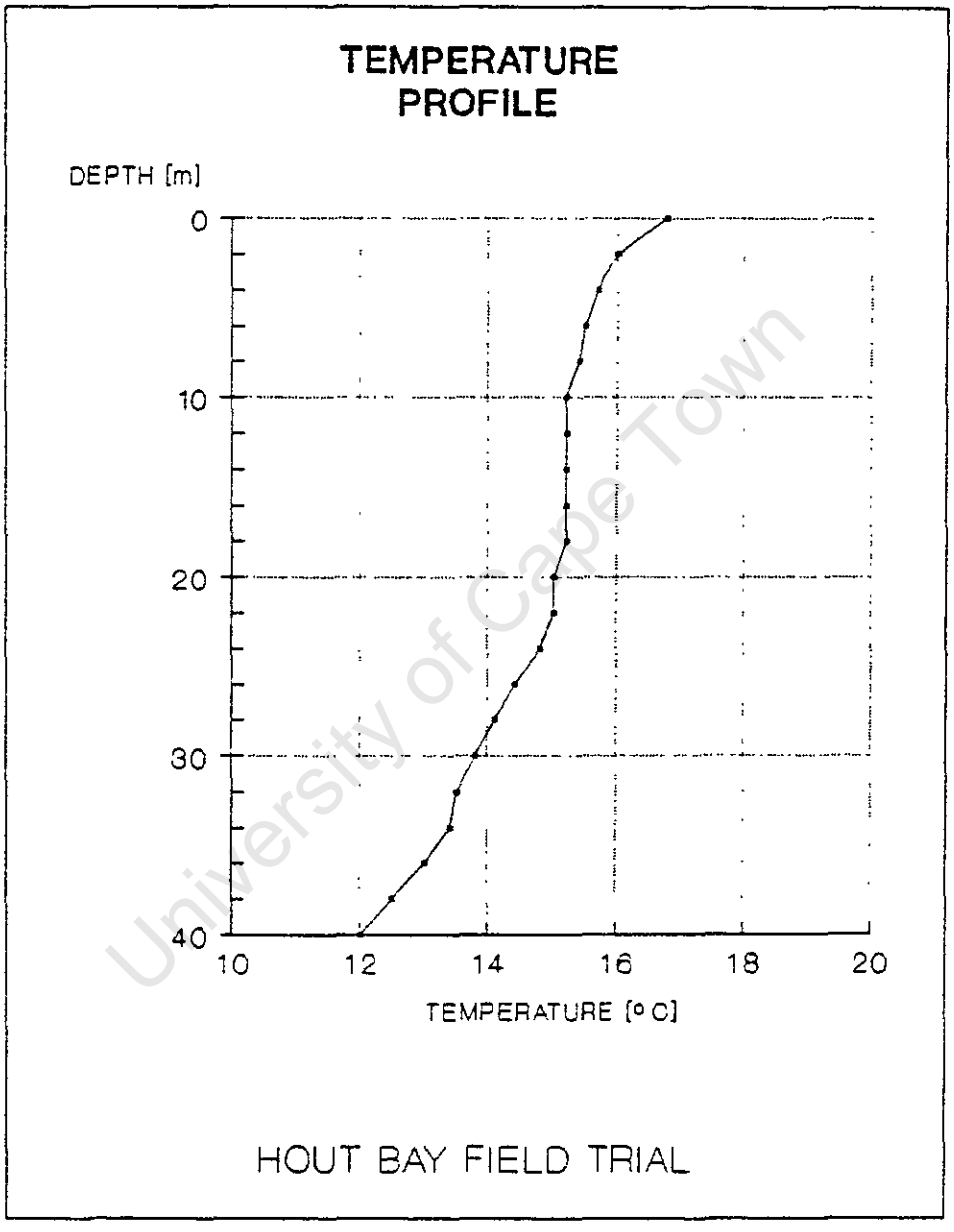

APPENDIX 35(b)

PRESSURE CHARACTERISTIC : HOUT BAY

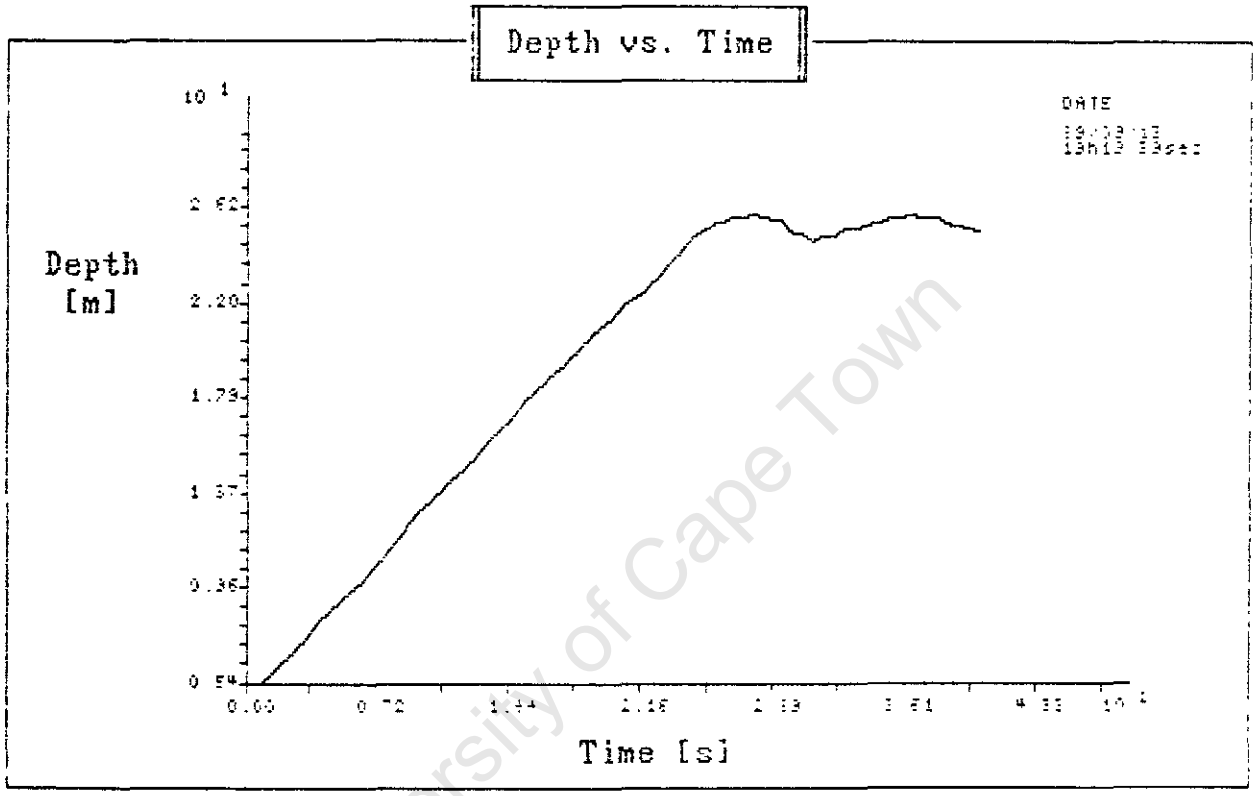

APPENDIX 35(c)

POWER SPECTRUM : HOUT BAY

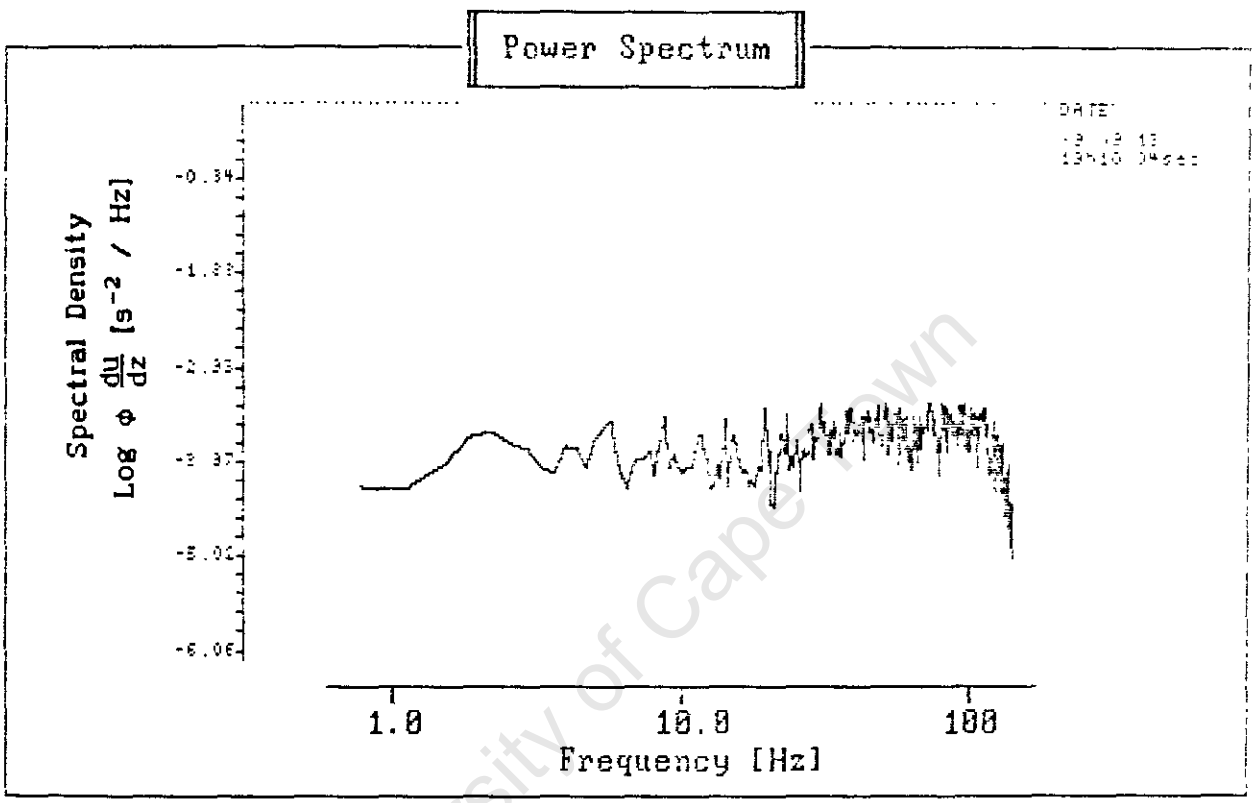

* Spectrum derived from average of 5 consecutive 4 second segments over depth interval 5 - 23 metres.
* Frequency spectrum over range 1 - 100 Hz corresponds to wavenumber spectrum over range 1.1 - 111 cycles per metre.

APPENDIX 35(d)

SHEAR TRACE : HOUT BAY

10 Second Trace (5m - 14m) Bandlimited to 100 Hz:

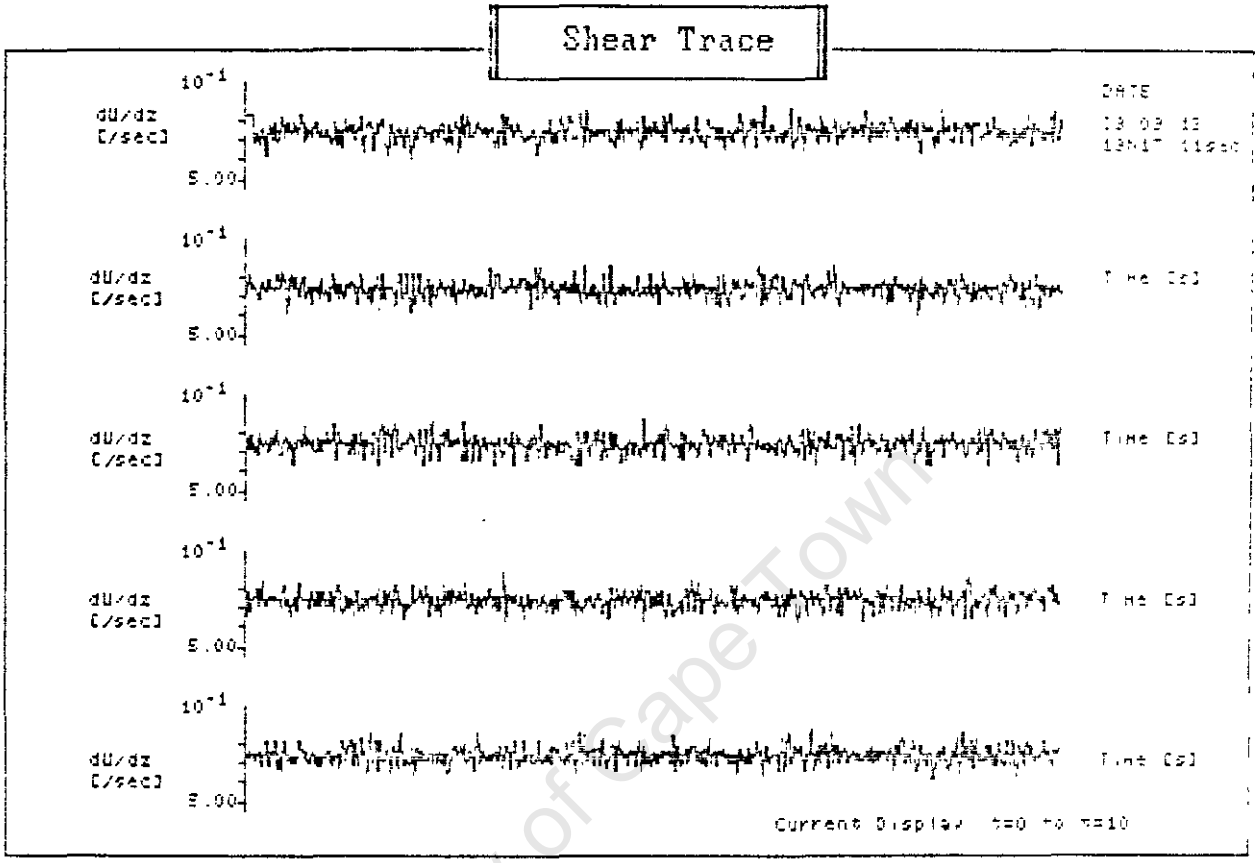

10 Second Trace (5m - 14m) Bandlimited to 25 Hz:

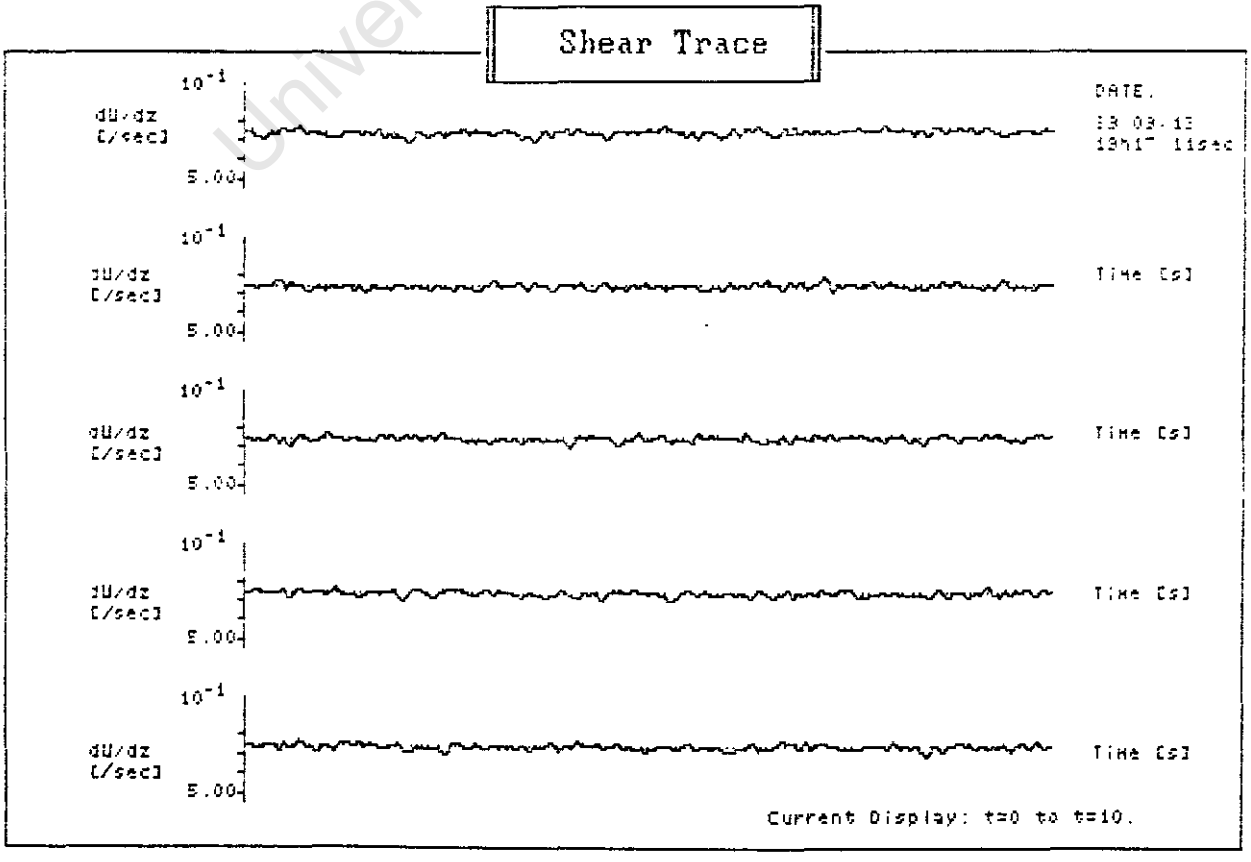

* Vehicle fall-speed is 0.9 ms^{-1}.